Summer 8-15-2016

Regulation of durable adaptive immune response by the c-MYC-AP4 transcriptional cascade

Chun Chou
Washington University in St. Louis

WASHINGTON UNIVERSITY IN ST. LOUIS

Division of Biology and Biomedical Sciences

Immunology

Dissertation Examination Committee:

Takeshi Egawa, Chair
Deepta Bhattacharya
Chyi-song Hsieh
Kenneth M. Murphy
Eugene M. Oltz
Emil R. Unanue

Regulation of durable adaptive immune response by the c-MYC-AP4 transcriptional cascade

by

Chun (Jim) Chou

A dissertation presented to the
Graduate School of Arts and Sciences
of Washington University in
partial fulfillment of the
requirements for the degree
of Doctor of Philosophy

August 2016

St. Louis, Missouri

TABLE OF CONTENTS

List of Figures

List of Tables

ACKNOLEDGEMENTS

The completion of this work could not have been possible without the guidance and support from friends and colleagues. I would like to thank Takeshi Egawa who has mentored me throughout my training. He has been instrumental in helping me develop lab techniques and refine skills of scientific inquiry. I would also like to thank members of my thesis committee, Ken Murphy, Emil Unanue, Eugene Oltz, Chyi Hsieh, and Deepta Bhattacharya who have provided guidance throughout my training.

I would also like to thank members outside the Egawa lab, Mike Diamond, Erika Pearce, Marco Colonna, Marina Cella, Amelia Pinto, Steve Persaud, Jonathon Curtis, Jennifer Govero, Yinan Wang, and Rachel Wong for technical support. I have acknowledged other collaborators at the end of each chapter.

This work was supported by the National Institute of Health. Additional funding sources are listed in each chapter.

ABSTRACT OF THE DISSERTATION

Regulation of durable adaptive immune response by the c-MYC-AP4 transcriptional cascade

by

Chun (Jim) Chou

Doctor of Philosophy in Biology and Biomedical Sciences
Immunology

Washington University St. Louis, 2016

Professor Takeshi Egawa, Chair

The process of amplifying immune responses by expanding a small number of antigen-specific cells, termed clonal expansion, is an important feature of the adaptive immunity. Whereas clonal expansion of cytotoxic T lymphocytes is required for complete eradication of intracellular pathogens, proliferation of B lymphocytes in the germinal centers (GC) is critical for generating a diverse immunoglobulin gene repertoire from which protective antibody carrying multiple mutations can arise. While the proto-oncogene c-MYC is absolutely required for the activation and cell cycle initiation in lymphocytes, its expression is temporally restricted. Activated lymphocytes, however, continue to proliferate after c-MYC levels decay to maximize clonal expansion. It remains unknown how lymphocytes sustain their proliferative program in the absence c-MYC. We demonstrated that the c-MYC-inducible transcription factor, AP4 is required for sustained expansion of antigen-specific lymphocytes. Mice lacking AP4 in CD8 T cells exhibited diminished T cell clonal expansion and succumbed to West Nile virus

infection due to uncontrolled viral replication in the central nervous system. Genetic ablation of AP4 in B lymphocytes impaired GC growth. These mice failed to control persistent viral infection due to blunted neutralizing antibody development. The accumulation of AP4 requires IL-2 and IL-21 signals in CD8 T cells and GC B cells, respectively, suggesting that AP4 functions as a gauge for extracellular microenvironment and scales the magnitude of lymphocyte expansion accordingly. Mechanistically, ChIP-seq and gene expression analyses suggest that AP4 compensates for early termination of c-MYC by maintaining the transcription of activation signature genes initiated by c-MYC. Thus, both CD8 T and GC B cells have evolved to utilize the c-MYC-AP4 transcription factor cascade to maximize immune responses.

CHAPTER 1:

Introduction

The central feature of the adaptive immune system is the use of an anticipatory repertoire in which each lymphocyte bears a unique antigen receptor [1]. This system allows for reactivity against a diverse array of antigens, but at the same time limits the number of lymphocytes for any given antigen at the steady-state, ranging between tens to hundreds for CD8 T cells [2]. Thus, an effective adaptive immune response requires the selective expansion of few antigen specific cells in a short period of time, a process termed 'clonal expansion,' to nullify pathogens.

The magnitude and duration of clonal expansion are commensurate with the strength and duration of activation signals that the lymphocytes receive. CD8 T cell expansion scales with the amount of pathogen in the initial inoculum and the levels of antigen expression by the pathogen [3, 4, 5]. Experiments using alternative peptide ligands, which represent a wide range of pMHC-TCR affinities, also showed a scaling effect [4, 6, 7, 8]. Similarly, during the germinal center (GC) response, B cells bearing a B cell receptor (BCR) of higher affinity than neighboring clones receive more help signals from follicular helper T (T_{FH}) cells and consequently undergo more rounds of cell division [9, 10, 11]. An insufficient CD8 T or GC B cell response may result in delayed pathogen clearance, leading to chronic infection or death of the hosts [5]. In contrast, an over-blown CD8 T cell response can cause excessive immunopathology[7, 12]. Uncontrolled expansion and survival of GC B cells nullify affinity maturation. Thus, the ability of lymphocytes to scale their responses according to the quality and quantity of activation stimuli is a functionally significant feature of the adaptive immune system.

In this work, we set forth to dissect the molecular mechanisms by which the magnitude and duration of adaptive immune responses are regulated. In particular, we

sought to identify transcription factors that translate extracellular stimuli, such as antigen load and cytokine levels, to the activation and expansion of lymphocytes during the course of infection.

1.1 CD8 T cell response during acute infection is controlled by the sequential expression of distinct transcription factors.

A typical course of acute CD8 T cell response consists of three distinct stages: priming, expansion, and contraction/memory formation (**Figure 1**) [13]. Once an antigen-specific CD8 T cell is optimally primed, it can divide as many as 19 times, generating a potential 500,000-fold expansion in 7 days [14]. In order to support proliferation at such dramatic rate, CD8 T cells must undergo drastic changes in metabolism [15]. In addition to enhanced glucose and amino acid uptake, an increase in aerobic glycolysis meets the demand for building blocks of proteins, nucleic acid, and lipids in order to make new cells [16]. The proto-oncogene c-MYC is rapidly up-regulated after CD8 T cell activation and stimulates transcription of key metabolic genes in the aforementioned pathways [17]. The transcription factor *Hif1a*, a downstream target of c-MYC, has also been shown to regulate glycolysis in activated CD8 T cells [18], but is dispensable for T cell expansion in an immunization model [19]. A recent report, however, showed hyperactive CD8 T cell response when *Hif1a* was constitutively expressed [20]. Although the expression of c-MYC is transient, its effects persist. Proliferation of CD8 T cells does not cease after the loss of c-MYC; rather, clonal expansion can continue even when mitogenic stimuli are limiting in the microenvironment as pathogens are being cleared [21, 22]. Maximal CD8 T cell expansion provides sufficient tissue surveillance to completely eradicate infected host

cells. The molecular mechanisms that sustain proliferation during this period have only begun to be understood.

As CD8 T cells proliferate, a subset differentiates into short-lived effector cells (SLECs) in response to environmental cues, including pro-inflammatory cytokines and antigen stimulation [23, 24, 25]. SLECs are terminally differentiated cells characterized by their ability to kill pathogen-infected cells, clonally expand and migrate to inflamed tissues and can be readily distinguished by the surface marker expression: $KLRG1^{hi}CD127^{lo}$ [26]. CD8 T cells acquire effector functions as they proliferate. However, whether effector differentiation is coupled to clonal expansion remains unclear: do pro-inflammatory cytokines induce distinct transcription factors to separately control proliferation and differentiation? Alternatively, can one transcription factor simultaneously regulate both processes? Recent evidence supports both models. T-bet (encoded by the gene Tbx21), a transcription factor induced by interleukin (IL)-12, is required for the up-regulation of KLRG1 [26]. In T-bet-deficient mice, CD8 T cell expansion was moderately reduced and effector cells exhibited slightly impaired cytotoxic activity [26]. Another transcription factor, Blimp-1 (encoded by the gene Prdm1), whose expression can be induced by IL-2, IL-12, and IL-21 [24, 27], has also been shown to regulate effector CD8 T cell response. Mice lacking Blimp-1 in CD8 T cells failed to clear influenza virus efficiently due to poor recruitment of CD8 T cells to the lungs [28] and reduced IFNγ and granzyme B expression in CD8 T cells [29]. However, expansion of Blimp1-deficient CD8 T cells appeared to be unaffected [28]. These limited examples beg for more extensive studies to identify additional transcription factors that instruct CD8 T cell response in a cytokine-dependent manner.

While over 90% of activated CD8 T cell undergo apoptosis during acute infection, a small fraction survive and mature to become memory cells [30]. Central memory T (T_{CM}) cells, characterized by high surface expression of CD62L and CD127, are capable of rapid response upon re-challenge and can be found in circulation and secondary lymphoid organs [31]. Memory CD8 T cells require IL-7 and IL-15 for survival and maintenance [32, 33]. Mice lacking the transcription factor Eomesodermin (*Eomes*) contained reduced number of T_{CM} cells due in part to decreased expression of CD122, which is involved in IL-15 signaling [34]. In spite of intensive studies in B cells response, the role of the transcription factor B cell lymphoma (Bcl)-6 in memory CD8 T cell differentiation is poorly understood. Current data suggest that *Bcl6* expression positively correlates with CD8 T cells with memory phenotype [35]. Thus, distinct transcription factors are activated in a stage-specific manner to program clonal expansion, effector differentiation, and memory formation of antigen specific CD8 T cells.

Despite current advancements in elucidating transcriptional control of CD8 T cell response, two important questions are yet to be answered. First, what are the transcription factors that sustain effector expansion after priming, and second, why do CD8 T cells continue to expand when pathogens are cleared from circulation and lymphoid organs?

1.2 Transient T-B interaction induces transcription factors that potentiate continued expansion of selected GC B cells.

The germinal center response (GC) is essential for generating highly protective affinity-matured antibody after immunization and pathogen challenge [36, 37, 38]. In response

to stimulation by T-dependent antigens, B cells form a specialized structure, GC, in which secondary diversification of B cell receptor (BCR) genes, expansion and affinity maturation take place [39, 40] (**Figure 2**). GC is functionally divided into the light zone (LZ) and the dark zone (DZ) [37, 38]. In the LZ, GC B cells compete for help signals from cognate follicular helper T cells (T_{FH}) on the basis of their BCR affinity for the antigen [11]. Clones expressing BCR of higher affinity than neighboring cells are selected for entry into the DZ where cell division and somatic hypermutation occur [9, 10, 11]. DZ cells then migrate back to the LZ to test their mutated BCR and the process of affinity-based selection repeats. Through iterative cycles of selection, proliferation, and somatic hypermutation, termed "cyclic re-entry", rare clones capable of producing high affinity antibody emerge and differentiate into memory or plasma cells, conferring long-term protective humoral immunity to the host.

The magnitude of GC expansion and the extent of somatic hypermutation are determined by the availability of T_{FH}-derived help. In the LZ, GC B cells capture antigen from follicular dendritic cells (FDCs) [38], process and present it to cognate T cells and receive help signal. Recent studies demonstrated that enhancing B-T interaction through targeted antigen delivery is sufficient to shorten S-phase length and promote cell division of GC B cells (**Figure 2**) [9]. During GC responses, T cell help is delivered to GC B via cell-cell contact or in the form of soluble factors. While stimulation through surface CD40L-CD40 ligation is critical for GC formation and maintenance [41], such an interaction is lost when selected cells migrate away from T cells towards the DZ. Secreted mediators by T_{FH} may provide sustained help to GC B cells at a relatively distant location in the LZ. Cytokine production by T_{FH} can be triggered by antigen

presentation of their cognate B cells [42]. Among several T_{FH}-derived cytokines, IL-21 in particular, is critical for GC growth, somatic hypermutation and affinity maturation, in part, by directly regulating Bcl-6 expression [43, 44]. Although it is evident that transient T cell help in the LZ can program the extent of proliferation in the anatomically remote DZ, the underlying molecular mechanisms remain elusive.

The proto-oncogene c-MYC is required for cellular activation and initiation of highly proliferative states in a variety of rapidly dividing cells, including GC B cells [45, 46]. Although *Myc* has recently been identified as an essential regulator for GC formation and maintenance downstream of T cell help, it is only expressed in a subset of LZ cells that have initiated cell cycle progression on route to DZ [45, 46]. However, these selected cells undergo extensive cell divisions without detectable levels of c-MYC in the DZ. Thus, additional transcription factors induced during transient T-B interaction are required to sustain proliferation of DZ GC B cells after c-MYC is downregulated.

1.3 AP4 (encoded by *Tfap4*) is a transcriptional target of c-MYC

AP4, encoded by the gene *Tfap4*, belongs to a superfamily of basic helix-loop-helix (bHLH) transcription factors (**Figure 3**) [47]. As the name implies, bHLH transcription factors contain two distinct and conserved structures: a basic region that binds a specific stretch of DNA sequence, so-called E-box motif, and a HLH domain that facilitates formation of homo- or hetero-dimers with other bHLH members [48]. AP4 has been shown to form homodimer with itself and generally does not interact with other bHLH factors [47]. Little has been known about the function of AP4 despite its

identification almost 30 years ago [49]. *In vitro* studies suggest that AP4 is an activator for SV40 late transcription [49]. A study previously published by our lab showed that AP4 promotes silencing of Cd4 gene in both the double-negative thymocytes and CD8 T cells [50]. Two reports by the Hermeking lab established AP4 as a downstream target of c-MYC. AP4 promotes c-MYC-dependent cell cycle progression by inhibiting the expression of p21 [51] and enhances c-MYC-mediated epithelial-mesenchymal transition of a colon tumor cell line [52]. Because c-MYC is absolutely necessary for activation and proliferation of lymphocytes, we suspected that AP4, as an inducible target of c-MYC, also plays a role during adaptive immune responses.

1.4 Conclusions

The mechanisms by which early activation programs are established during lymphocyte priming have been studied in details. How these programs are maintained over time in proliferating lymphocytes is less understood. Key transcription factors, including *Myc*, *Batf* and *Irf4* are rapidly induced after activation in both CD8 T cells [53, 54, 55] and GC B cells [45, 46]. Deficiencies in any one of these genes result in early defects in CD8 T cell clonal expansion [54] [53], with *Myc* ablation showing the most severe phenotypes presumably because its master regulator role in initiating general activation programs. These data indicate that *Myc*, *Batf*, and *Irf4* play non-redundant roles in promoting the initial expansion of CD8 T cells. None of the three transcription factors, however, persist throughout the entire course of clonal expansion. Thus, it remains unclear how CD8 T cells continue to expand in the later phase of the immune response. Similarly, *Myc*, *Batf*, and *Irf4* expression are restricted to recently selected cells in the GC, and are

downregulated when selected cells proliferate in the DZ. In this study, we identified the novel transcription factor AP4, as a key regulator that maintains rapid proliferation of lymphocytes after the initial expansion upon activation. In Chapter 2, we demonstrated the critical requirement for AP4 in maximizing CD8 T cell clonal expansion and host protection from lethal challenge by the neurotropic human pathogen, West Nile virus. In Chapter 3, we extended our findings to explain how selected GC B cells undergo continued proliferation in the DZ after receiving help signals from T_{FH} in the physically separated LZ. The significance of AP4-dependent GC expansion was highlighted by the finding that mice lacking AP4 in B cells failed to generate high quality antibody response that helps resolve chronic viral infection. Mechanistically, AP4 maintains the transcription of activation signature genes induced by c-MYC, thereby sustaining proliferation and activation of lymphocytes.

1.6 REFERENCES

1. Cooper, M.D. & Alder, M.N. The evolution of adaptive immune systems. *Cell* **124**, 815-822 (2006).
2. Jenkins, M.K. & Moon, J.J. The role of naive T cell precursor frequency and recruitment in dictating immune response magnitude. *J Immunol* **188**, 4135-4140 (2012).
3. van Heijst, J.W. *et al.* Recruitment of antigen-specific CD8+ T cells in response to infection is markedly efficient. *Science* **325**, 1265-1269 (2009).
4. Corse, E., Gottschalk, R.A. & Allison, J.P. Strength of TCR-peptide/MHC interactions and in vivo T cell responses. *J Immunol* **186**, 5039-5045 (2011).
5. Tscharke, D.C., Croft, N.P., Doherty, P.C. & La Gruta, N.L. Sizing up the key determinants of the CD8(+) T cell response. *Nat Rev Immunol* **15**, 705-716 (2015).
6. Zehn, D., Lee, S.Y. & Bevan, M.J. Complete but curtailed T-cell response to very low-affinity antigen. *Nature* **458**, 211-214 (2009).
7. King, C.G. *et al.* T cell affinity regulates asymmetric division, effector cell differentiation, and tissue pathology. *Immunity* **37**, 709-720 (2012).
8. Marchingo, J.M. *et al.* T cell signaling. Antigen affinity, costimulation, and cytokine inputs sum linearly to amplify T cell expansion. *Science* **346**, 1123-1127 (2014).
9. Gitlin, A.D. *et al.* HUMORAL IMMUNITY. T cell help controls the speed of the cell cycle in germinal center B cells. *Science* **349**, 643-646 (2015).
10. Gitlin, A.D., Shulman, Z. & Nussenzweig, M.C. Clonal selection in the germinal centre by regulated proliferation and hypermutation. *Nature* **509**, 637-640 (2014).

11. Victora, G.D. *et al.* Germinal center dynamics revealed by multiphoton microscopy with a photoactivatable fluorescent reporter. *Cell* **143**, 592-605 (2010).

12. Enouz, S., Carrie, L., Merkler, D., Bevan, M.J. & Zehn, D. Autoreactive T cells bypass negative selection and respond to self-antigen stimulation during infection. *J Exp Med* **209**, 1769-1779 (2012).

13. Zhang, N. & Bevan, M.J. CD8(+) T cells: foot soldiers of the immune system. *Immunity* **35**, 161-168 (2011).

14. Badovinac, V.P., Haring, J.S. & Harty, J.T. Initial T cell receptor transgenic cell precursor frequency dictates critical aspects of the CD8(+) T cell response to infection. *Immunity* **26**, 827-841 (2007).

15. MacIver, N.J., Michalek, R.D. & Rathmell, J.C. Metabolic regulation of T lymphocytes. *Annual review of immunology* **31**, 259-283 (2013).

16. Vander Heiden, M.G., Cantley, L.C. & Thompson, C.B. Understanding the Warburg effect: the metabolic requirements of cell proliferation. *Science* **324**, 1029-1033 (2009).

17. Wang, R. & Green, D.R. Metabolic checkpoints in activated T cells. *Nat Immunol* **13**, 907-915 (2012).

18. Finlay, D.K. *et al.* PDK1 regulation of mTOR and hypoxia-inducible factor 1 integrate metabolism and migration of CD8+ T cells. *The Journal of experimental medicine* **209**, 2441-2453 (2012).

19. Wang, R. *et al.* The transcription factor Myc controls metabolic reprogramming upon T lymphocyte activation. *Immunity* **35**, 871-882 (2011).

20. Doedens, A.L. *et al.* Hypoxia-inducible factors enhance the effector responses of CD8(+) T cells to persistent antigen. *Nat Immunol* **14**, 1173-1182 (2013).

21. Blair, D.A. *et al.* Duration of antigen availability influences the expansion and memory differentiation of T cells. *J Immunol* **187**, 2310-2321 (2011).

22. Prlic, M., Hernandez-Hoyos, G. & Bevan, M.J. Duration of the initial TCR stimulus controls the magnitude but not functionality of the CD8+ T cell response. *The Journal of experimental medicine* **203**, 2135-2143 (2006).

23. Mescher, M.F. *et al.* Signals required for programming effector and memory development by CD8(+) T cells. *Immunol Rev* **211**, 81-92 (2006).

24. Kalia, V. *et al.* Prolonged interleukin-2Ralpha expression on virus-specific CD8+ T cells favors terminal-effector differentiation in vivo. *Immunity* **32**, 91-103 (2010).

25. Pipkin, M.E. *et al.* Interleukin-2 and inflammation induce distinct transcriptional programs that promote the differentiation of effector cytolytic T cells. *Immunity* **32**, 79-90 (2010).

26. Joshi, N.S. *et al.* Inflammation directs memory precursor and short-lived effector CD8(+) T cell fates via the graded expression of T-bet transcription factor. *Immunity* **27**, 281-295 (2007).

27. Kwon, H. *et al.* Analysis of Interleukin-21-Induced Prdm1 Gene Regulation Reveals Functional Cooperation of STAT3 and IRF4 Transcription Factors. *Immunity* **31**, 941-952 (2009).

28. Kallies, A., Xin, A., Belz, G.T. & Nutt, S.L. Blimp-1 Transcription Factor Is Required for the Differentiation of Effector CD8(+) T Cells and Memory Responses. *Immunity* **31**, 283-295 (2009).

29. Rutishauser, R.L. *et al.* Transcriptional Repressor Blimp-1 Promotes CD8(+) T Cell Terminal Differentiation and Represses the Acquisition of Central Memory T Cell Properties. *Immunity* **31**, 296-308 (2009).

30. Kaech, S.M. & Cui, W. Transcriptional control of effector and memory CD8+ T cell differentiation. *Nat Rev Immunol* **12**, 749-761 (2012).

31. Sarkar, S. *et al.* Functional and genomic profiling of effector CD8 T cell subsets with distinct memory fates. *Journal of Experimental Medicine* **205**, 625-640 (2008).

32. Schluns, K.S. & Lefrancois, L. Cytokine control of memory T-cell development and survival. *Nat Rev Immunol* **3**, 269-279 (2003).

33. Tan, J.T. *et al.* Interleukin (IL)-15 and IL-7 jointly regulate homeostatic proliferation of memory phenotype CD8+ cells but are not required for memory phenotype CD4+ cells. *J Exp Med* **195**, 1523-1532 (2002).

34. Banerjee, A. *et al.* Cutting Edge: The Transcription Factor Eomesodermin Enables CD8(+) T Cells To Compete for the Memory Cell Niche. *J Immunol* **185**, 4988-4992 (2010).

35. Ichii, H. *et al.* Role for Bcl-6 in the generation and maintenance of memory CD8+ T cells. *Nat Immunol* **3**, 558-563 (2002).

36. De Silva, N.S. & Klein, U. Dynamics of B cells in germinal centres. *Nat Rev Immunol* **15**, 137-148 (2015).

37. Victora, G.D. & Nussenzweig, M.C. Germinal centers. *Annual review of immunology* **30**, 429-457 (2012).

38. MacLennan, I.C. Germinal centers. *Annual review of immunology* **12**, 117-139 (1994).

39. Jacob, J., Kelsoe, G., Rajewsky, K. & Weiss, U. Intraclonal generation of antibody mutants in germinal centres. *Nature* **354**, 389-392 (1991).

40. Berek, C., Berger, A. & Apel, M. Maturation of the immune response in germinal centers. *Cell* **67**, 1121-1129 (1991).

41. Han, S. *et al.* Cellular interaction in germinal centers. Roles of CD40 ligand and B7-2 in established germinal centers. *J Immunol* **155**, 556-567 (1995).

42. Shulman, Z. *et al.* Dynamic signaling by T follicular helper cells during germinal center B cell selection. *Science* **345**, 1058-1062 (2014).

43. Zotos, D. *et al.* IL-21 regulates germinal center B cell differentiation and proliferation through a B cell-intrinsic mechanism. *J Exp Med* **207**, 365-378 (2010).

44. Linterman, M.A. *et al.* IL-21 acts directly on B cells to regulate Bcl-6 expression and germinal center responses. *J Exp Med* **207**, 353-363 (2010).

45. Calado, D.P. *et al.* The cell-cycle regulator c-Myc is essential for the formation and maintenance of germinal centers. *Nat Immunol* **13**, 1092-1100 (2012).

46. Dominguez-Sola, D. *et al.* The proto-oncogene MYC is required for selection in the germinal center and cyclic reentry. *Nat Immunol* **13**, 1083-1091 (2012).

47. Hu, Y.F., Luscher, B., Admon, A., Mermod, N. & Tjian, R. Transcription factor AP-4 contains multiple dimerization domains that regulate dimer specificity. *Genes Dev* **4**, 1741-1752 (1990).

48. Jones, S. An overview of the basic helix-loop-helix proteins. *Genome Biol* **5** (2004).

49. Mermod, N., Williams, T.J. & Tjian, R. Enhancer binding factors AP-4 and AP-1 act in concert to activate SV40 late transcription in vitro. *Nature* **332**, 557-561 (1988).

50. Egawa, T. & Littman, D.R. Transcription factor AP4 modulates reversible and epigenetic silencing of the Cd4 gene. *Proc Natl Acad Sci U S A* **108**, 14873-14878 (2011).

51. Jung, P., Menssen, A., Mayr, D. & Hermeking, H. AP4 encodes a c-MYC-inducible repressor of p21. *Proceedings of the National Academy of Sciences of the United States of America* **105**, 15046-15051 (2008).

52. Jackstadt, R. *et al.* AP4 is a mediator of epithelial-mesenchymal transition and metastasis in colorectal cancer. *J Exp Med* **210**, 1331-1350 (2013).

53. Kurachi, M. *et al.* The transcription factor BATF operates as an essential differentiation checkpoint in early effector CD8(+) T cells. *Nature Immunology* **15**, 373-+ (2014).

54. Yao, S. *et al.* Interferon regulatory factor 4 sustains CD8(+) T cell expansion and effector differentiation. *Immunity* **39**, 833-845 (2013).

55. Wang, R. & Green, D.R. Metabolic checkpoints in activated T cells. *Nature immunology* **13**, 907-915 (2012).

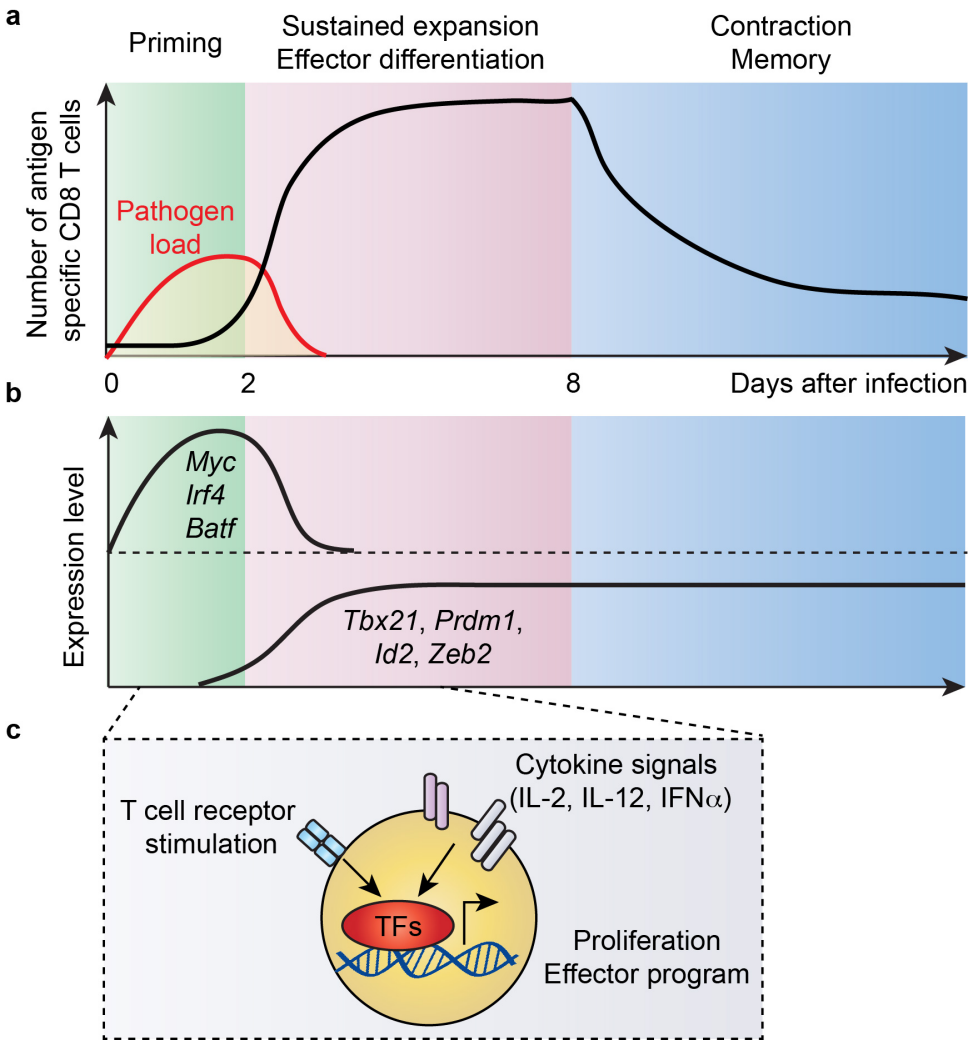

Figure 1.1. Sequential activation of transcription factors programs effector CD8 T cell responses. a, A schematic diagram showing expansion kinetics of antigen-specific CD8 T cells and kinetics of pathogen clearance during acute infection. Priming of CD8 T cells in the early phase of infection initiates sustained clonal expansion and effector differentiation over a course of week, followed by massive contraction, leaving behind a population of memory cells. During acute responses, pathogen is eradicated in the lymphoid organ by days 4 to 5 after infection, before the peak of CD8 T cell number on day 7. **b**, Stage-specific activation of distinct transcription factors. *Myc*, *Irf4*, and *Batf* are induced early after priming and regulate initial expansion of CD8 T cells. *Tbx21*, *Prdm1*, *Id2*, and *Zeb2* upregulation is delayed, but essential for proper differentiation into effector cells. **c**, Distinct environmental cues program CD8 T cell response by inducing transcription factors.

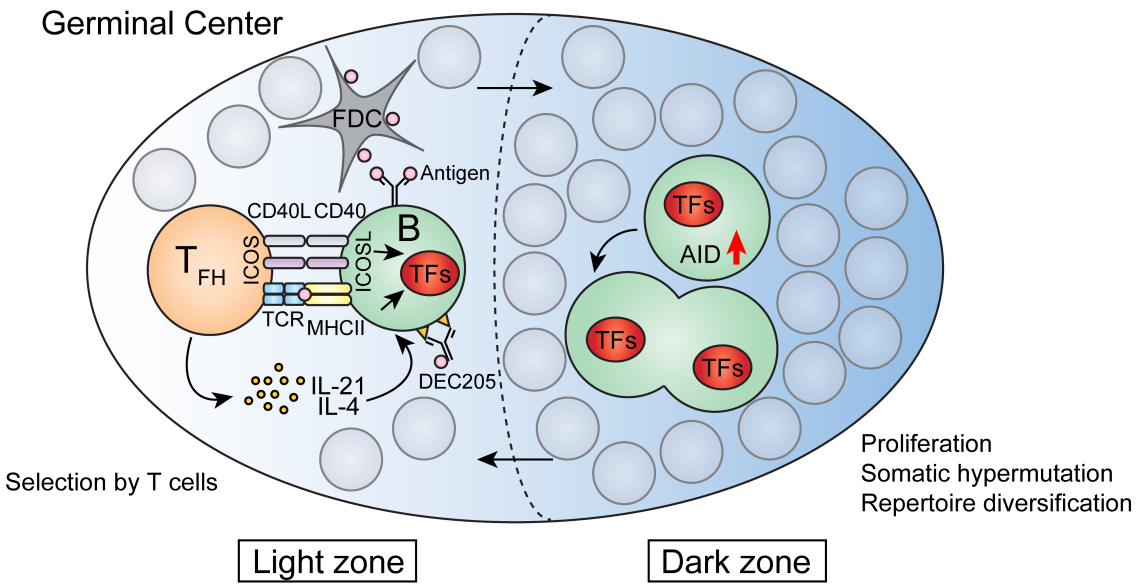

Figure 1.2. Transient interaction with T cells in the LZ potentiates expansion of selected GC B cells in the DZ. A schematic diagram showing spatial separation of selection events and proliferation of selected cells in the germinal center (GC). In the light zone (LZ), GC B cells capture antigen, internalize, and present to cognate follicular helper T cells (T_{FH}) and receive help signals through CD40 ligation and cytokine receptors. Selected GC B cells migrate to the dark zone (DZ) and undergo rounds of proliferation as well as somatic hypermutation. Daughter cells re-enter the LZ to test their mutated B cell receptor for antigen capture. Enhanced antigen presentation by B cells through DEC205-mediated antigen delivery activates T cells to produced elevated level of cytokines. This in turn promotes B cells to increase proliferation in the DZ.

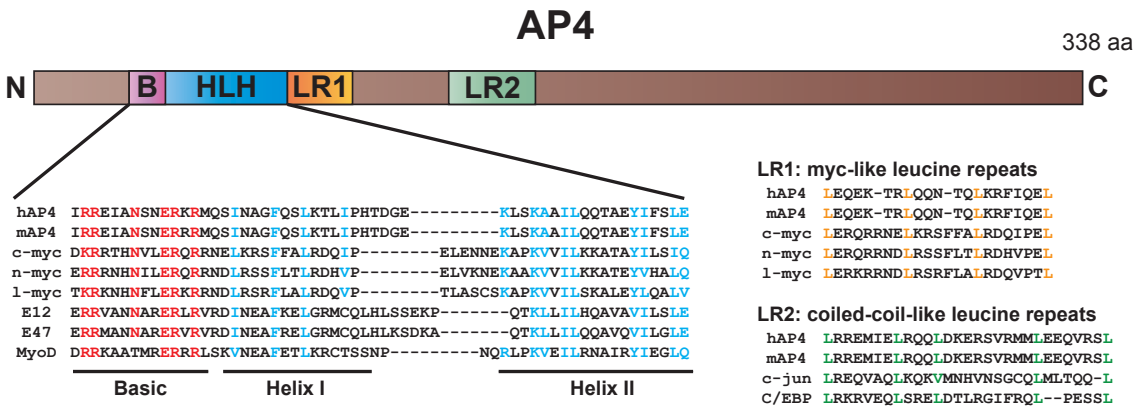

Figure 1.3. Domain structure of the AP4 protein. AP4 belongs to the basic helix-loop-helix (bHLH) transcription factor super family, sharing a domain homology with other bHLH family members. The bHLH region contains conserved basic amino acid residues (shown in red) and two helices that facilitate binding to DNA with the consensus motif, CAGCTG. Unlike most bHLH factors, AP4 also contains two additional leucine rich (LR) domains that are required for homodimerization. The C-terminal poly-glutamine domain is hypothesized to have transactivation function, but this remains to be tested.

CHAPTER 2:

c-Myc-induced transcription factor AP4 is required for host protection mediated by $CD8^+$ T cells.

The contents of this chapter have been previously published in *Nature Immunology*.

Chou C, Pinto AK, Curtis JD, Persaud SP, Cella M, Lin CC, Edelson BT, Allen PM, Colonna M, Pearce EL, Diamond MS, Egawa T. c-Myc-induced transcription factor AP4 is required for host protection mediated by $CD8^+$ T cells. *Nat Immunol*. 2014 Sep;15(9):884-93

2.1 ABSTRACT

Although cMyc is an essential transcription factor that establishes a metabolically active and proliferative state in T cells after antigen priming, its expression is transient. To date, it remains unknown how T cell activation is maintained after cMyc down-regulation. Here, we identify AP4, encoded by the gene *Tfap4*, as the transcription factor that is induced by cMyc and sustains activation of antigen-specific $CD8^+$ T cells. Despite normal priming, *Tfap4*$^{-/-}$ $CD8^+$ T cells fail to continue transcription of a broad range of cMyc-dependent targets necessary for sustained proliferation. Mice lacking AP4 specifically in $CD8^+$ T cells showed enhanced susceptibility to West Nile virus infection. Genome-wide analysis suggests that many activation-induced metabolic genes are shared targets of cMyc and AP4. Thus, AP4 maintains cMyc-initiated cellular activation programs in $CD8^+$ T cells to control microbial infections.

2.2 INTRODUCTION

Protective immunity by $CD8^+$ T cells is critical for host defense against many pathogens that cause death or chronic infection. During an acute infection by a virus or intracellular bacterium, antigen (Ag)-specific $CD8^+$ T cells are primed by signals through the T cell receptor (TCR), co-stimulatory molecules and cytokine receptors and undergo rapid expansion, effector differentiation, and memory cell formation[1, 2]. In the priming phase, activated $CD8^+$ T cells grow in size by increasing global gene transcription and protein translation, and enter the cell cycle[3]. Activated T cells utilize aerobic glycolysis pathways to produce the energy and materials for biosynthesis that enables rapid cell division and enhanced cytokine expression[4, 5, 6, 7]. Previous studies established that the transcription factor cMyc is essential for the initiation of global cellular activation in activated lymphocytes, as well as other rapidly proliferating cells, including cancers and embryonic stem cells[8, 9, 10, 11]. cMyc is induced by signals through the TCR and IL-2 receptor (IL-2R)[12] and is essential for activation of glycolysis and other metabolic programs. cMyc-deficient T cells fail to increase their size and glycolytic activities upon activation[13].

During acute infection, $CD8^+$ T cell expansion persists even after levels of Ag and inflammation wane[3]. While this persistent proliferation may be driven by residual Ag on Ag-presenting cells (APCs), other evidence suggests that $CD8^+$ T cells, once optimally primed, continue to proliferate after levels of Ag and cytokines diminish to sub-optimal concentrations or in the absence of Ag *in vitro* and *in vivo*[14, 15, 16, 17]. Expression of cMyc is rapidly induced in activated T cells[9, 13]. Its expression, however, is transient and does not persist throughout the duration of T cell expansion[9, 18]. These findings suggest that other transcription factors maintain cMyc-initiated global cellular activation to maximize clonal expansion and effector differentiation of T cells during acute responses to pathogen infection.

We hypothesized that TCR and cytokine receptor signals during the early stage of pathogen infection induce transcription factors, which program $CD8^+$ T cells for a durable response. Among the multiple cytokines established as important for $CD8^+$ T cell immune responses, IL-2 sustains clonal expansion *in vitro* and possibly, *in vivo*[19, 20, 21] as well as differentiation into effector cells[20, 22, 23]. In this study, we identified AP4 as a transcription factor regulated by TCR and IL-2R signals and demonstrated that AP4 sustains proliferation of Ag-specific $CD8^+$ T cells in a cell-autonomous manner in acute infection models *in vivo*. Whereas $CD8^+$ T cells lacking AP4 were primed normally and initiated rapid proliferation, they failed to sustain clonal expansion compared to control wild-type (WT) cells, leading to a substantial reduction in clonal frequency at the peak of response. Although AP4 was dispensable for clearance of pathogens in the spleen, mice lacking AP4 specifically in $CD8^+$ T cells failed to control infection of West Nile virus (WNV) in the central nervous system, which requires sustained antigen-specific $CD8^+$ T cell effector responses for hos*t*-mediated clearance and survival. Finally, our data suggest that AP4 is necessary to sustain global cellular activity, including transcriptome amplification and aerobic glycolysis initiated by cMyc, through regulation of a substantial proportion of cMyc target genes. Thus, our data establish that AP4 regulates the magnitude of acute $CD8^+$ T cell responses to control microbial infection.

2.3 RESULTS

Regulation of AP4 by signaling via the TCR and IL-2R

Using microarray analysis, we identified ~70 transcription factors whose expression changed by greater than 1.8-fold in $CD8^+$ T cells following neutralization of IL-2 (**Fig. 1a**). In addition to previously known IL-2-regulated genes, including *Bcl6* and *Eomes*[23], we identified *Tfap4*, which encodes AP4, as a gene that required IL-2 receptor (IL-2R) signaling for sustained expression. AP4 is a basic helix-loop-helix protein that regulates viral gene transcription and *Cd4* gene repression in immature thymocytes and $CD8^+$ T cells[24, 25, 26]. Although AP4 mRNA expression was reduced only modestly (2-fold, $P < 0.05$) upon withdrawal of IL-2 (**Fig. 1b**), its protein expression was substantially diminished (**Fig. 1c**), suggesting that signals through IL-2R are required for sustained AP4 expression at both transcriptional and post-transcriptional levels. As retrovirus-driven AP4 expression also required continuous IL-2R stimulation (**Fig. 1d**), AP4 protein expression appears regulated predominantly at the post-transcriptional level. The half-life of AP4 protein was two to three hours under permissive (+IL-2) or non-permissive (+ anti-IL-2 neutralizing mAb) conditions (**Fig. 1e**), with its degradation mediated by the ubiquitin-proteasome pathway (**Fig. 1f**). AP4 protein expression was sustained by TCR stimuli or other gamma chain cytokines (IL-7 and IL-15) but not by IL-12 or type I interferons (**Fig. 2a,b**). These results suggest that a common pathway converging from TCR and IL-2Rγ chain signaling sustains AP4 protein expression. To test this hypothesis, we treated $CD8^+$ T cells with small molecule inhibitors of relevant signaling pathways in the presence of TCR or IL-2R signals. Both MEK and p38 MAPK inhibitors U0126 and SB203580, respectively, attenuated the accumulation of AP4 protein in the presence of TCR or IL-2R stimulation (**Fig. 2c**). To validate the roles of TCR and IL-2R in sustained AP4 expression *in vivo,* we examined AP4 levels in Ag-

specific $CD8^+$ T cells during acute infection with the Armstrong strain of lymphocytic choriomeningitis virus (LCMV-Arm) (**Fig. 3a**). AP4 protein was expressed highly in $CD8^+$ T cells on days 4 and 5 after infection and the level declined substantially as T cell clonal expansion slowed on day 6. By day 7 after infection, AP4 protein expression was abolished and correspondingly, Ag-specific T cells showed markedly reduced proliferation. In activated $CD8^+$ T cells on day 4.5 after LCMV-Arm infection, AP4 protein was detected specifically in $CD25^+$ cells, which receive TCR and/or IL-2R stimulation, but not in $CD25^-$ cells, despite similar mRNA levels in both subpopulations (**Fig. 3b**). Furthermore, Ag-specific $CD8^+$ T cells lacking CD25/IL-2Rγ expressed reduced, yet still substantial, amounts of AP4 protein four days after LCMV-Arm infection (**Fig. 3c**). We conclude that AP4 is regulated post-transcriptionally in $CD8^+$ T cells during their response to pathogens via signaling through TCR and IL-2R *in vitro* and *in vivo*.

$CD8^+$ T cell population expansion requires AP4

To assess the function of AP4 in immune responses, we infected *Tfap4*$^{-/-}$ (ref. [24]) and congenic wild-type (WT) C57BL/6 mice with LCMV-Arm and examined expansion and differentiation of $CD8^+$ T cells. At the peak of acute response in *Tfap4*$^{-/-}$ mice, the total number of $CD8^+$ T cells was reduced by ~3-fold ($P < 0.0001$), and the number of $KLRG1^+$ terminally differentiated $CD8^+$ T cells[1] was reduced by 8-fold ($P < 0.0001$) compared to WT mice (**Fig. 4a,c**). T cells specific for the LCMV GP33 epitope also were decreased by 5-fold ($P < 0.0001$) and, among them, $KLRG1^+$ terminal effector cells were diminished by 8-fold ($P < 0.0001$) in *Tfap4*$^{-/-}$ compared to WT mice (**Fig. 4b,d**). To determine whether the requirement for AP4 is $CD8^+$ T cell-intrinsic, we deleted a loxP-flanked conditional *Tfap4* allele specifically in $CD8^+$ T

cells using a CD8-Cre transgenic deleter[27] (**Fig. 5**); in these mice, AP4 deletion occurs after thymic selection because a Cre transgene is expressed under the control of a *Cd8a* enhancer activated only after thymic selection. We observed a similar reduction in numbers of polyclonal and GP33-specific $CD8^+$ T cells and $KLRG1^+$ $CD8^+$ T cells in *Tfap4*$^{-/-}$ and CD8-Cre^+ *Tfap4*$^{F/F}$ mice (**Fig. 6**). These results indicate that the requirement for AP4 is $CD8^+$ T cell-intrinsic and that diminished clonal expansion of *Tfap4*$^{-/-}$ $CD8^+$ T cells is not due to developmental defects in the thymus. $CD8^+$ T cell clonal expansion and effector differentiation also were reduced in *Tfap4*$^{-/-}$ mice infected with the intracellular bacterium *Listeria monocytogenes* expressing ovalbumin (Lm-Ova) (**Fig. 7**). Memory cells were generated and maintained comparably between *Tfap4*$^{-/-}$ and WT mice following acute infection with LCMV-Arm or Lm-Ova. Numbers of GP33-specific $CD8^+$ T cells in the spleen were comparable between *Tfap4*$^{-/-}$ and control WT mice (**Fig. 8a,b)**, and frequencies of GP33-specific memory $CD8^+$ T cells in peripheral blood also were similar in *Tfap4*$^{-/-}$, CD8-Cre^+ *Tfap4*$^{F/F}$ and control WT mice 60 days after LCMV-Arm infection (**Fig. 8c).** Frequencies of Ova-specific $CD8^+$ T cells in the spleen also were comparable between *Tfap4*$^{-/-}$ and control WT mice 45 days after Lm-Ova infection (**Fig. 8d)**. However, *Tfap4*$^{-/-}$ memory T cells failed to expand efficiently upon secondary challenge (**Fig. 9**). The numbers of Ag-specific $CD8^+$ T cells in the spleen after re-infection with LCMV-Arm or Lm-Ova were reduced by 4-fold and 8-fold, respectively. Thus, AP4 is essential for expansion of Ag-specific $CD8^+$ T cells both in primary and recall responses.

AP4 sustains $CD8^+$ T cell clonal expansion

To compare expansion of *Tfap4*$^{-/-}$ and WT $CD8^+$ T cells in an identical environment, we generated *Tfap4*$^{-/-}$ mice expressing a $V_\alpha2^+$ $V_\beta8^+$ TCR transgene specific for LCMV GP33 (P14)

(ref. [28]). A 1:1 mixture of $V_{\alpha}2^{+}$ $V_{\beta}8^{+}$ naive $CD8^{+}$ T cells from *Tfap4*$^{-/-}$ (Thy1.2/CD45.2) and WT (Thy1.1/CD45.2) P14 TCR transgenic mice was adoptively transferred to congenic host CD45.1 mice. Prior to infection with LCMV-Arm, the ratio of *Tfap4*$^{-/-}$ to WT P14 T cells was approximately 1:1 in the spleen (**Fig. 10a**). This result is consistent with comparable frequencies of $CD8^{+}$ T cells in various tissues in *Tfap4*$^{-/-}$ mice under steady state conditions compared to control WT mice (**Fig. 10b**), and indicates that AP4 is dispensable for survival of $CD8^{+}$ T cells and their homing to the spleen and peripheral tissues. To determine whether AP4 was required for priming and initial proliferation of P14 T cells, we labeled donor P14 T cells with carboxyfluorescein succinimidyl ester (CFSE) prior to adoptive transfer. On day 3 after LCMV-Arm infection, both *Tfap4*$^{-/-}$ and WT P14 T cells diluted CFSE to undetectable levels (**Fig. 10c**), which was consistent with the comparable numbers of P14 T cells recovered from the spleen and the frequencies of bromodeoxyuridine $(BrdU)^{+}$ cells following a pulse labeling (**Fig. 10d-g**). These results establish that AP4 is not required for priming and initial proliferation of $CD8^{+}$ T cells during the acute Ag-specific response. Despite the rapid early expansion, the absolute number of *Tfap4*$^{-/-}$ donor cells was substantially reduced compared to WT donor cells at the peak of the response after LCMV-Arm infection ($P < 0.0001$ on day 7, **Fig. 10d-f**). Control P14 T cells continued to expand until day 7 post-infection (**Fig. 10d**). While *Tfap4*$^{-/-}$ cells continued to proliferate until day 7 post-infection, they failed to maintain rapid proliferation rates, as judged by frequencies of BrdU-labeled cells on day 4 and later (**Fig. 10g**). Because $CD8^{+}$ T cells divide as many as 6-7 times per day during a response to acute infection[29], the effect of mild but continued reduction in BrdU incorporation rates could result in a greater than 10-fold reduction in clonal expansion of *Tfap4*$^{-/-}$ donors compared to control WT cells over 4 days (**Fig. 10e,g**). We also observed reduced clonal expansion, BrdU incorporation, and activation of the mTOR

pathway of *Tfap4*$^{-/-}$ OT-I T cells following Lm-Ova infection (**Fig. 11a-c**). We did not, however, observe changes in the frequency of Annexin V^{+} cells between *Tfap4*$^{-/-}$ and WT P14 T cells on day 6 after LCMV-Arm infection (**Fig. 11d,e**). Moreover, ratios between *Tfap4*$^{-/-}$ and WT P14 T cells were similar in the spleen, peripheral blood, mesenteric lymph nodes, lung, liver and kidney 7 days after LCMV-Arm infection (**Fig. 11f**), suggesting no substantial difference in trafficking of Ag-specific T cells during the acute response to LCMV infection. Furthermore, *Tfap4*$^{-/-}$ OT-I T cells proliferated at similar rates with co-cultured WT OT-I T cells when they were stimulated with various concentrations of Ova peptide for 3 days (**Fig. 12a**). However, *Tfap4*$^{-/-}$ cells were outcompeted in numbers by co-cultured WT cells and failed to blast when kept for a longer duration with low concentration of peptide (**Fig. 12a,b**). Because the induction of IFN-γ expression by *Tfap4*$^{-/-}$ and WT OT-I T cells in response to Ag was comparable (**Fig. 12c**), it is unlikely that AP4 regulates TCR sensitivity *per se*. These results suggest that AP4 is required for sustained T cell proliferation after TCR stimulation.

Protection against infection with WNV requires AP4

We next tested the contribution of AP4 to CD8^{+} T cell-mediated protection against a lethal viral infection. For this purpose, we utilized the mouse model of WNV infection. WNV is a virulent zoonotic RNA virus that causes fatal encephalitis in humans and many strains of inbred mice[30, 31]. CD8^{+} T cells are required for clearance of the virus in both the peripheral and central nervous system (CNS) tissue compartments[32]. To determine whether AP4 was required for protection against WNV infection in a CD8^{+} T cell-dependent manner, we infected CD8-Cre^{+} *Tfap4*$^{F/F}$ mice and age-matched control Cre^{-} *Tfap4*$^{F/F}$ mice with WNV (New York 1999 strain). While the majority of control Cre^{-} *Tfap4*$^{F/F}$ mice survived as expected (compared to WT

C57BL/6 mice[33]), all CD8-Cre^{+} *Tfap4*$^{F/F}$ mice died from WNV between days 8 and 13 (**Fig. 13a,** $P < 0.0001$), which was similar to the lethality observed in *Cd8a*$^{-/-}$ or MHC class Iα$^{-/-}$ mice[32]. CD8-Cre^{+} *Tfap4*$^{F/F}$ mice sustained higher viral loads in the brain compared to control mice on day 9 post-infection (**Fig. 13b,** $P < 0.05$), indicating that AP4 expression in CD8^{+} T cells is essential for the control of WNV in the CNS. Consistent with our results with LCMV-Arm and Lm-Ova infection models, Ag-specific CD8^{+} T cell expansion was diminished in WNV-infected *Tfap4*$^{-/-}$ and CD8-cre^{+} *Tfap4*$^{F/F}$ mice compared to control WT mice in the spleen on day 7 after infection (**Fig. 14**). However, AP4 was dispensable for control of WNV infection in the spleen (**Fig. 13c**). Consistent with this observation, no differences in LCMV-Arm or Lm-Ova burden were detected in the spleen and peripheral tissues following acute infection (**Fig. 15**). These results indicate that AP4 is dispensable for control of LCMV-Arm and Lm-Ova in the peripheral tissues and WNV in the spleen presumably because clearance of these pathogens begins at an early phase of the acute response. In contrast, control of WNV in the CNS requires a more prolonged CD8^{+} T cell response. Thus, AP4-mediated sustained activation of Ag-specific CD8^{+} T cells may be critical for control of certain CNS pathogens. These results also establish that AP4 is required for host protection against WNV infection in the CNS in a CD8^{+} T cell-intrinsic manner.

AP4 sustains T cell activation

Upon priming, T cells expand in size prior to cell division and activate an aerobic glycolysis program[5, 34]. The transcription factor, cMyc, activates glycolysis and amplifies global gene transcription and protein synthesis in activated lymphocytes[9, 13]. cMyc mRNA and protein expression was induced rapidly after TCR stimulation, followed by AP4 mRNA up-regulation in

activated $CD8^+$ T cells (**Fig. 16a,b**). AP4 expression in activated $CD8^+$ T cells lacking *Myc* was absent at both protein and mRNA levels, indicating that cMyc is essential for AP4 up-regulation (**Fig. 16c,d**). In agreement with a prior study using human cancer cell lines[35], cMyc binds to the *Tfap4* locus in activated $CD8^+$ T cells (**Fig. 16e**), further suggesting that AP4 expression is augmented by cMyc through direct binding in activated $CD8^+$ T cells. Given these results, we hypothesized that AP4 and cMyc might cooperate to regulate cell growth associated with T cell activation. In contrast to defective cell growth and metabolic changes in *Myc*-deficient T cells[13], activated *Tfap4*$^{-/-}$ $CD8^+$ T cells underwent normal blast development accompanied by active glycolysis *in vitro* (**Fig. 17a-c**). Moreover, *Tfap4*$^{-/-}$ and WT Ag-specific T cells were of comparable size three days after LCMV-Arm or Lm-Ova infection *in vivo* (**Fig. 18a-c**). Differences in gene expression between *Tfap4*$^{-/-}$ and control WT $CD8^+$ T cells either 3 days after anti-CD3 and anti-CD28 antibody-mediated activation *in vitro* or 2 days after Lm-Ova infection *in vivo* were substantially smaller compared to that observed at later time points with few genes relevant to T cell activation or metabolisms altered in culture or at the early time point (**Fig. 18d**). These results suggest that AP4 is dispensable for establishment of the cMyc-dependent cellular response to T cell activation. However, at later time points (days 4 and 6), *Tfap4*$^{-/-}$ P14 or OT-I $CD8^+$ T cells were smaller in size than control cells (**Fig. 18a-c**). The size difference between *Tfap4*$^{-/-}$ and control cells coincided with cMyc down-regulation in Ag-specific $CD8^+$ T cells after Lm-Ova infection (**Fig. 19**). A small fraction of OT-I T cells primed by Lm-Ova infection *in vivo* started to up-regulate cMyc protein as determined using the Myc-GFP fusion protein knock-in allele[36]. Activated OT-I T cells uniformly expressed Myc-GFP as they expanded in size until day 3 *in vivo* (**Fig. 19a**). Although the activated OT-I cells continued to proliferate and only slowly reduced their size on day 4 post-infection, Myc-GFP was down-regulated approximately

by 14-fold compared to day 2 and 10-fold compared to day 3 (**Fig. 19**). In comparison, AP4 expression in WT cells also was up-regulated as the cMyc level increased after priming and then began to decline on day 3 (**Fig. 19a**). In contrast to the rapid decay of cMyc, AP4 protein expression was still detected on day 4 (**Fig. 19**). Although the methods used to quantitate cMyc and AP4 levels are not directly comparable, these results suggest that AP4 expression persists longer than cMyc. In addition to the cell size, total RNA content per cell also was reduced in *Tfap4*$^{-/-}$ OT-I T cells compared to WT cells on day 4 (**Fig. 20a,** $P < 0.05$). Furthermore, basal aerobic glycolysis and the maximum glycolytic capacity in the presence of oligomycin, as measured by extracellular acidification rates (ECAR)[37] were significantly reduced in *Tfap4*$^{-/-}$ OT-I cells compared to WT cells recovered from the same recipient mice infected with Lm-Ova on days 4 and 6 after infection (**Fig. 20b**, $P < 0.0001$). Consistent with the metabolic measurements, expression of key glycolytic enzymes normalized to a per cell basis by using spiked-in control RNA[38] was reduced (1.5 to 2.2-fold, $P < 0.05$) in *Tfap4*$^{-/-}$ CD8^{+} T cells compared to WT cells on day 4 post-infection (**Fig. 20c**). The difference was enhanced on day 6 (4.0 to 5.2-fold, $P < 0.05$), indicating that AP4 is required for sustained expression of genes regulating the glycolytic activity (**Fig. 20c**). These results suggest that AP4 sustains T cell activation after cMyc down-regulation as reflected by glycolytic rates and cell sizes.

AP4 sustains c-Myc-initiated global cellular activity

To further define how AP4 is required for maintenance of the activation-induced global cellular activity established by early expression of cMyc, we analyzed gene expression programs of *in vivo*-activated *Tfap4*$^{-/-}$ and WT CD8^{+} T cells using microarray transcriptional profiling at the time point in which we detected cell size differences. For accurate assessment of gene

expression on a per cell basis, we spiked the cellular RNA with a mixture of control RNAs in proportion to the cell number prior to reverse transcription and then profiled cell number-normalized gene expression in *Tfap4*$^{-/-}$ and control WT OT-I T cells[9, 10]. Consistent with the smaller size and reduced RNA content of *Tfap4*$^{-/-}$ cells compared to control WT OT-I T cells, global gene expression in *Tfap4*$^{-/-}$ cells, as determined by the slopes of scatter plots, was reduced ($P < 0.01$) compared to control WT cells (**Fig. 21a,b**). We identified 1,784 genes that showed more than 1.8-fold difference between *Tfap4*$^{-/-}$ and WT OT-I cells 4 days after Lm-Ova infection. A pathway analysis highlighted an enrichment of the 1,784 genes in those related to metabolism, transcription and translation (**Fig. 21c**). To determine whether these differentially expressed genes were directly regulated by AP4, cMyc or both, we performed chromatin immunoprecipitation analysis (ChIP) using anti-AP4 and anti-cMyc antibodies and profiled AP4- and cMyc-bound genes in activated CD8$^+$ T cells that express both AP4 and cMyc (**Fig. 22**). Unbiased analysis of 7,000 peaks of AP4 and cMyc that were selected as statistically significant ($P < 1.5e-65$ for AP4 and $P < 5e-9$ for cMyc based on peak-calling in Homer[39]) remarkably revealed that more than 50% of AP4 and cMyc peaks overlapped at the gene level (**Fig. 23a**). While transcription factor binding does not necessarily establish biological significance, we further examined overlaps between the AP4-cMyc co-bound genes and the 1,784 differentially expressed genes. Among the 1,784 genes, nearly a quarter (479 genes) were bound by both AP4 and cMyc (**Fig. 6a**), AP4-cMyc co-bound genes were highly enriched in those annotated in pathways related to metabolism, general transcription and translation (**Fig. 21c marked in red and Fig. 22e**). Furthermore, the majority of these 479 genes were up-regulated on day 2 after Lm-Ova infection in WT OT-I cells that express both cMyc and AP4, remained highly expressed on day 4 when cMyc levels waned, and were eventually down-regulated on day 6 following the

decline of AP4, suggesting that AP4 regulated these shared cMyc-AP4 target genes as expression of cMyc decayed (**Fig. 23b**). Because expression of these 479 genes was not different between *Tfap4*$^{-/-}$ and WT OT-I T cells on day 2 post-infection (**Fig. 18d**), the altered expression of these genes on day 4 may explain the phenotypes observed in the *Tfap4*$^{-/-}$ CD8^{+} T cells. Since the ChIP-seq analysis was performed using cells which co-expressed AP4 and cMyc, it remained unknown whether AP4 still bound to these loci after cMyc down-regulation in Ag-specific CD8^{+} T cells in response to acute infection. Therefore, we purified CD25^{+} P14 T cells 5 days after LCMV-Arm infection and examined AP4 binding by ChIP assays. As expected, cMyc was down-regulated on day 5 after LCMV-Arm infection compared to earlier time points (**Fig. 23c**). Even after the cMyc decay, the majority of previously identified AP4-c-Myc-bound loci retained AP4 binding, as assessed by anti-AP4 ChIP (**Fig. 23d**). These results suggest that cMyc-induced AP4 expression is required for sustained transcription of genes associated with CD8^{+} T cell activation and clonal expansion, including metabolism, general transcription and translation pathways through direct binding, after cMyc is down-regulated.

AP4 supplements c-Myc function

Our data thus far suggest that AP4 and cMyc have overlapping functions in activated in CD8^{+} T cells. To determine whether AP4 is dispensable if cMyc expression is sustained, we retrovirally expressed a stabilized form of cMyc (Myc^{T58A} mutant[40, 41]) in *Tfap4*$^{-/-}$ CD8^{+} T cells in our *in vitro* culture system that recapitulates the cell size difference between *Tfap4*$^{-/-}$ and WT cells (**Fig. 24a**). In this assay, we optimally primed *Tfap4*$^{-/-}$ and WT OT-I cells with anti-CD3 and anti-CD28 antibodies for two days and transferred the activated OT-I cells to a culture of irradiated splenocytes pulsed with a low concentration of OVA peptide for 24 h. Ectopic

expression of Myc^{T58A} or AP4 itself in *Tfap4*$^{-/-}$ $CD8^+$ T cells rescued the cell size defects under conditions of threshold Ag stimulation (**Fig. 24b,c**). In addition to cell size, Myc^{T58A} or AP4 restored glycolysis, BrdU incorporation, and expression of a subset of cMyc-AP4-cobound genes that were down-regulated in *Tfap4*$^{-/-}$ $CD8^+$ T cells on day 4 post Lm-Ova infection *in vivo* (**Fig. 24d-f**). To determine whether Myc^{T58A} expression restored clonal expansion of *Tfap4*$^{-/-}$ $CD8^+$ T cells *in vivo*, we adoptively transferred cMyc- or AP4-transduced naive *Tfap4*$^{-/-}$ OT-I T cells and control WT OT-I T cells into congenic hosts that were subsequently infected with Lm-Ova. Although retroviral expression of AP4 in *Tfap4*$^{-/-}$ OT-I T cells fully restored clonal expansion and KLRG1 expression, Myc^{T58A} expression only partially restored clonal expansion (**Fig. 24g-i**). Nevertheless, Myc^{T58A} expression increased cell sizes and BrdU incorporation of *Tfap4*$^{-/-}$ OT-I cells comparably to AP4 ectopic expression (**Fig. 24j,k**). These results suggest that AP4 and cMyc have partially overlapping functions in regulating T cell activation and that a temporal switch from cMyc to AP4 is necessary for optimal $CD8^+$ T cell clonal expansion.

To determine whether ectopic expression of AP4 correspondingly rescues defective proliferation or cell growth of *Myc*-deficient cells, we retrovirally expressed AP4 in $CD8^+$ T cells in which cMyc was deleted by tamoxifen-inducible Cre recombinase fused to the estrogen receptor ligand binding domain ($CreER^{T2}$)[42]. To express AP4, we infected $CD8^+$ T cells from *ROSA26*-$CreER^{T2}$ *Myc*$^{F/F}$ and control Cre^- *Myc*$^{F/+}$ (*Myc*$^{+/+}$) or *ROSA26*-$CreER^{T2}$ *Myc*$^{+/+}$ mice with retrovirus following stimulation with anti-CD3 and anti-CD28 antibodies for 24 h. The activated T cells were treated with 4-hydroxytamoxifen (4OHT) under resting conditions for two days, and proliferation and gene expression of transduced cells were tested upon re-stimulation with anti-CD3 and anti-CD28 antibodies (**Fig. 25a**). We confirmed the absence of cMyc expression and ectopic expression of AP4 at the protein level before and after TCR re-

stimulation and at the mRNA level after re-stimulation (**Fig. 25b,c**). Retroviral cMyc expression rescued, albeit partially, proliferation and cell size increase of *Myc*$^{-/-}$ cells (**Fig. 25d**). The incomplete rescue by retroviral cMyc expression was probably caused by a delay in cMyc expression from the retrovirus immediately after TCR stimulation compared to that from the endogenous locus (**Fig. 25c**). In contrast, AP4 ectopic expression, which was detected already in cells prior to TCR stimulation (**Fig 25b**), failed to rescue proliferation or cell size increases of *Myc*$^{-/-}$ cells (**Fig. 25d**). Consistent with these results, gene expression profiling by microarray revealed little difference between AP4- and empty virus-transduced *Myc*$^{-/-}$ cells and partially rescued gene expression by cMyc transduction (**Fig. 25e**). These results indicate that AP4 requires prior expression of cMyc to mediate its effects. Thus, AP4 functionally supplements cMyc activity to prolong global cellular metabolism and maximize clonal expansion of CD8^{+} T cells.

2.4 DISCUSSION

Our study defines a critical role of AP4 in regulating clonal expansion and antiviral function of $CD8^+$ T cells *in vivo*. Our data indicate that AP4 regulates the maintenance phase but not the initiation of rapid clonal expansion after antigen priming. Although AP4 is rapidly induced after priming of T cells in a cMyc-dependent manner, it is not necessary for initial cell growth, induction of glycolytic activity and proliferation during the early phase of acute $CD8^+$ T cell responses presumably because cMyc is highly expressed during this phase. Ag-specific $CD8^+$ T cells rapidly proliferate and control LCMV-Arm or Lm-Ova infection in an AP4-independent manner as clearance of these microbes occurs rapidly and does not require full clonal expansion of Ag-specific $CD8^+$ T cell. This also is consistent with the normal thymocyte cellularity in *Tfap4*$^{-/-}$ mice[24], because cMyc is sufficient for preTCR-driven thymocyte proliferation in the late double-negative stage that is relatively short compared to Ag-specific $CD8^+$ T cell proliferation in acute responses. In contrast, AP4 expression in $CD8^+$ T cells is essential for protection against neurotropic WNV infection likely because control of WNV in the CNS requires sustained activity and proliferation of Ag-specific $CD8^+$ T cells. The increased susceptibility could be due to reduced clonal expansion leading to fewer cells reaching the tissue (quantitative defects) or to defective differentiation as effector cells (qualitative defects). Reduced clonal expansion could result from defective proliferation, increased cell death, or a migration defect. Our data suggest that AP4 is required predominantly for sustained rapid proliferation. Because $CD8^+$ T cells proliferate rapidly during their acute response to microbial infection over several days, even modest reductions in the rate of proliferation can translate into substantial reductions in the magnitude of clonal expansion. Because clearance of WNV in the spleen and that of LCMV-Arm or Lm-Ova in multiple peripheral tissues was comparable

between AP4-deficient and -sufficient mice, it is unlikely that the killing activity or trafficking is inherently compromised in the absence of AP4.

Mechanistically, there are two major possible interpretations of AP4 function in the regulation of acute $CD8^+$ T cell responses. One interpretation is that AP4 directly regulates genes that are essential for T cell activation. Identification of AP4 and $cMyc^-$bound genes in activated $CD8^+$ T cells revealed substantial overlap between targets of the two transcription factors. Combined analysis of binding targets and genes down-regulated in AP4-KO cells (1,784 genes) showed that approximately a quarter of these differentially expressed genes were shared binding targets of AP4 and cMyc. However, when we examined 85 genes out of 1,748 genes that were annotated in pathways for metabolism, general transcription and translation, AP4 and cMyc co-binding was further enriched (~75%). Although transcription factor binding to the genome can be promiscuous and does not always have biological significance, this considerable enrichment of AP4 and Myc co-targets in the set of genes relevant to T cell activation also supports the hypothesis that AP4 contributes to maintenance of expression of these genes. AP4 was dispensable for initial up-regulation of these genes upon T cell priming because these pathways already are activated by cMyc. In contrast, after cMyc down-regulation during the late phase of the acute response, the contribution of AP4 in the regulation of these genes may become critical for the maintenance of expression. AP4 binds to these loci not only in $CD8^+$ T cells activated *in vitro*, but also in $CD8^+$ T cells activated *in vivo* after cMyc expression wanes. With respect to cellular carbohydrate metabolism, the differentially expressed genes were enriched for enzymes but not transporters, suggesting the altered glucose utilization in *Tfap4*$^{-/-}$ $CD8^+$ T cells results from defective glycolysis rather than its uptake. In contrast, since many genes encoding enzymes for glutaminolysis, amino acid transport, and components of protein translation machinery were

down-regulated in *Tfap4*$^{-/-}$ CD8^{+} T cells, the smaller cell size likely reflects reduced protein synthesis from defects at multiple stages. Since expression of *Hif1a* and components of the mTOR pathway was not reduced, the diminished activity of the mTOR pathway may be regulated indirectly by AP4.

As an alternative explanation, AP4 might indirectly sustain activity of Ag-specific T cells through sensitizing T cell activation by TCR or cytokine receptor signals independent of cMyc. Sensitivity to extrinsic stimuli may not be critical for initial activation of CD8^{+} T cells *in vitro* or Ag-specific CD8^{+} T cells during the early phase of acute responses *in vivo* in the presence of abundant Ag or inflammatory cytokines. However, it may be essential in the late phase of the CD8^{+} T cell response *in vivo* due to declines in Ag and cytokine concentrations. Under these circumstances, *Tfap4*$^{-/-}$ cells might prematurely lose activation, which would secondarily cause reduced metabolic activity and clonal expansion. A previous study using *Listeria* expressing altered Ova peptide ligands demonstrated that duration and magnitude of acute CD8^{+} T cell responses *in vivo* are determined by affinity between TCR and peptide ligands[43]. Compared to Lm-Ova expressing the canonical SIINFEKL epitope, engineered strains expressing low affinity variant epitopes showed a reduced magnitude of clonal expansion of OT-I T cells at the peak despite normal initial activation and proliferation during the early phase of acute responses. Although these phenotypes are similar to those in *Tfap4*$^{-/-}$ mice, there are differences. Infection by pathogens expressing low affinity ligands shortens the duration of clonal expansion by triggering earlier contraction and also generates reduced numbers of memory cells after the clearance of the infection[43]. We observed neither of these phenotypes in *Tfap4*$^{-/-}$ mice after infection with Lm-Ova or LCMV-Arm.

Although we favor the former interpretation of AP4-dependent maintenance of cMyc targets, the two models are not mutually exclusive. Regardless, our results indicate that cMyc-induced AP4 expression is essential for maximal clonal expansion and sustained T cell activity in a temporally regulated manner. Another potential mechanism is the direct regulation of cell cycle by AP4. A study using colon cancer cell lines suggested that AP4 is regulated by cMyc and promotes cell cycle progression through direct binding to multiple CAGCTG motifs of the *CDKN1A* (p21 CIP1/WAF1) promoter[35]. While both AP4 and cMyc bind to the *Cdkn1a* locus, *Cdkn1a* mRNA expression was not different between *Tfap4*$^{-/-}$ and WT CD8^{+} T cells. Because our data indicate that AP4 is dispensable for cell cycle entry of activated T cells when cMyc is expressed, it is unlikely that reduced proliferation of *Tfap4*$^{-/-}$ CD8^{+} T cells is caused by derepression of *Cdkn1a*.

Although mechanisms by which cMyc induces expression of a large set of genes have not fully been elucidated, recent studies using activated lymphocytes, embryonic stem cells and highly proliferative cancer cells demonstrate that cMyc increases their transcription rates rather than simply turning-on and off target genes containing the consensus binding motif ("transcriptome amplification")[9, 10, 11]. Our data suggests that AP4 has similar functions. While both cMyc and AP4 peaks are highly enriched in promoter regions, only one-third of statistically significant cMyc binding peaks and 60% of AP4 peaks contain the canonical E-box consensus motif (CACGTG for cMyc and CAGCTG for AP4), respectively. These findings suggest that AP4 recruitment to target sites may be mediated through protein-protein interactions with transcriptional activator complexes for some target genes.

In conclusion, our study demonstrates that AP4 is a transcription factor that is critical for regulation of CD8^{+} T cell-mediated acute anti-pathogen responses by sustaining metabolic gene

expression in the post-Myc phase. Activated T cells utilize AP4 to maintain their activated states under conditions of threshold antigen or signaling for complete elimination of pathogens or clearance of pathogen-infected cells in non-lymphoid organs.

2.5 MATERIALS AND METHODS

Mice

Mice containing a loxP-flanked *Tfap4* allele were generated in 129P2/Ola-derived E14TG2a ES cells essentially as described (**Fig. 5a**)[24]. *Tfap4*$^{-/-}$ mice were described previously[24]. Both AP4 mutant strains were backcrossed to C57BL6 mice for more than 10 generations before intercrossing or breeding to other transgenic mice. *cMyc*-flox mice and cMyc-GFP fusion protein knock-in mice were described previously[36, 44]. C57BL6 and B6-Ly5.2 (CD45.1) mice were purchased from the National Cancer Institute. OT-I transgenic mice[45], *Tcra*$^{-/-}$ mice[46], *Il2ra*$^{-/-}$ mice[47], *ROSA26*-Cre^{ERT2} (ref. [48]) and B6-Thy1.1 were purchased from the Jackson Laboratory and P14 transgenic mice[28] were purchased from Taconic. *Il2ra*$^{-/-}$ P14 T cells were collected from mixed bone marrow chimeric mice reconstituted with a mixture of bone marrow cells from *Il2ra*$^{-/-}$ (Thy1.2) and WT (Thy1.1) P14 mice. CD8-Cre mice were generated previously in the C57BL6 background[27]. All mice were maintained in a specific pathogen free facility at Washington University in St. Louis, and all experiments were performed according to the protocol approved by Washington University's Animal Studies Committee.

Infection Experiments

LCMV-Arm stocks were prepared by infecting BHK cells and titering culture supernatants by plaque assay on Vero cells. Mice were infected with 2 x 10^5 plaque forming units (PFU) of LCMV-Arm by intraperitoneal injection. Lm-Ova was inoculated intravenously at a dose of 1 x 10^4 colony-forming units (CFU). Infection with WNV (New York 1999 strain) was performed as previously described[32]. For adoptive transfer experiments, CD44$^-$ CD62L$^+$ $V_\alpha2^+$ $V_\beta5^+$ OT-I or

$CD44^{-}$ $CD62L^{+}$ $V_{\alpha}2^{+}$ $V_{\beta}8^{+}$ P14 donor T cells were purified by fluorescence activated cell sorting, and 5 x 10^5 (for day 3 analysis), 1 to 2 x 10^4 (for day 4 analysis), or 1 to 3 x 10^4 (for days 5 to 12 analysis) cells were transferred intravenously to recipient mice one day before infection. All experiments using infectious agents were performed in biosafety level 2 and 3 facilities according to the protocols approved by Washington University Institutional Biological and Chemical Safety Committee.

Flow Cytometry

Single cell suspensions were prepared by disrupting spleens manually with frosted glass slides followed by erythrocyte lysis with ACK (Ammonium-Chloride-Potassium) solution, or by digesting mesenteric lymph nodes, liver, lung and kidney with collagenase B or D (Roche) followed by purification using Percoll gradient (GE Healthcare Life Sciences). For sorting of naive $CD8^{+}$ T cells, splenocytes were initially depleted of $B220^{+}$ cells using magnetic beads (Life Technologies) and then stained with monoclonal antibodies prior to sorting $CD62L^{+}$ $CD44^{-}$ $CD8^{+}$ $CD4^{-}$ cells using a FACS AriaII (BD Biosciences). For analysis, cells were stained with monoclonal antibodies, D^{b}-GP33 (Beckman Coulter), or K^{b}-OVA single chain tetramer and analyzed using a FACS LSRII (BD Biosciences) with DAPI staining to exclude dead cells. Data were analyzed using FlowJo software (Tree Star Inc.). All antibodies were purchased from Biolegend. For intracellular staining for AP4, cells were fixed with 2% paraformaldehyde (PFA) for 10 minutes, permeabilized with ice-cold 100% methanol for 30 minutes, and then stained for markers with fluorochrome-conjugated monoclonal antibodies and AP4 with affinity-purified anti-AP4 polyclonal antibody[24] at a concentration of 1.25 μg/ml and Alexa-647 conjugated anti-

rabbit IgG secondary antibody (Cell Signaling). For detection of phosphorylated S6 (p-S6) ribosomal protein, cells were fixed with PFA, permeabilized with methanol, and stained for surface markers and p-S6 with an anti-p-S6 antibody (Cell signaling #4858P) and Alexa-647 conjugated anti-rabbit IgG secondary antibody (Cell Signaling).

BrdU labeling

At different time points after infection mice were administered with 1 mg BrdU by i.p. injection two hours before euthanasia. BrdU incorporation was analyzed using an APC-BrdU Flow Kit (BD Biosciences) according to the manufacturer's instruction. For proliferation assays *in vitro*, cells were cultured in media containing 10 μM BrdU for 1 hour prior to analysis.

***In vitro* T cell stimulation**

Naive $CD8^+$ T cells were cultured in RPMI supplemented with 10% fetal bovine serum (Life Technologies) in the presence of soluble anti-CD3 (145-2C11, Biolegend) and anti-CD28 (37.51, Bio X Cell) at 0.1 μg/ml and 1 μg/ml, respectively, unless otherwise specified, in multi-well tissue culture plates coated with rabbit anti-hamster IgG (MP Biomedicals). For retroviral transduction of activated T cells, viral supernatants were prepared by transfecting PlatE cells[49] with TransIT 293 (Mirus Bio) and primed T cells were spinoculated following overnight stimulation as described previously[24]. To retrovirally transduce $CD8^+$ T cells without TCR stimulation, naive $CD8^+$ T cells were cultured in the presence of IL-7 (10 ng/ml, Peprotech) and IL-15 (100 ng/ml, Peprotech) for 2 days prior to spinoculation. For IL-2 blockade, 2 μg/ml of anti-IL-2 (JES6-1A12, Biolegend) was added to the culture.

Real-time qRT-PCR

RNA was extracted using Trizol (Life Technologies), and reverse transcribed using qScript supermix (Quanta Bio). Real-time qRT-PCR was performed using DyNAmo ColorFlash SYBR green qPCR mix (Thermofisher) and Roche LightCycler 480. Quantities of transcripts were normalized against 18S ribosomal RNA (rRNA) using the ΔΔCt method unless otherwise specified. Primer sequences are available upon request. For quantitation of gene expression normalized against spiked-in RNA, 1 μL of 1:1,000 diluted External RNA Controls Consortium (ERCC) RNA Spike-In Control Mixes (Ambion) was added to total RNA extracted from 1 x 10^5 cells prior to reverse-transcription. The mixed RNA was used for reverse-transcription and real-time PCR quantitation. The following primers were used: 18S-rRNA, CGGCTACCACATCCAAGGAA and GCTGGAATTACCGCGGCT;
Bcl6, CCTGTGAAATCTGTGGCACTCG and CGCAGTTGGCTTTTGTGACG;
Eomes, ACCCAGCTAAAGATCGACCA and GACCTCCAGGGACAATCTGA;
Gapdh, CTCACAATTTCCATCCCAGACC and CATCAATGGTGCAGCGAACTTTATTGATG;
Hif1a, CTGGAAACGAGTGAAAGGATTC and CGTAACTGGTCAGCTGTGGTAA;
Hk2, CAACTCCGGATGGGACAG and CACACGGAAGTTGGTTCCTC;
Hprt1, AGGTTGCAAGCTTGCTGGT and TGAAGTACTCATTATAGTCAAGGGCA;
Il2ra, CTCACCTGGCAACACAGATG and GGCTCTGACTTTTCTAGCTTGC;
Ldha, CTGTTGGCATGGCTTGTG and CATCATCTCGCCCTTGAGTT;
Myc: AGTGCTGCATGAGGAGACAC and GGTTTGCCTCTTCTCCACAG;

Pkm2, CTGTCTGGAGAAACAGCCAAG and TCGAATAGCTGCAAGTGGTAGA; Slc2a1, ATGGATCCCAGCAGCAAG and CCAGTGTTATAGCCGAACTGC; *Tfap4*, GGAGAAGCTAGAGCGGGAAC and TTTTGCCGGGATGTAGAGAC; ERCC00108, CTATCAGCTTGCGCCTATTAT and GTTGAGTCCACGGGATAGAGTC; and LCMV-GP, CATTCACCTGGACTTTGTCAGACTC and GCAACTGCTGTGTTCCCGAAAC.

Microarray Analysis

Total RNA was extracted with a Nucleospin RNA XS extraction kit (Macherey-Nagel). 5 to 50 ng of total RNA was amplified using PicoSL RNA amplification kit (Nugen) and biotinylated with Encore biotin module (Nugen). Labeled RNA was hybridized to Mouse Gene 1.0ST microarray (Affymetrix) according to the manufacturer's instruction. For each experiment, RNA was prepared from two to three biological replicates, amplified, labeled and hybridized in a single experiment. Data were analyzed using Arraystar (DNA Star) with Robust Multi-array Average (RMA) normalization[50]. For spiked-in microarray analysis, ERCC RNA Spike-In Control Mixes were added as described above followed by RNA amplification, labeling and hybridization. CEL files were generated using a modified CDF file provided by Affymetrix. Data were initially normalized by RMA and signal intensities were further converted by formula obtained from linear regression of signals for spiked-in control RNA between samples.

Chromatin Immunoprecipitation

$CD8^+$ T cells were purified from C57BL6 mice by positive selection with FlowComp CD8 Dynabeads (Life Technologies). Purified $CD8^+$ T cells were stimulated with anti-CD3 and anti-CD28 for 2 days, and fixed with 1% PFA for 10 minutes at room temperature. Chromatin shearing and immunoprecipitation were performed as described previously[51]. Anti-AP4 antibody was previously described[24]. cMyc antibody (sc-764) and anti-phosphorylated RNA polII antibodies (ab5095 and ab5131) were purchased from Santa Cruz and Abcam, respectively. After immunoprecipitation, DNA was purified with a purification kit (Sigma), and 1-10 ng of DNA was used for library construction followed by 50 bp single read sequencing on HiSeq2000 (Illumina). Sequence tags were mapped onto the NCBI37/mm9 assembly of mouse genome using Bowtie2 (ref.[52]). BedGraph histograms normalized to 1 x 10^7 reads were generated using the Homer package[39] (http://biowhat.ucsd.edu/homer/ngs/) and visualized in the IGV browser (http://www.broadinstitute.org/igv/). Peak calling was performed using Homer with a -style factor option. For analysis of overlapping binding targets and binding motifs, 7,000 AP4 binding peaks filtered by P < 1.5e-65 and 7,000 cMyc-binding peaks (P < 5e-9) were analyzed. The following primers were used for real-time PCR analysis: Adsl, GGAATAATTCTGACAGGCTGCT and GCCCTAGTGGACACTTGGAGTA; Cd4 (promoter), TGGCCTTGAGCTTGTGATTTTTCT and GAATCAAGCTGGAGTCTGGAATGT;

Cd4 (silencer), TACGAAGCTAGGCAACAGAGGAAG and TGTGGTCCCGAATGCGTTT; Eif1a, ATCACCAAACAGGCAAGATTTC and GGGTTGCCCTTTTTACATTTCT; Eif4a1, ACAACAGACAAGCGAAACAGG and ACATGGCCGCTTGAGAGATT; Gapdh, CGCGAGGCTAGAACTTCTCC and TAGTAATCCAACACCCCGACTT; Hk2, AGGCCTCTTCAACACATCCTTA and GTGGGGAAGAATCCTGCTTAG;

Hoxa13, TTGTTTCCTGTTGGTTCCAG and AGCCCAAACTTCCCAGAGA; Ldha, CTTCTGAGGCTGAGGAGCAT and CACGATGTCCCTGCAAGAGT; Mthfd2, TGAGGCATTGCAGATTACCATA and CTGTCATACGAGCAGACACAGG; Pfkl, GGCTGTGCTTCTCTTAGAGGTC and CTATTCCTTTCTAGGCCACACG; Pkm (promoter), AGCGACTCGTCTTCACTTGACT and GTTCCTGCTGCGATACCTAGAG; Pkm (intron), CTACTCAGGTTTGGAGGTGGTC and GAGATGCTCAGAGCTCCCTAGA; Ppat, CACCCAAACACACCACATTC and CCTCTTGAGGCGTTCGATAG; Shmt2, AGCAAAGAGAAGGATACCATCG and GCCTCTTTCACTCGAACTTCAC; *Tfap4* (promoter), CTGATCAGATGTCTGTTTCAAGG and CGCTGCAAATAGTCCTTTGTTT;

Tfap4 CNS1 (Myc-1), CGAGTAAGCAAGGAAAAGGAAG and AGTCGCGACGTTTGTAAATTG;

Tfap4 CNS2 (Myc-2), GACCCGGCATAGAGAACTACAG and AGTCACTAGTCGCACGTTCTCC;

Tpi1, GATGTCAAGGAAGGGGGTCT and GTGCAGACCTCTCGAATAGCC; and Yars, ATCGATTCTTTCGACTCTCTGC and GGGAACTGTCACGCTAGTCC.

Metabolic Measurements

Extracellular acidification rates (ECARs) were measured using a Seahorse XF96 Analyzer (Seahorse Bioscience) essentially as described[37]. Briefly, $CD8^+$ T cells were purified from uninfected mice (for naive) or chimeric mice transferred with a mixture of *Tfap4*$^{-/-}$ and control WT OT-I T cells and infected with 1 x 10^4 CFU of Lm-Ova. To prepare *in vitro* activated $CD8^+$ T cells, purified naive $CD8^+$ T cells were activated with anti-CD3 and anti-CD28 antibodies

without exogenous IL-2 for 24 hours. 0.15 x 10^6 cells/well of $CD8^+$ T cells from three biological replicates were seeded onto a 96 well plate and ECARs were measured in duplicate in XF media (non buffered RPMI 1640 containing 25 mM glucose, 2 mM L-glutamine, and 1 mM sodium pyruvate) under basal conditions and in response to 1 μM oligomycin. Experiments were repeated three times for *in vivo* activated $CD8^+$ T cell samples and four times for naive and *in vitro* activated $CD8^+$ T cells.

Western blotting

Whole cell extracts were prepared by lysing cells in Laemmli buffer containing 1% SDS and 2% 2-mercaptoethanol. Lysates from equal numbers of cells were separated by 8 or 10% SDS PAGE, transferred to PVDF membranes (GE Healthcare), incubated with primary antibodies and detected with HRP-conjugated species-specific anti-immunoglobulin light chain antibodies (Jackson ImmunoResearch) and a Luminata HRP substrate (Millipore). Anti-HDAC1 (ab7028, Abcam) and anti-Tubulin beta (Developmental Studies Hybridoma Bank, University of Iowa) were used as loading controls. Anti-AP4 antibody was previously described[24]. The following antibodies were purchased: anti-Myc (Cell Signaling, 9402S), anti-phospho Stat5 (PY694) (BD Biosciences, 611964), anti-Blimp1 (Genscript, A01647-40), anti-T-Bet (Santa Cruz, sc-21003). For translation inhibition and proteasome inhibition, 10 μM of cycloheximide (Sigma) or MG-132 (Sigma) was added to the cell culture. For inhibition of signaling pathways, 20 nM of U0126 (Cayman Chemical), 10 μM of SB203580 (Cayman Chemical), 50 nM of wortmannin (Cayman Chemical), 5 nM of FK506 (Cayman Chemical), or 2.5 nM of rapamycin (Cayman Chemical) was added to the cell culture.

Statistical Analysis

P values were calculated with unpaired two-tailed Student's *t*-test for two group comparisons and with ANOVA for multiple group comparisons with the Tukey post-hoc test in Prism 6 (Graphpad) unless otherwise specified. *P* values < 0.05 were considered significant.

2.6 ACKNOWLEDGMENTS

We thank M. J. Bevan (University of Washington, Seattle, WA) for Lm-Ova, I. Taniuchi (RIKEN, Yokohama, Japan) and D. R. Littman (New York University, New York, NY) for CD8-Cre mice, B. P. Sleckman (Washington University School of Medicine, St. Louis) for cMyc-GFP knock-in mice, F. W. Alt (Harvard Medical School, Boston, MA) and D. R. Green (St. Jude Children's Research Hospital, Memphis, TN) for *Myc*-flox mice, T.Hansen (Washington University School of Medicine, St. Louis, MO) for the K^b-OVA single chain tetramer, S. Hsiung, J. Govero and M. J. Sunshine for technical assistance, E. Oltz, C.-s.Hsieh and D. R. Littman for discussions and critical reading of the manuscript. This study was supported by the Lucille P. Markey Pathway Program (C.C.) and grants from the National Institutes of Health (NIH) (R01 AI097244-01A1 to T.E., and U54 AI081680 to M.S.D.), and the Edward Mallinckrodt Jr. Foundation (T.E.). This study also was supported in part by an NIH grant to the Rheumatic Diseases Core Center (P30AR048335) and by the Washington University Institute of Clinical and Translational Sciences grant UL1 TR000448 from the National Center for Advancing Translational Sciences (NCATS) of NIH.

2.7 AUTHOR CONTRIBUTIONS

C.C. and T.E. designed the study with help with M. Cella, M. Colonna, P.M.A., E.L.P and M.S.D. C.C., A.K.P., J.D.C., S.P.P., C-C. L., B.T.E. and T.E. performed experiments. C.C., E.L.P., M.S.D. and T.E. analyzed data. T.E. wrote the manuscript with the other authors providing editorial comments.

2.8 REFERENCES

1. Kaech, S.M. & Wherry, E.J. Heterogeneity and cell-fate decisions in effector and memory CD8+ T cell differentiation during viral infection. *Immunity* **27**, 393-405 (2007).
2. Zhang, N. & Bevan, M.J. CD8(+) T cells: foot soldiers of the immune system. *Immunity* **35**, 161-168 (2011).
3. Kaech, S.M. & Cui, W. Transcriptional control of effector and memory CD8+ T cell differentiation. *Nature reviews. Immunology* **12**, 749-761 (2012).
4. MacIver, N.J., Michalek, R.D. & Rathmell, J.C. Metabolic regulation of T lymphocytes. *Annual review of immunology* **31**, 259-283 (2013).
5. van der Windt, G.J. & Pearce, E.L. Metabolic switching and fuel choice during T-cell differentiation and memory development. *Immunological reviews* **249**, 27-42 (2012).
6. Wang, R. & Green, D.R. Metabolic reprogramming and metabolic dependency in T cells. *Immunol Rev* **249**, 14-26 (2012).
7. Chang, C.H. *et al.* Posttranscriptional control of T cell effector function by aerobic glycolysis. *Cell* **153**, 1239-1251 (2013).
8. Kim, J. *et al.* A Myc network accounts for similarities between embryonic stem and cancer cell transcription programs. *Cell* **143**, 313-324 (2010).
9. Nie, Z. *et al.* c-Myc is a universal amplifier of expressed genes in lymphocytes and embryonic stem cells. *Cell* **151**, 68-79 (2012).
10. Lin, C.Y. *et al.* Transcriptional amplification in tumor cells with elevated c-Myc. *Cell* **151**, 56-67 (2012).
11. Rahl, P.B. *et al.* c-Myc regulates transcriptional pause release. *Cell* **141**, 432-445 (2010).

12. Sinclair, L.V. *et al.* Control of amino-acid transport by antigen receptors coordinates the metabolic reprogramming essential for T cell differentiation. *Nat Immunol* **14**, 500-508 (2013).

13. Wang, R. *et al.* The transcription factor Myc controls metabolic reprogramming upon T lymphocyte activation. *Immunity* **35**, 871-882 (2011).

14. Kaech, S.M. & Ahmed, R. Memory CD8+ T cell differentiation: initial antigen encounter triggers a developmental program in naive cells. *Nature immunology* **2**, 415-422 (2001).

15. Prlic, M., Hernandez-Hoyos, G. & Bevan, M.J. Duration of the initial TCR stimulus controls the magnitude but not functionality of the CD8+ T cell response. *The Journal of experimental medicine* **203**, 2135-2143 (2006).

16. Blair, D.A. *et al.* Duration of antigen availability influences the expansion and memory differentiation of T cells. *Journal of immunology* **187**, 2310-2321 (2011).

17. Porter, B.B. & Harty, J.T. The onset of CD8+-T-cell contraction is influenced by the peak of Listeria monocytogenes infection and antigen display. *Infect Immun* **74**, 1528-1536 (2006).

18. Best, J.A. *et al.* Transcriptional insights into the CD8(+) T cell response to infection and memory T cell formation. *Nature immunology* **14**, 404-412 (2013).

19. Williams, M.A., Tyznik, A.J. & Bevan, M.J. Interleukin-2 signals during priming are required for secondary expansion of CD8+ memory T cells. *Nature* **441**, 890-893 (2006).

20. Obar, J.J. *et al.* CD4+ T cell regulation of CD25 expression controls development of short-lived effector CD8+ T cells in primary and secondary responses. *Proceedings of the National Academy of Sciences of the United States of America* **107**, 193-198 (2010).

21. D'Souza, W.N. & Lefrancois, L. IL-2 is not required for the initiation of CD8 T cell cycling but sustains expansion. *Journal of immunology* **171**, 5727-5735 (2003).

22. Kalia, V. *et al.* Prolonged interleukin-2Ralpha expression on virus-specific CD8+ T cells favors terminal-effector differentiation in vivo. *Immunity* **32**, 91-103 (2010).

23. Pipkin, M.E. *et al.* Interleukin-2 and inflammation induce distinct transcriptional programs that promote the differentiation of effector cytolytic T cells. *Immunity* **32**, 79-90 (2010).

24. Egawa, T. & Littman, D.R. Transcription factor AP4 modulates reversible and epigenetic silencing of the Cd4 gene. *Proc Natl Acad Sci U S A* **108**, 14873-14878 (2011).

25. Hu, Y.F., Luscher, B., Admon, A., Mermod, N. & Tjian, R. Transcription factor AP-4 contains multiple dimerization domains that regulate dimer specificity. *Genes Dev* **4**, 1741-1752 (1990).

26. Mermod, N., Williams, T.J. & Tjian, R. Enhancer binding factors AP-4 and AP-1 act in concert to activate SV40 late transcription in vitro. *Nature* **332**, 557-561 (1988).

27. Maekawa, Y. *et al.* Notch2 integrates signaling by the transcription factors RBP-J and CREB1 to promote T cell cytotoxicity. *Nature immunology* **9**, 1140-1147 (2008).

28. Pircher, H., Burki, K., Lang, R., Hengartner, H. & Zinkernagel, R.M. Tolerance induction in double specific T-cell receptor transgenic mice varies with antigen. *Nature* **342**, 559-561 (1989).

29. Yoon, H., Kim, T.S. & Braciale, T.J. The cell cycle time of CD8+ T cells responding in vivo is controlled by the type of antigenic stimulus. *PloS one* **5**, e15423 (2010).

30. Petersen, L.R. & Fischer, M. Unpredictable and difficult to control--the adolescence of West Nile virus. *N Engl J Med* **367**, 1281-1284 (2012).

31. Suthar, M.S., Diamond, M.S. & Gale, M., Jr. West Nile virus infection and immunity. *Nat Rev Microbiol* **11**, 115-128 (2013).

32. Shrestha, B. & Diamond, M.S. Role of CD8+ T cells in control of West Nile virus infection. *J Virol* **78**, 8312-8321 (2004).

33. Diamond, M.S., Shrestha, B., Marri, A., Mahan, D. & Engle, M. B cells and antibody play critical roles in the immediate defense of disseminated infection by West Nile encephalitis virus. *Journal of virology* **77**, 2578-2586 (2003).

34. Wang, R. & Green, D.R. Metabolic checkpoints in activated T cells. *Nat Immunol* **13**, 907-915 (2012).

35. Jung, P., Menssen, A., Mayr, D. & Hermeking, H. AP4 encodes a c-MYC-inducible repressor of p21. *Proceedings of the National Academy of Sciences of the United States of America* **105**, 15046-15051 (2008).

36. Huang, C.Y.B., A. L.; Walker, L. M.; Bassing, C. H.; Sleckman, B. P. Dynamic regulation of c-Myc proto-oncogene expression during lymphocyte development revealed by a GFP-c-Myc knock-in mouse. *Eur J Immunol* **38**, 342-349 (2008).

37. van der Windt, G.J. *et al.* Mitochondrial respiratory capacity is a critical regulator of CD8+ T cell memory development. *Immunity* **36**, 68-78 (2012).

38. Loven, J. *et al.* Revisiting global gene expression analysis. *Cell* **151**, 476-482 (2012).

39. Heinz, S. *et al.* Simple combinations of lineage-determining transcription factors prime cis-regulatory elements required for macrophage and B cell identities. *Molecular cell* **38**, 576-589 (2010).

40. Chang, D.W., Claassen, G.F., Hann, S.R. & Cole, M.D. The c-Myc transactivation domain is a direct modulator of apoptotic versus proliferative signals. *Molecular and cellular biology* **20**, 4309-4319 (2000).

41. Yeh, E. *et al.* A signalling pathway controlling c-Myc degradation that impacts oncogenic transformation of human cells. *Nature cell biology* **6**, 308-318 (2004).

42. Indra, A.K. *et al.* Temporally-controlled site-specific mutagenesis in the basal layer of the epidermis: comparison of the recombinase activity of the tamoxifen-inducible Cre-ER(T) and Cre-ER(T2) recombinases. *Nucleic Acids Res* **27**, 4324-4327 (1999).

43. Zehn, D., Lee, S.Y. & Bevan, M.J. Complete but curtailed T-cell response to very low-affinity antigen. *Nature* **458**, 211-214 (2009).

44. de Alboran, I.M. *et al.* Analysis of C-MYC function in normal cells via conditional gene-targeted mutation. *Immunity* **14**, 45-55 (2001).

45. Hogquist, K.A. *et al.* T cell receptor antagonist peptides induce positive selection. *Cell* **76**, 17-27 (1994).

46. Mombaerts, P. *et al.* Mutations in T-cell antigen receptor genes alpha and beta block thymocyte development at different stages. *Nature* **360**, 225-231 (1992).

47. Willerford, D.M. *et al.* Interleukin-2 receptor alpha chain regulates the size and content of the peripheral lymphoid compartment. *Immunity* **3**, 521-530 (1995).

48. Ventura, A. *et al.* Restoration of p53 function leads to tumour regression in vivo. *Nature* **445**, 661-665 (2007).

49. Morita, S., Kojima, T. & Kitamura, T. Plat-E: an efficient and stable system for transient packaging of retroviruses. *Gene Ther* **7**, 1063-1066 (2000).

50. Bolstad, B.M., Irizarry, R.A., Astrand, M. & Speed, T.P. A comparison of normalization methods for high density oligonucleotide array data based on variance and bias. *Bioinformatics* **19**, 185-193 (2003).

51. Ciofani, M. *et al.* A validated regulatory network for Th17 cell specification. *Cell* **151**, 289-303 (2012).

52. Langmead, B. & Salzberg, S.L. Fast gapped-read alignment with Bowtie 2. *Nat Methods* **9**, 357-359 (2012).

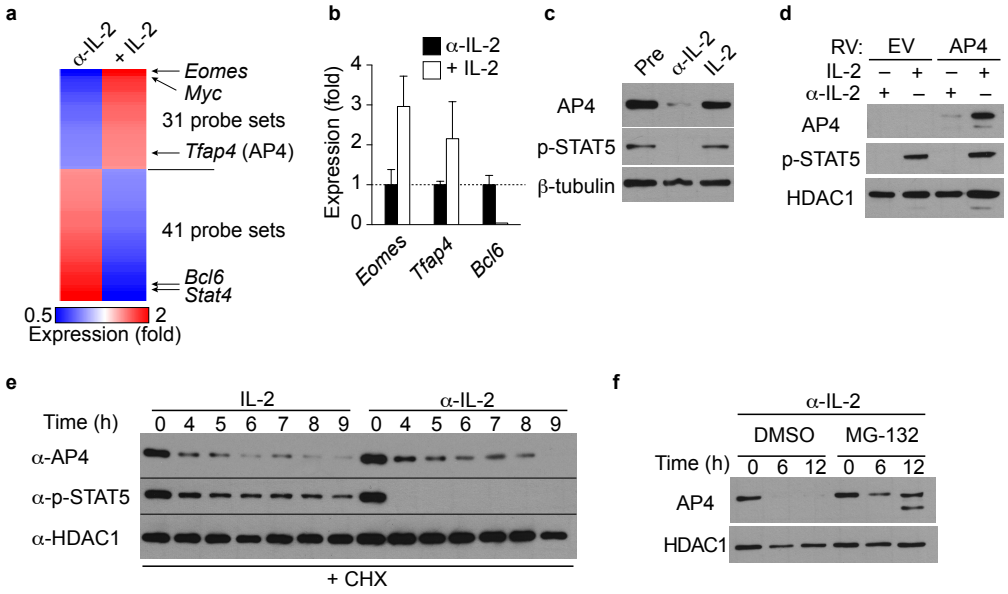

Figure 2.1. IL-2 signals maintain AP4 expression. (a) Microarray analysis of transcription factor–encoding genes with a difference in expression of >1.8-fold in activated $CD8^+$ T cells treated for 12 h with IL-2 (100 U/ml; + IL-2) relative to their expression in activated $CD8^+$ T cells treated for 12 h with anti−IL-2 (2 μg/ml; α-IL-2); results are presented as mean signal intensity. **(b)** Quantitative RT-PCR analysis of Eomes, *Tfap4* and Bcl6 in $CD8^+$ T cells treated as in a; results for cells treated with IL-2 are presented relative to those of cells treated with anti−IL-2, set as 1 (dashed line). **(c)** Immunoblot analysis of AP4 in $CD8^+$ T cells before treatment (Pre) or treated as in a; phosphorylated STAT5 (p-STAT5) and β-tubulin serve as loading controls. **(d)** Immunoblot analysis of AP4 in *Tfap4*$^{-/-}$ $CD8^+$ T cells transduced with retrovirus (RV) containing an empty vector (EV) or vector expressing AP4 (above blot) and treated as in a (above lanes); the histone deacetylase HDAC1 serves as a loading control throughout. **(e)** Immunoblot analysis of AP4 in $CD8^+$ T cells treated for 0−9 h (above lanes) with IL-2 or anti−IL-2 (above blot) in the presence of cycloheximide (10 μM). **(f)** Immunoblot analysis of AP4 in $CD8^+$ T cells treated for 0−12 h (above lanes) with anti−IL-2 in the presence of dimethyl sulfoxide (DMSO) or the proteasome inhibitor MG132 (10 μM). Data are from one experiment **(a)**, are pooled from two experiments (**b**; error bars, s.d.) or are representative of four experiments **(c)**, or three experiments **(d-f)**.

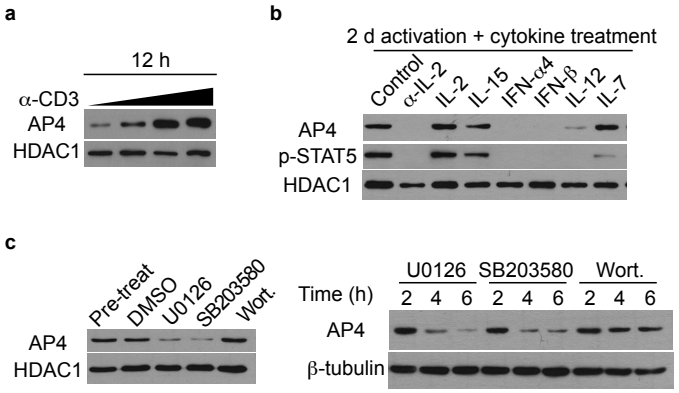

Figure 2.2. Sustained AP4 expression requires signaling via the MAPK pathway. (a,b) Immunoblot analysis of AP4 in $CD8^+$ T cells stimulated for 12 h with increasing concentrations (wedge) of anti-CD3 (12 h act) or stimulated for 2 d with anti-CD3 alone (Control) or with subsequent treatment for 12 h with anti−IL-2 or various cytokines (above lanes; 2 d act + 12 h Tx). IFN, interferon. **(c)** Immunoblot analysis of AP4 in $CD8^+$ T cells stimulated for 48 h with anti-CD3 and anti-CD28 alone (Pre-treat) or subsequently treated for 6 h with DMSO, U0126, SB203580 or wortmannin (Wort) (left blot), or treated for 24 h with IL-2 followed by treatment for various times (above lanes) with U0126, SB203580 or wortmannin (right blot). Data are representative of three experiments.

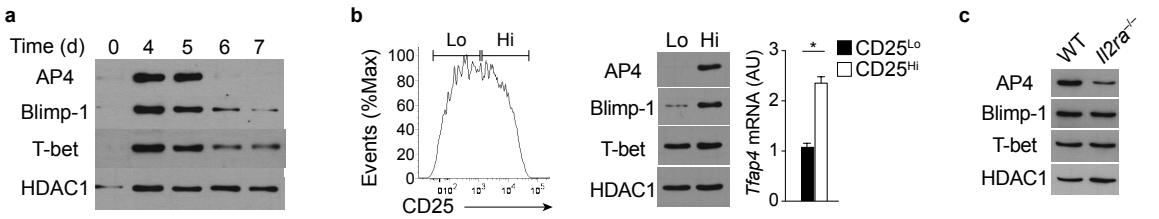

Figure 2.3. Signals through CD25 sustain AP4 expression *in vivo*. (a) Immunoblot analysis of AP4, Blimp-1 and T-Bet in P14 T cells adoptively transferred into host mice, assessed at 0−7 d (above lanes) after infection of the host with LCMV-Arm. **(b)** CD25 expression in $CD44^{+}CD62L^{-}$ $CD8^{+}$ T cells from C57BL/6 mice at day 4.5 after infection with LCMV-Arm (left), and immunoblot analysis of AP4, Blimp-1 and T-Bet (middle) and quantitative RT-PCR analysis of *Tfap4* (right) in the $CD25^{lo}$ and $CD25^{hi}$ cells sorted at left. **(c)** Immunoblot analysis of AP4 in $Il2ra^{+/+}$ and $Il2ra^{-/-}$ P14 donor T cells adoptively transferred into host mice and assessed on day 4 after infection of the host with LCMV-Arm. Data are representative of two **(a)**, or three **(b,c)** experiments.

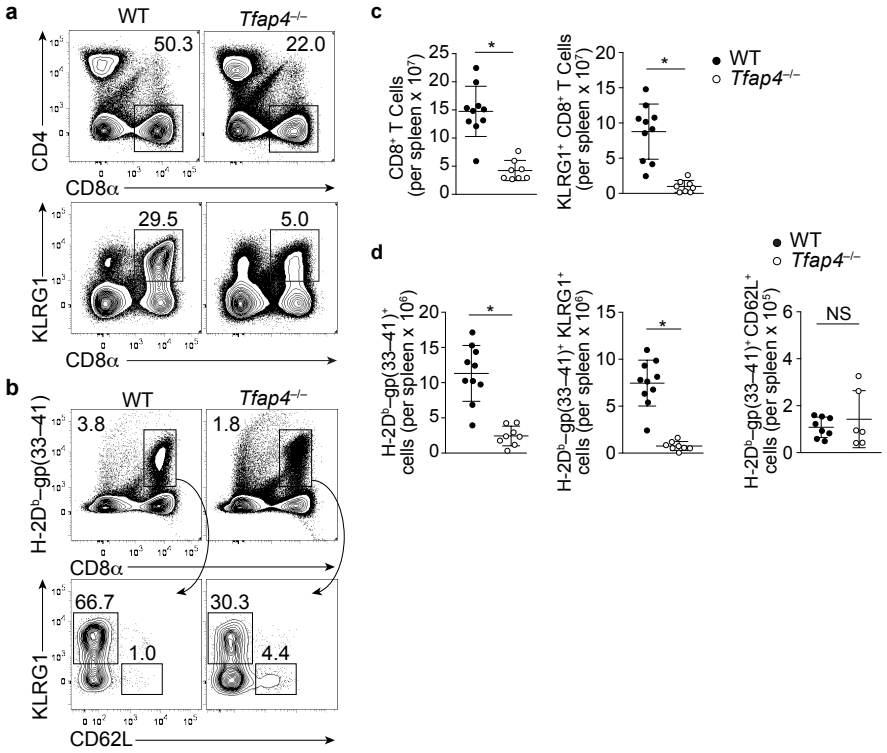

Figure 2.4. AP4 is required for the population expansion of antigen-specific CD8$^+$ T cells following infection with LCMV-Arm. (a,b) Expression of CD4, CD8α and KLRG1 **(a)** and binding of an H-2D^b–gp(33–41) tetramer and expression of CD8α, KLRG1 and CD62L **(b)** in splenocytes from wild-type (WT) and *Tfap4*$^{-/-}$ mice, assessed by flow cytometry 8 d after infection with LCMV. Numbers adjacent to outlined areas (gates) indicate percent CD8α$^+$ T cells **(a, top)**, KLRG1$^+$ CD8α$^+$ effector cells **(a, bottom)**, gp(33–44)-specific CD8α$^+$ T cells among total splenocytes (b, top), and CD62L$^+$ cells (top left) or KLRG1$^+$ cells **(bottom right)** among gp(33–41)-specific CD8α$^+$ T cells **(b, bottom)**. (c,d) Cumulative results from a **(c)** and b **(d)**: each symbol represents an individual mouse (n = 10 (wild-type) or 8 (*Tfap4*$^{-/-}$) mice); small horizontal lines indicate the mean (± s.d.). Each symbol represents an individual mouse (n = 5 per genotype); small horizontal lines indicate the mean (± s.d.); long dashed horizontal lines indicate the limit of detection. NS, not significant; *P < 0.0001 (unpaired *t*-test). Data are representative of three experiments **(a,b)** or are pooled from three experiments (c,d).

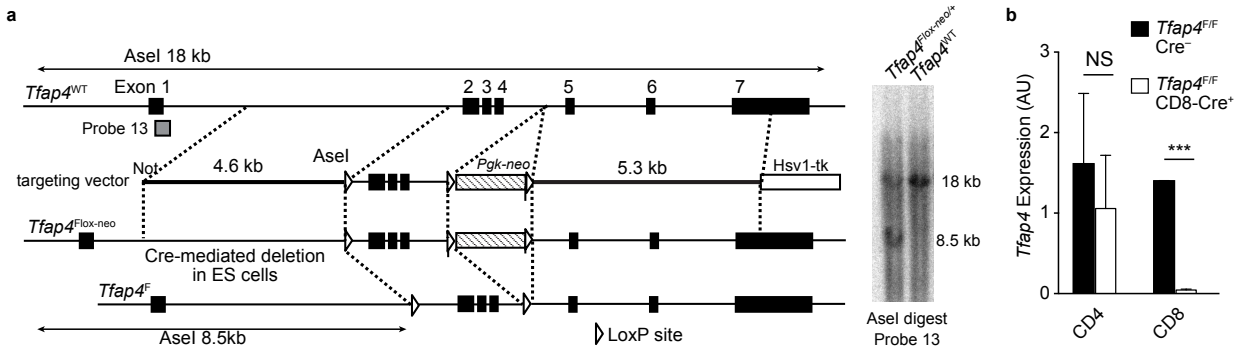

Figure 2.5. Generation of *Tfap4*^{F} allele. (a) A gene-targeting strategy shown with representative restriction enzyme sites used for screening by Southern blot with a 5' external probe (gray square). LoxP sites were inserted to flank exons 2 to 4 of *Tfap4* in ES cells. The loxP-neo cassette was deleted in vitro by transient Cre transfection in ES cells prior to blastocyst injection. **(b)** Quantitative RT-PCR analysis of RNA of CD4^{+} and CD8^{+} T cells purified from *Tfap4*$^{F/F}$ Cre^{-} or *Tfap4*$^{F/F}$ CD8-Cre^{+} mice showing the abundance of the transcript encoding *Tfap4*. Error bars, s.d. (n = 3). *** $P < 0.001$, NS: not significant by unpaired *t*-test.

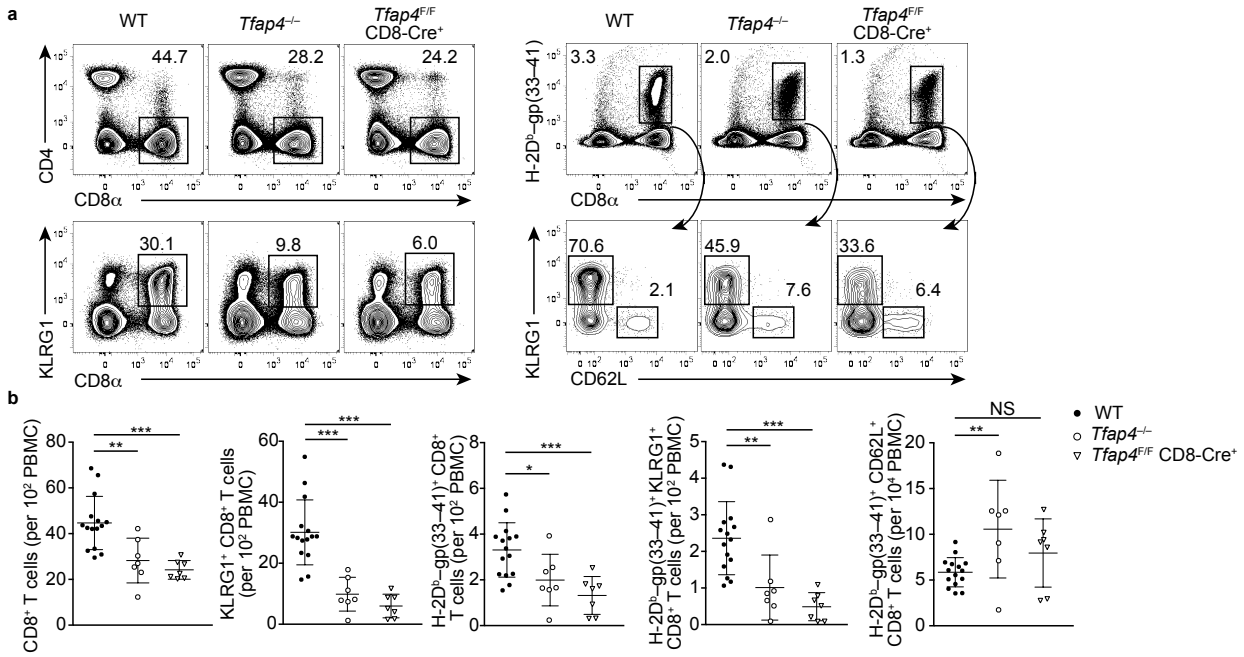

Figure 2.6. AP4 is required in a cell-autonomous way for the population expansion of CD8$^+$ T cells. (a,b) Flow cytometry analysis showing expression of CD4, CD8α, KLRG1, CD62L and H-2D^b–gp(33–41)-specific TCR in peripheral blood mononuclear cells (PBMC) from *Tfap4*$^{-/-}$ (n = 7), *Tfap4*$^{F/F}$ CD8-Cre$^+$ (n = 7) and control C57BL/6 mice (n = 15) on day 8 after LCMV-Arm infection. Statistical analysis is shown in **(b)**. Each symbol in d represents an individual mouse; small horizontal lines indicate the mean (± s.d.). * $P < 0.05$, ** $P < 0.01$, *** $P < 0.001$, NS: not significant by one-way ANOVA. Data pooled from three experiments.

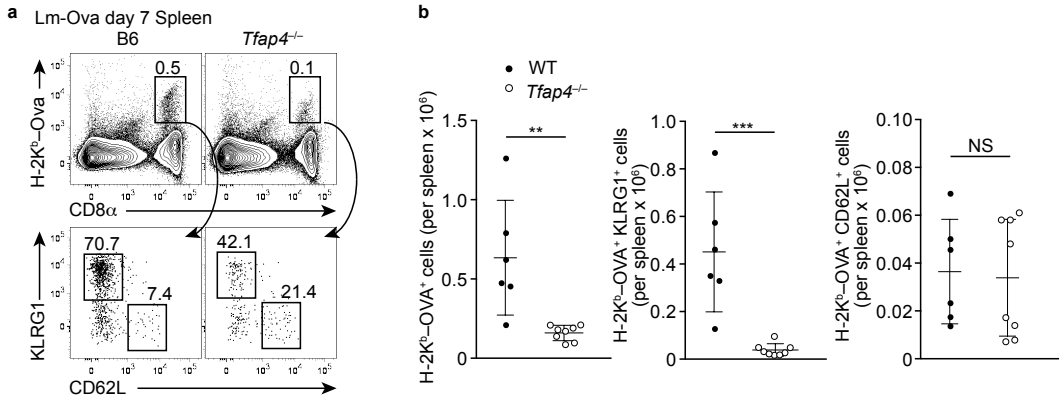

Figure 2.7. AP4 is required for the population expansion of antigen-specific CD8$^+$ T cells in response to infection with LM-OVA. (a) Flow cytometry analysis showing expression of CD8α, KLRG1, CD62L and H2-K^b–OVA-specific TCR in splenocytes of *Tfap4*$^{-/-}$ and age-matched C57BL/6 mice on day 7 after LM-OVA infection. OVA-specific CD8$^+$ T cells, and KLRG1$^+$ CD62L$^-$ effectors and KLRG1$^-$ CD62L$^+$ memory precursors are shown with rectangular gates with percentages. **(b)** Statistical analysis of total, KLRG1$^+$ and CD62L$^+$ H2-K^b–OVA-specific CD8$^+$ T cells. (n = 6 for C57BL/6, 8 for *Tfap4*$^{-/-}$ mice in two independent experiments). Error bars, s.d. Each symbol represents an individual mouse; small horizontal lines indicate the mean (± s.d.). * $P < 0.05$, ** $P < 0.01$, *** $P < 0.001$, NS: not significant by unpaired *t*-test. Data are representative of three experiments.

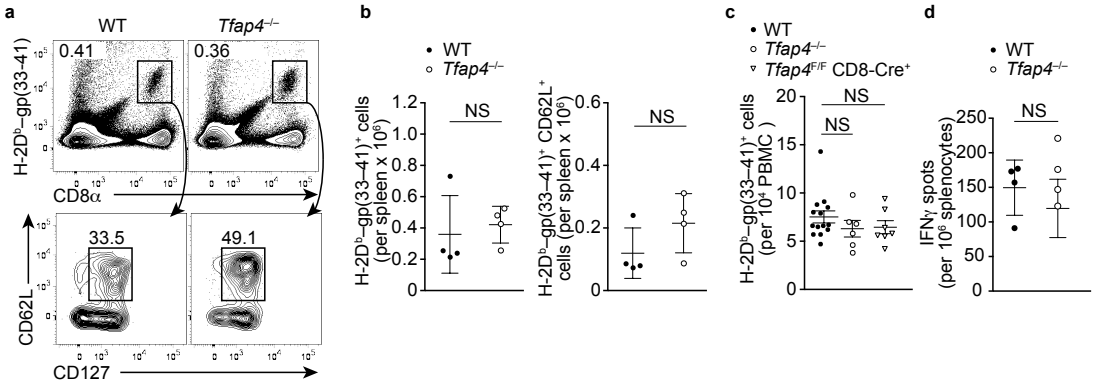

Figure 2.8. AP4 is dispensable for CD8 T cell memory formation. (a) Flow cytometry analysis of splenocytes showing expression of CD8α, CD127, CD62L and H-2D^b–gp(33–41)-specific TCR on day 60 after LCMV-Arm infection. (n = 4). **(b,c)** Statistical analysis of absolute numbers of gp(33–41)-specific total memory CD8$^+$ T cells and CD62L$^+$ central memory CD8$^+$ T cells in the spleen on day 60 after LCMV-Arm infection **(b)** and frequencies of gp(33–41)-specific memory CD8$^+$ T cells in peripheral blood mononuclear cells (PBMC) in *Tfap4*$^{-/-}$ (n = 6), *Tfap4*$^{F/F}$ CD8-Cre$^+$ (n = 7) or control C57BL/6 mice (n = 14) on day 60 after LCMV-Arm infection **(c)**. **(d)** IFN-γ ELISPOT assay showing frequencies of OVA-specific memory CD8$^+$ T cells in splenocytes of *Tfap4*$^{-/-}$ (n = 4) and control C57BL/6 mice (n = 4) on day 45 after LM-OVA infection. All mice had less than 11 spots per million splenocytes when no antigen was included. NS: not significant by unpaired *t*-test.

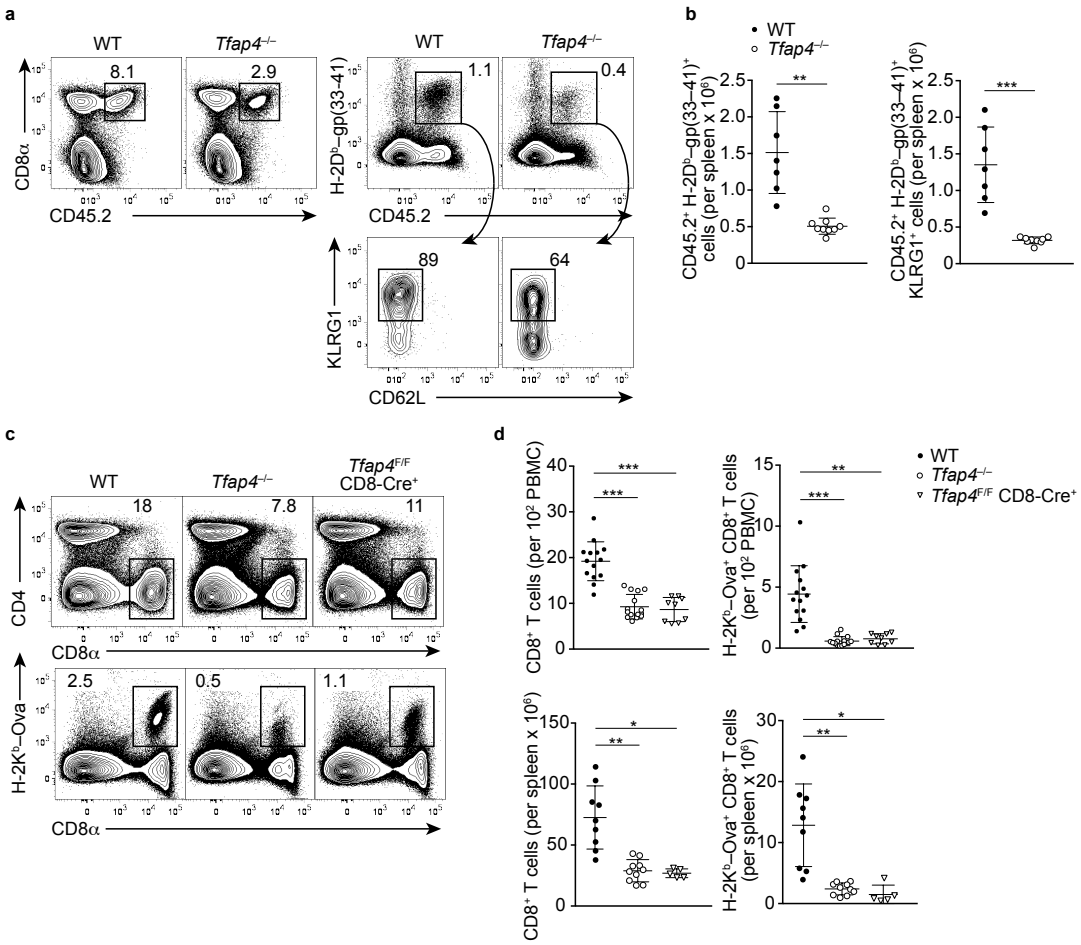

Figure 2.9. AP4 is essential for the secondary population expansion of memory CD8$^+$ T cells. (a,b) Flow cytometry analysis showing expression of CD8α, CD45.2, CD62L, KLRG1 and H-2D^b–gp(33–41)-specific TCR in splenocytes of CD45.1 wild-type host mice on day 5 after LCMV-Arm infection. Before infection, the host mice received CD8$^+$ T cells from *Tfap4*$^{-/-}$ or C57BL/6 mice, which were infected with LCMV-Arm 60 days before. (n = 8 in two independent experiments). Statistical analysis is shown in **(f)**. **(c)** Flow cytometry analysis of PBMC of *Tfap4*$^{-/-}$ (n = 15), *Tfap4*$^{F/F}$ CD8-Cre$^+$ (n = 9), or control C57BL/6 mice (n = 14) 5 days after secondary challenge with LM-OVA. **(d)** Statistical analysis of numbers of total CD8$^+$ T cell and OVA-specific CD8$^+$ T cells numbers in blood and spleen 5 days after secondary challenge with LM-OVA is shown. Each symbol represents an individual mouse; small horizontal lines indicate the mean (± s.d.). * $P < 0.01$, ** $P < 0.001$, *** $P < 0.0001$, NS: not significant by unpaired *t*-test **(b)** or one-way ANOVA **(d)**. Data are representative of three experiments.

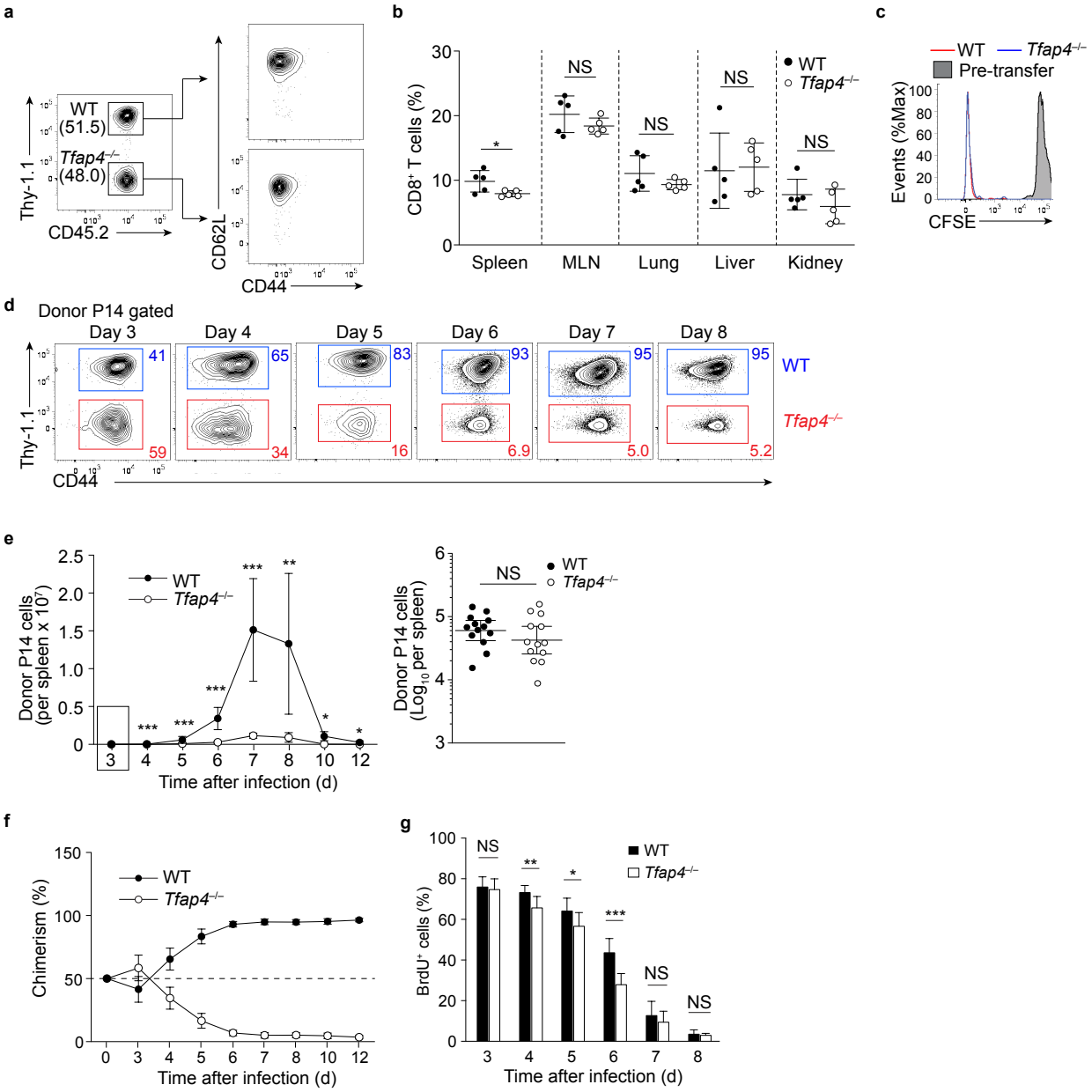

Figure 2.10. AP4 is required for the sustained clonal expansion of CD8$^+$ T cells but not for their initial proliferation. (a) Expression of CD62L and CD44 (right) by *Tfap4*$^{+/+}$ and *Tfap4*$^{-/-}$ P14 T cells (sorted by marker expression at left), assessed by flow cytometry 16 h after transfer together (at a ratio of 1:1) into congenic host mice. Numbers adjacent to outlined areas (left) indicate percent Thy-1.1$^+$CD45.2$^+$ (*Tfap4*$^{+/+}$) P14 T cells (top) or Thy-1.1−CD45.2$^+$ (*Tfap4*$^{-/-}$) P14 T cells (bottom). **(b)** Frequency of CD8$^+$ T cells in the spleen, mesenteric lymph nodes (MLN), lungs, liver and kidneys of *Tfap4*$^{-/-}$ mice and control wild-type C57BL/6 mice (WT) under steady-state conditions. Each symbol represents an individual mouse; small horizontal lines indicate the mean (± s.d.). **(c)** Flow cytometry of CFSE-labeled *Tfap4*$^{+/+}$ and *Tfap4*$^{-/-}$ P14 donor T cells before transfer (Pre-transfer) and after transfer into host mice, assessed 3 d after infection of the host with LCMV-Arm. **(d)** Flow cytometry of *Tfap4*$^{+/+}$ and *Tfap4*$^{-/-}$ P14 donor cells transferred into host mice at a starting ratio of 1:1, assessed at various time points after

infection of the host with LCMV-Arm (numbers in plots as in a). **(e)** Quantification of *Tfap4*$^{+/+}$ and *Tfap4*$^{-/-}$ P14 donor cells in the spleen of host mice as in d (n = 9−13 (day 3), 8−18 (day 4), 8−13 (day 5), 9−19 (day 6), 4−8 (day 7), 4−9 (day 8), 3 (day 10) or 5 (day 12)), normalized to 1 × 104 transferred cells (left), and data for day 3 (outlined at left) on a log10 scale (right): each symbol represents an individual mouse; small horizontal lines indicate the mean (± s.d.). (f,g) Frequency of *Tfap4*$^{+/+}$ and *Tfap4*$^{-/-}$ donor T cells in the mice in e, assessing chimerism **(f)**, and frequency of BrdU^{+} cells following 2 h of pulse labeling in vivo in those mice **(g)**. *P < 0.05, **P < 0.01 and ***P < 0.001 (unpaired *t*-test **(b,e,g)** or one-way analysis of variance (ANOVA) **(j)**). Data are representative of three **(a,d)** or two **(c)** experiments or are pooled from three **(b,e**−**g)**.

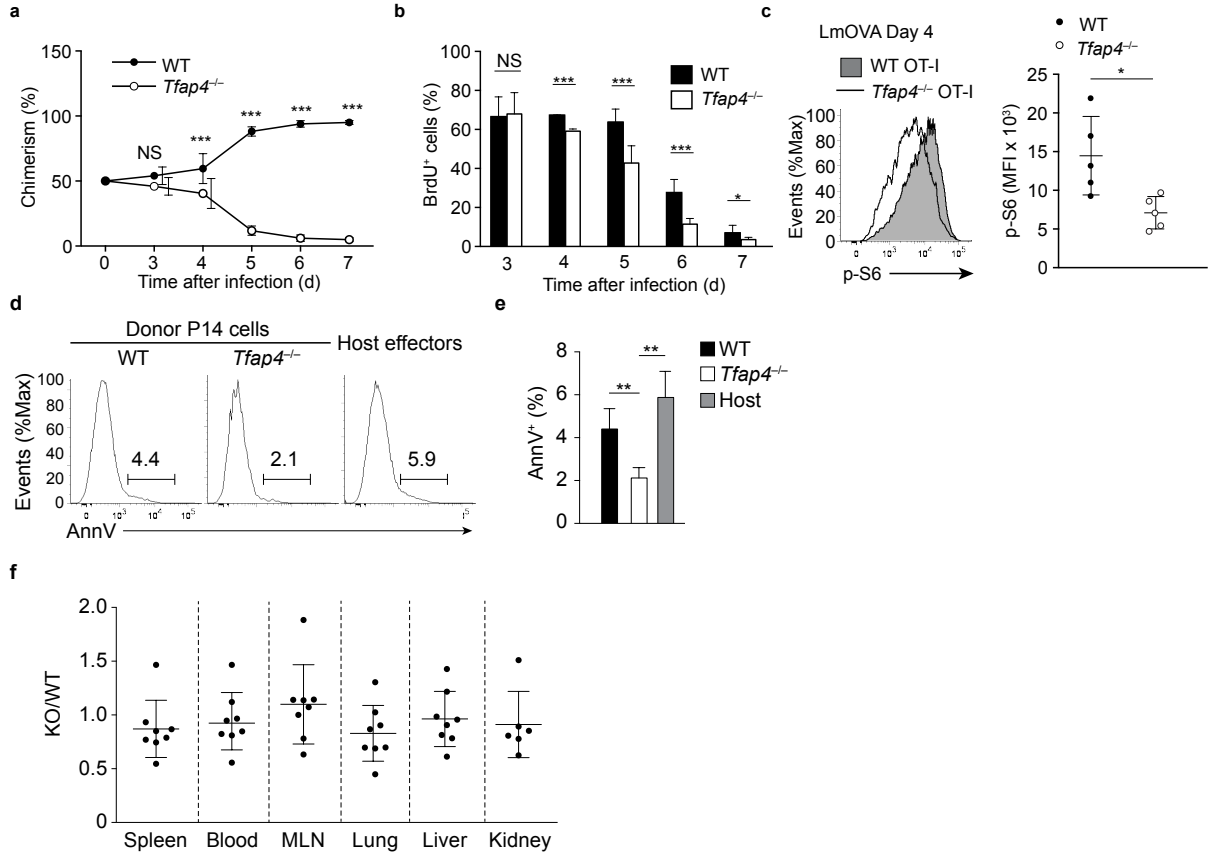

Figure 2.11. AP4-deficiency does not result in increased cell death or impaired CD8 T cell trafficking. (a) Statistical analysis of ratios between *Tfap4*$^{-/-}$ and *Tfap4*$^{+/+}$ OT-I T cells. (n = 15 for day 3, 18 for day 4, 6 for day 5, 8 for day 6, 8 for day 7). **(b)** Statistical analysis of percentages of BrdU^{+} OT-I T cells following 2 h pulse labeling. (n = 9 for day 3, 5 for day 4, 7 for day 5, 6 for day 6, 8 for day 7). **(c)** Flow cytometry analysis of OT-I T cells showing levels of phosphorylated serine 235/236 of S6 ribosomal protein (p-S6) on day 4 after LM-OVA infection shown as histogram overlays. (n = 5). **(d)** Binding of annexin V (AnnV) in *Tfap4*$^{+/+}$ and *Tfap4*$^{-/-}$ P14 donor cells and CD8^{+}CD44^{+} effector host cells (Host) in the spleen 6 d after infection of the host with LCMV-Arm, assessed by flow cytometry. Numbers above bracketed lines indicate percent annexin V^{-}positive cells. **(e)** Cumulative results from h (n = 5 host mice). **(f)** Ratio of *Tfap4*$^{-/-}$ P14 donor cells to *Tfap4*$^{+/+}$ P14 donor cells (KO/WT) (transferred at a starting ratio of 6:1) in various organs and blood of host mice 7 d after infection with LCMV-Arm. Each symbol represents an individual host mouse (n = 8); small horizontal lines indicate the mean (± s.d.). *P < 0.05, **P < 0.01 and ***P < 0.001 unpaired *t*-test.

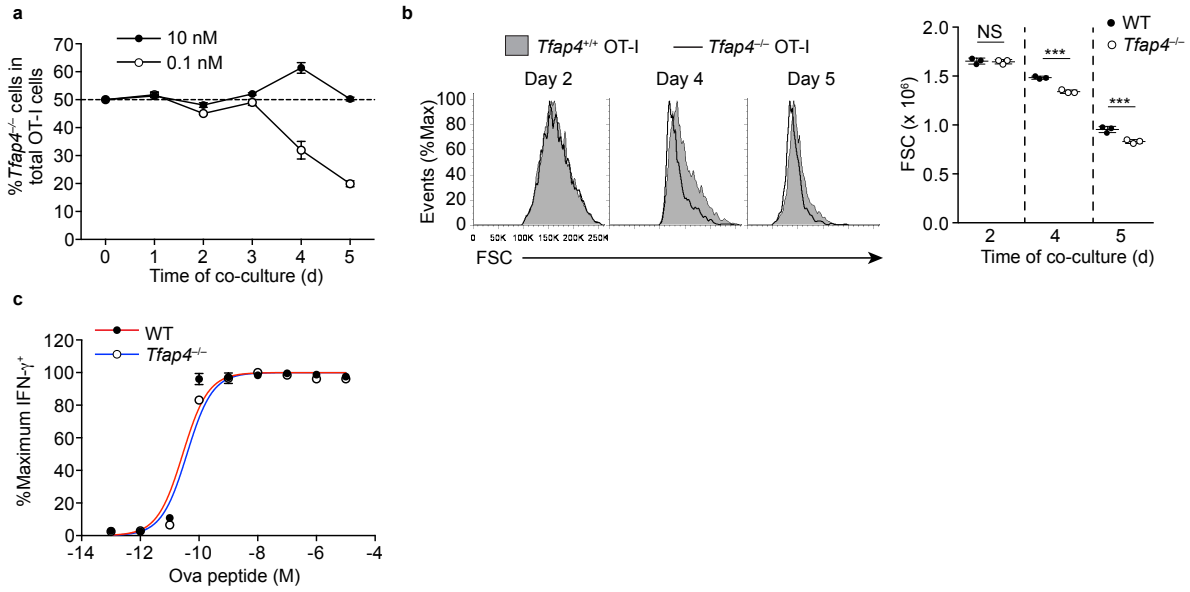

Figure 2.12. AP4 is dispensable for early T cell activation *in vitro*. (a) Statistical analysis of ratios of *Tfap4*$^{-/-}$ and *Tfap4*$^{+/+}$ OT-I T cells co-cultured with OVA peptide-pulsed irradiated splenocytes. Percentages of *Tfap4*$^{-/-}$ OT-I cells in total OT-I T cells are shown. **(b)** Flow cytometry analysis of *Tfap4*$^{-/-}$ and *Tfap4*$^{+/+}$ OT-I T cells showing FSC after co-culture in the presence of irradiated splenocytes pulsed with 0.1 nM of OVA peptide. (n = 3). **(c)** Statistical analysis of percentages of IFN-γ-producing *Tfap4*$^{-/-}$ and *Tfap4*$^{+/+}$ OT-I cells that had been initially activated by anti-CD3 and anti-CD28 and re-stimulated with OVA-peptide pulsed irradiated splenocytes. Values were normalized to the maximum percentage of cells producing IFN-γ. (n = 2). *** $P < 0.001$, NS: not significant by unpaired *t*-test.

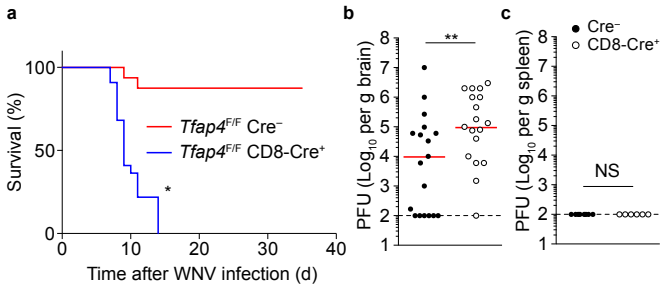

Figure 2.13. AP4 is essential for host protection against infection with WNV, in a CD8$^+$ T cell$^-$intrinsic manner. (a) Survival of *Tfap4*$^{F/F}$Cre− control mice (Cre$^-$; n = 16) and *Tfap4*$^{F/F}$CD8-Cre$^+$ mice (CD8-Cre$^+$; n = 22) following infection with WNV. **(b,c)** Viral titers in the brain **(b)** and spleen **(c)** of *Tfap4*$^{F/F}$ Cre$^-$ and *Tfap4*$^{F/F}$ CD8-Cre$^+$ mice on day 9 after infection with WNV. Each symbol represents an individual mouse (n = 18 **(b)** or 7 **(c)** per genotype); red horizontal lines **(b)** indicate the median; dashed horizontal lines indicate limit of detection. *P < 0.05 and **P < 0.001 (log-rank test **(a)** or Mann-Whitney U-test (b,c)). Data are pooled from three **(a)**, four **(b)** or two **(c)** independent experiments.

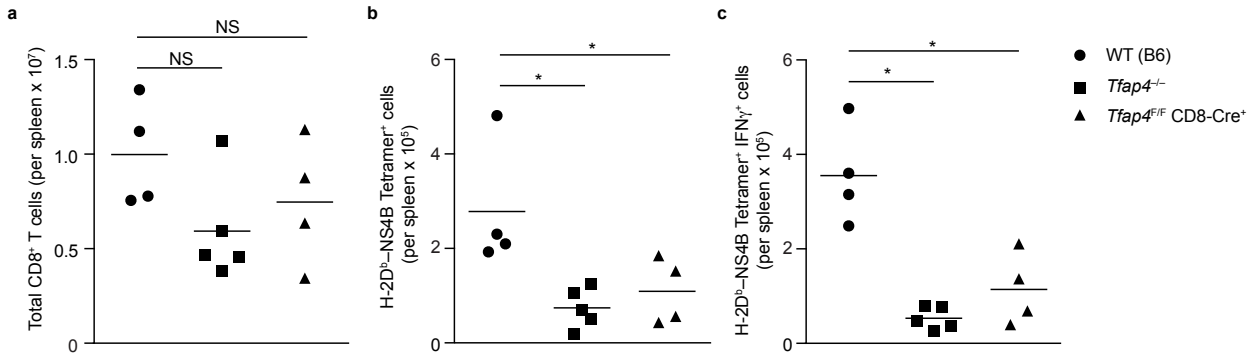

Figure 2.14. AP4 is required for the population expansion of antigen-specific CD8$^+$ T cells after infection with WNV. Statistical analysis showing absolute numbers of total CD8$^+$ T cells **(a)** H-2D^b–NS4B-specific T cells as determined by H-2D^b–NS4B tetramer binding **(b)** or intracellular staining for IFN-γ following NS4B peptide stimulation **(c)** in the spleen on day 7 after WNV infection. Data is from one experiment using five *Tfap4*$^{-/-}$, four *Tfap4*$^{F/F}$ CD8-Cre$^+$, and four control age- and sex-matched C57BL/6 mice. * $P < 0.05$, NS: not significant by Mann Whitney U-test. Each symbol represents an individual mouse; small horizontal lines indicate median.

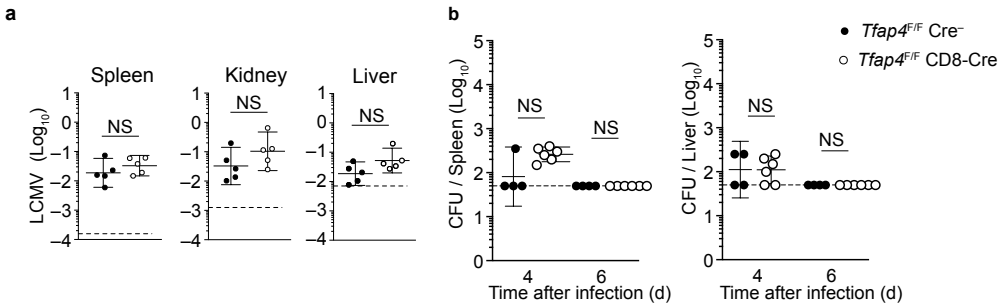

Figure 2.15. AP4 is dispensable for clearance of LM-OVA or LCMV Arm. (a) Quantitative RT-PCR analysis of the abundance of transcripts encoding LCMV-gp in the spleen, kidneys and liver of *Tfap4*$^{F/F}$CD8-Cre^{+} and control *Tfap4*$^{F/F}$Cre^{-} mice 6 d after infection with LCMV-Arm; results are presented relative to those of control transcripts encoding hypoxanthine guanine phosphoribosyl transferase (Hprt1). long dashed horizontal lines indicate the limit of detection. **(b)** Statistical analysis of LM-OVA bacterial titers in spleens and livers of *Tfap4*$^{F/F}$ CD8-Cre^{+} and *Tfap4*$^{F/F}$ Cre^{-} mice on days 4 and 6 after infection. (n = 4 for *Tfap4*$^{F/F}$ Cre^{-}, 6 for *Tfap4*$^{F/F}$ CD8-Cre^{+} in two experiments). Each symbol represents an individual mouse (n = 5 per genotype); small horizontal lines indicate the mean (± s.d.); NS, not significant by unpaired *t*-test.

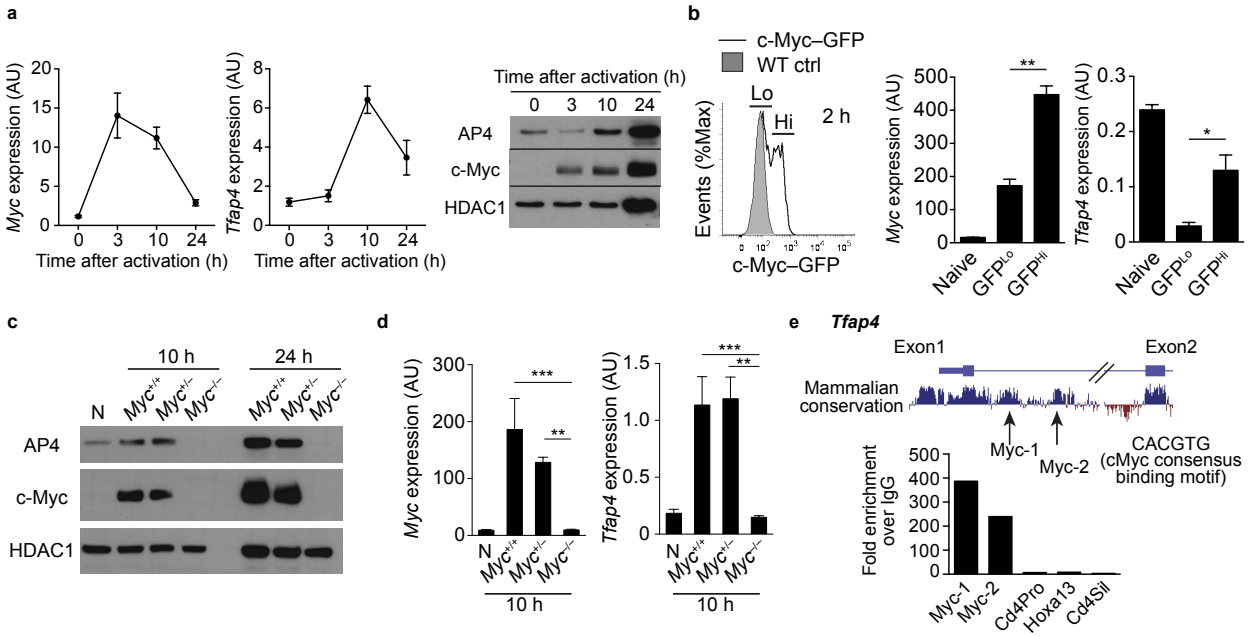

Figure 2.16. Myc induces AP4 after T cell activation. (a) Quantitative RT-PCR and immunoblot analysis showing c-Myc and AP4 expression at mRNA and protein levels in $CD8^+$ T cells following stimulation with anti-CD3 and anti-CD28. (n = 2). **(b)** Flow cytometry of $CD8^+$ T cells from OT-I c-Myc−GFP^+ mice showing c-Myc−GFP expression after two-hour stimulation with anti-CD3 and anti-CD28 and quantitative RT-PCR analysis of transcripts encoding Myc or *Tfap4* in purified GFP^{Lo} and GFP^{Hi} cells. (n = 2). **(c,d)** Immunoblot analysis of AP4 and c-Myc **(c)** and quantitative RT-PCR analysis of Myc and *Tfap4* **(d)** in wild-type naive $CD8^+$ T cells treated with 4-hydroxytamoxifen (N) and in $Myc^{F/+}$Cre− ($Myc^{+/+}$), $Myc^{F/+}$ Rosa26-Cre-ERT2 ($Myc^{+/–}$) and $Myc^{F/F}$ Rosa26-Cre-ERT2 ($Myc^{–/–}$) $CD8^+$ T cells treated with 4-hydroxytamoxifen and stimulated for 10 or 24 h in vitro with anti-CD3 and anti-CD28. **(e)** Quantitative PCR analysis of anti-c-Myc immunoprecipitated chromatin of activated $CD8^+$ T cells showing enrichment of the *Tfap4* intronic fragments containing c-Myc consensus binding sequences. PCR primers for *Cd4* promoter (Cd4Pro), *Hoxa13* promoter (Hoxa13) and *Cd4* silencer (Cd4Sil) were used as negative control (n = 2). *P < 0.05, **P < 0.01 and ***P < 0.001 by unpaired *t*-test.

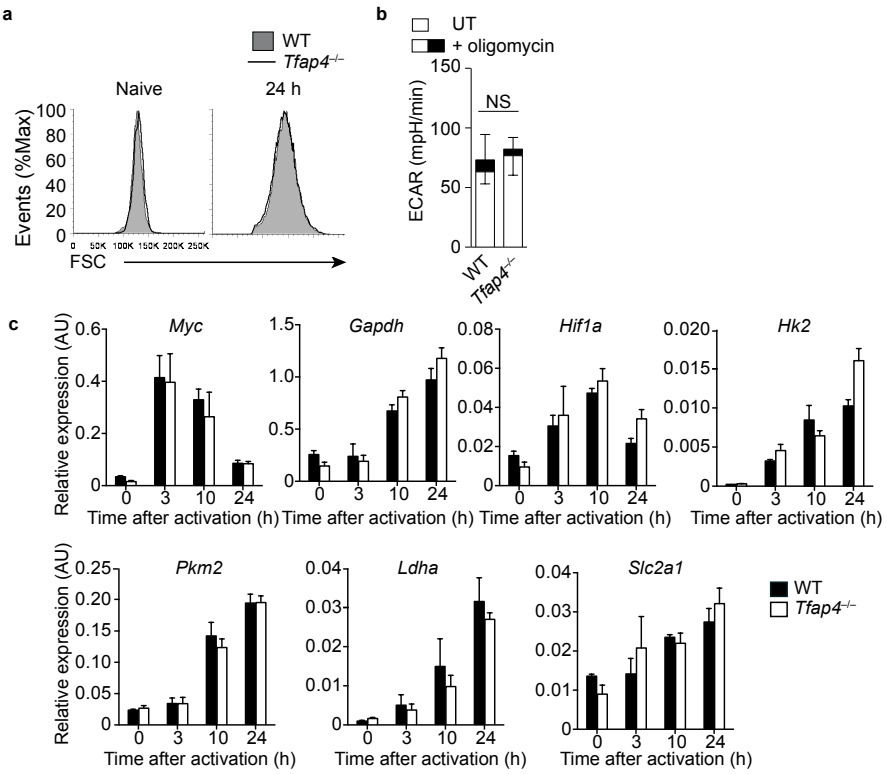

Figure 2.17. AP4 is dispensable for initial blasting and increase in glycolysis after T cell activation *in vitro*. (a) Flow cytometry of $CD8^+$ T cells showing FSC in the naive state and following 24 h stimulation with anti-CD3 and anti-CD28 antibodies in vitro. (n = 3). **(b)** ECAR measurement showing glycolytic rates of *Tfap4*$^{-/-}$ and C57BL/6 $CD8^+$ T cells after stimulation with anti-CD3 and anti-CD28 for 24 h. Data represent three independent experiments with three to four biological replicates in each experiment. **(c)** qRT-PCR analysis of RNA from $CD8^+$ T cells showing 18S rRNA-normalized expression of *Myc*, *Hif1a* and genes encoding glycolytic enzymes at different time points following stimulation with anti-CD3 and anti-CD28 antibodies in vitro. (n = 3). NS: not significant by unpaired *t*-test.

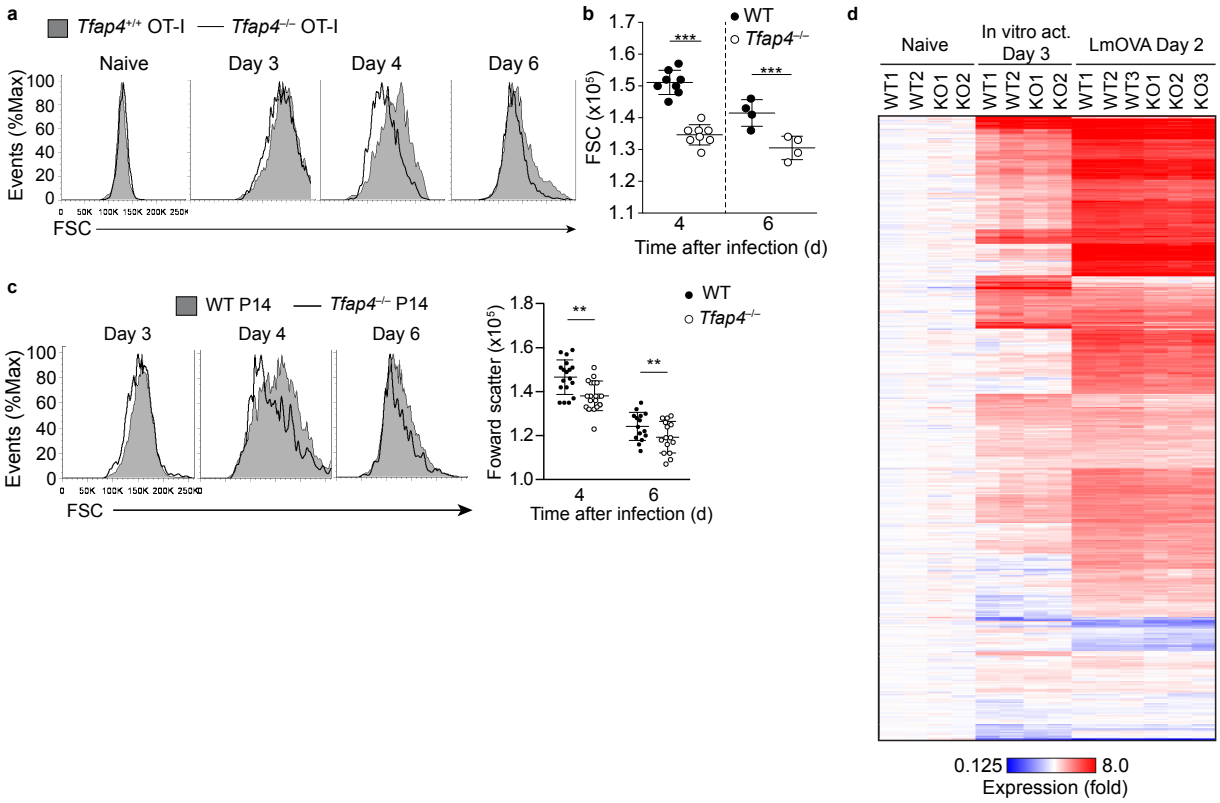

Figure 2.18. AP4-deficient CD8 T cells fail to maintain cell growth. (a) Flow cytometry of *Tfap4*$^{+/+}$ and *Tfap4*$^{-/-}$ OT-I donor T cells adoptively transferred into host mice, assessed before (Naive) or 3, 4 or 6 d after infection of the host with LM-OVA, assessing cell size as forward scatter (FSC). **(b)** Cumulative results for cells as in a: each symbol represents an individual host mouse (n = 8 (day 4) or 4 (day 6)); small horizontal lines indicate the mean (± s.d.). **(c)** Flow cytometry of co-transferred *Tfap4*$^{-/-}$ and *Tfap4*$^{+/+}$ P14 T cells showing FSC after infection of recipient mice with LCMV-Arm. Representative histogram overlays at each time point are shown in the left panel. (n = 3). **(d)** Microarray gene expression analysis of C57BL/6 CD8^{+} T cells in the naive state, or after activation with anti-CD3 and anti-CD28 in vitro for 3 days (n = 2), and OT-I T cells 2 days after LM-OVA infection in vivo (n = 3). Expression levels of the 479 AP4/Myc co-regulated genes are shown by a heat map. Expression levels are normalized to those of naive CD8^{+} T cells. **P < 0.01 and ***P < 0.001 by unpaired *t*-test.

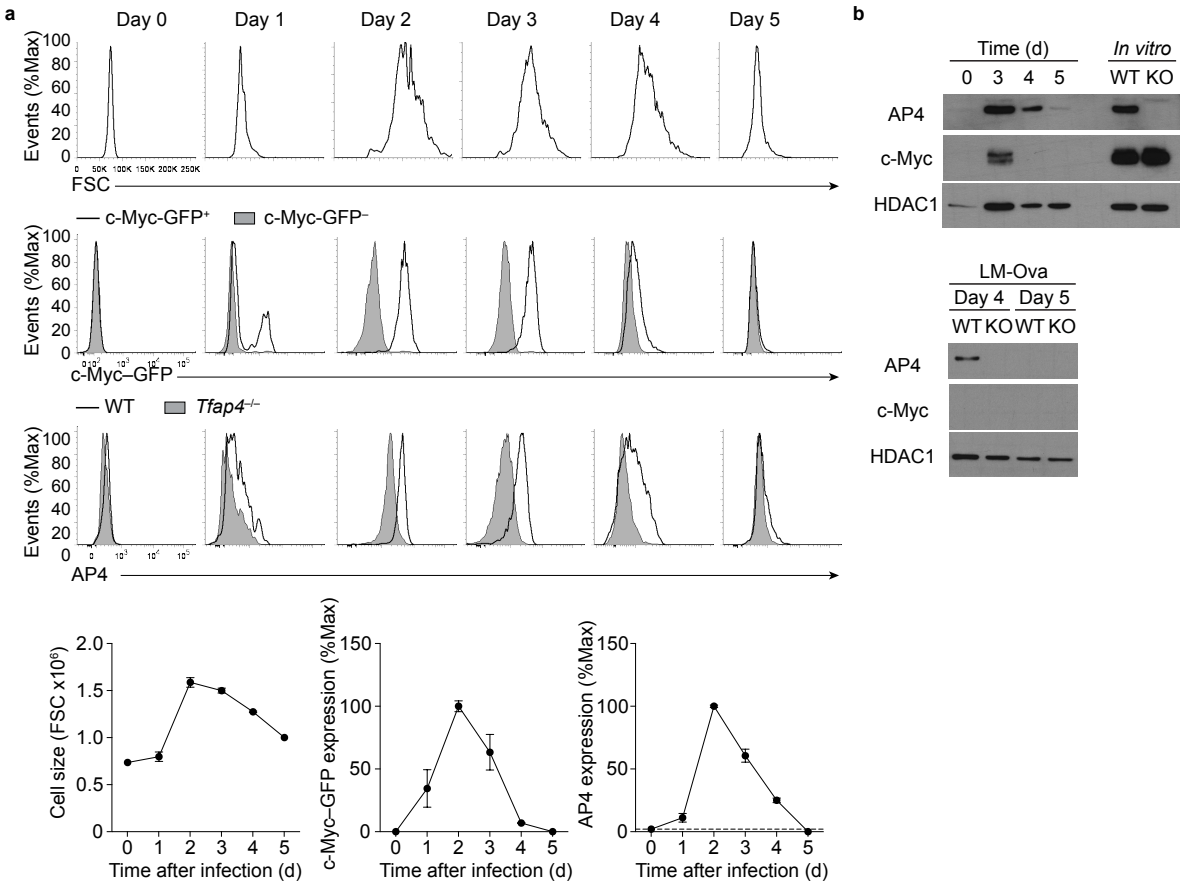

Figure 2.19. AP4 expression persists longer than MYC. (a) Size of *Tfap4*$^{+/+}$ OT-I donor T cells (assessed as forward scatter; top) and expression of c-Myc−GFP (middle) and AP4 (bottom) by *Tfap4*$^{+/+}$ and *Tfap4*$^{-/-}$ OT-I T cells on days 0−5 after infection with LM-OVA, assessed by flow cytometry; c-Myc^{-}GFP results obtained by subtraction of autofluorescence from the GFP fluorescence of OT-I T cells heterozygous for the knock-in allele encoding c-Myc−GFP. Below, cumulative results obtained as above. **(b)** Immunoblot analysis of AP4 and c-Myc in *Tfap4*$^{+/+}$ OT-I donor T cells adoptively transferred into host mice, assessed in the naive state (0) or on days 3−5 after infection of the host with LM-OVA (left), and in *Tfap4*$^{+/+}$ (WT) and *Tfap4*$^{-/-}$ (KO) OT-I donor T cells activated for 24 h in vitro with anti-CD3 and anti-CD28 (In vitro) or adoptively transferred into host mice and activated in vivo by infection of the host for 4 or 5 d with LM-OVA (bottom), to demonstrate antibody specificity.

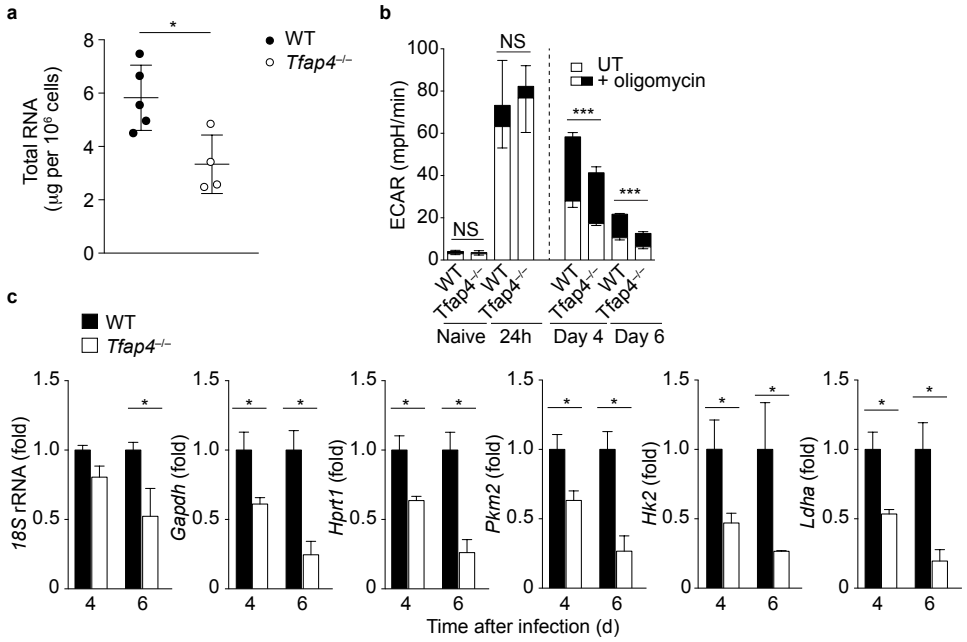

Figure 2.20. AP4 sustains active transcription and glycolysis of CD8 T cells. (a) Total RNA in *Tfap4*$^{+/+}$ and *Tfap4*$^{-/-}$ OT-I donor T cells adoptively transferred into host mice and assessed 4 d after infection of the host with LM-OVA. Each symbol represents an individual host mouse (n = 5); small horizontal lines indicate the mean (± s.d.). **(b)** ECAR of *Tfap4*$^{+/+}$ and *Tfap4*$^{-/-}$ OT-I CD8^{+} T cells left unstimulated (Naive), stimulated for 24 h in vitro with anti-CD3 and anti-CD28 (middle) or adoptively transferred into host mice and analyzed on days 4 and 6 after infection of the host with LM-OVA, all assessed at baseline (without additional treatment (UT)) and after treatment with oligomycin (olig). **(c)** Quantitative RT-PCR analysis of genes encoding molecules involved in glycolysis in *Tfap4*$^{+/+}$ and *Tfap4*$^{-/-}$ OT-I T cells adoptively transferred into host mice and assessed on day 4 or 6 after infection of the host with LM-OVA; results were normalized to those of 'spiked-in' control RNA ERCC-00108 and are presented relative to those of *Tfap4*$^{+/+}$ OT-I T cells. *P < 0.05, **P < 0.01 and ***P < 0.001, NS: not significant by unpaired *t*-test.

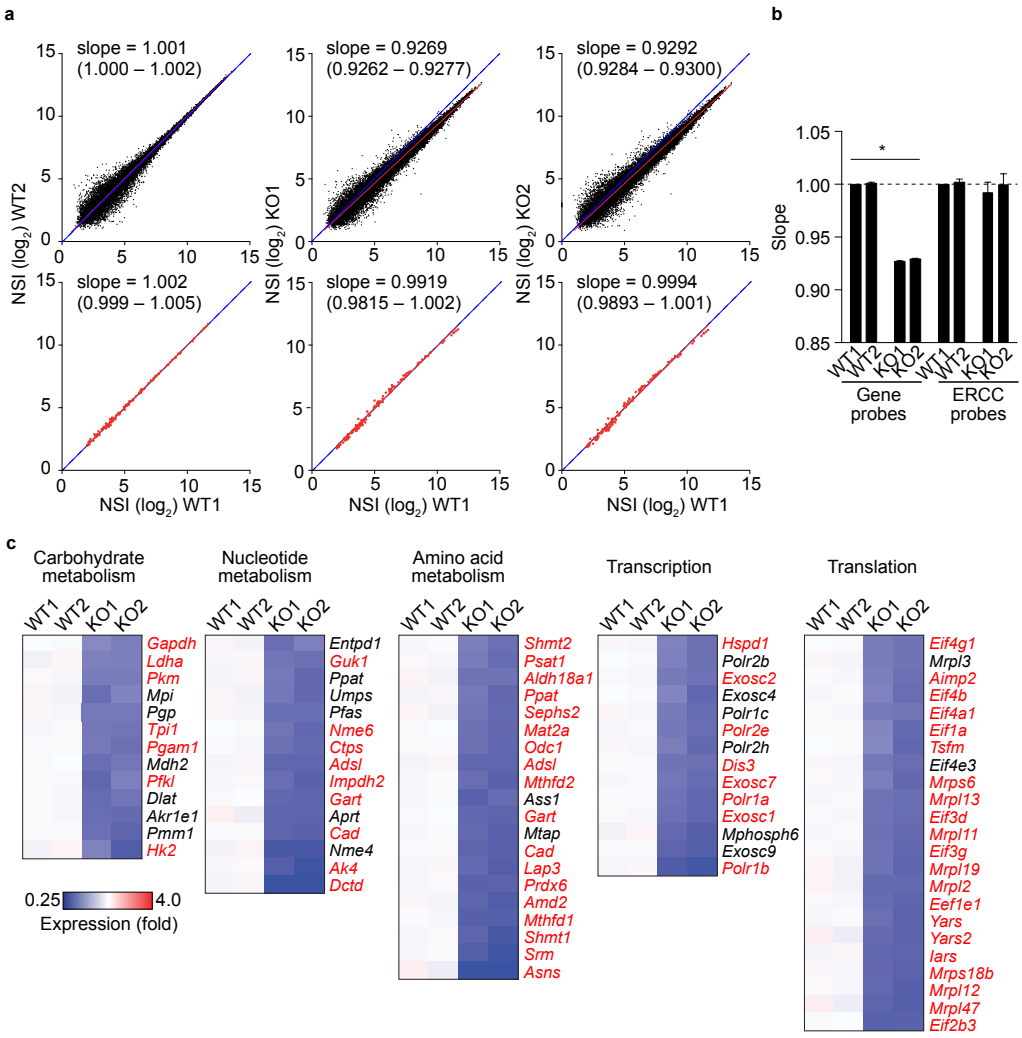

Figure 2.21. AP4 is required for sustaining the expression of activation signature genes. (a) Normalized signal intensity (NSI) of endogenous transcripts in *Tfap4*$^{+/+}$ and *Tfap4*$^{-/-}$ OT-I donor T cells adoptively transferred into host mice and assessed on day 4 after infection of the host with LM-OVA (top), and that of ERCC control RNA (bottom); numbers in plots indicate slope values obtained by linear regression (with 95% confidence interval in parentheses); slope of blue dashed lines, 1. WT1 and WT2, and KO1 and KO2, indicate two biological replicates of *Tfap4*$^{+/+}$ OT-I samples and of *Tfap4*$^{-/-}$ OT-I samples, respectively (throughout). **(b)** Slopes of plots in a. **(c)** Heat maps of the expression of genes encoding molecules in pathways (top) identified by the bioinformatics database DAVID (version 6.7), assessed in cells as in **(a)** and presented relative to results for *Tfap4*$^{+/+}$ OT-I T cells; red indicates genes bound by both c-Myc and AP4. *P < 0.05 (unpaired *t*-test).

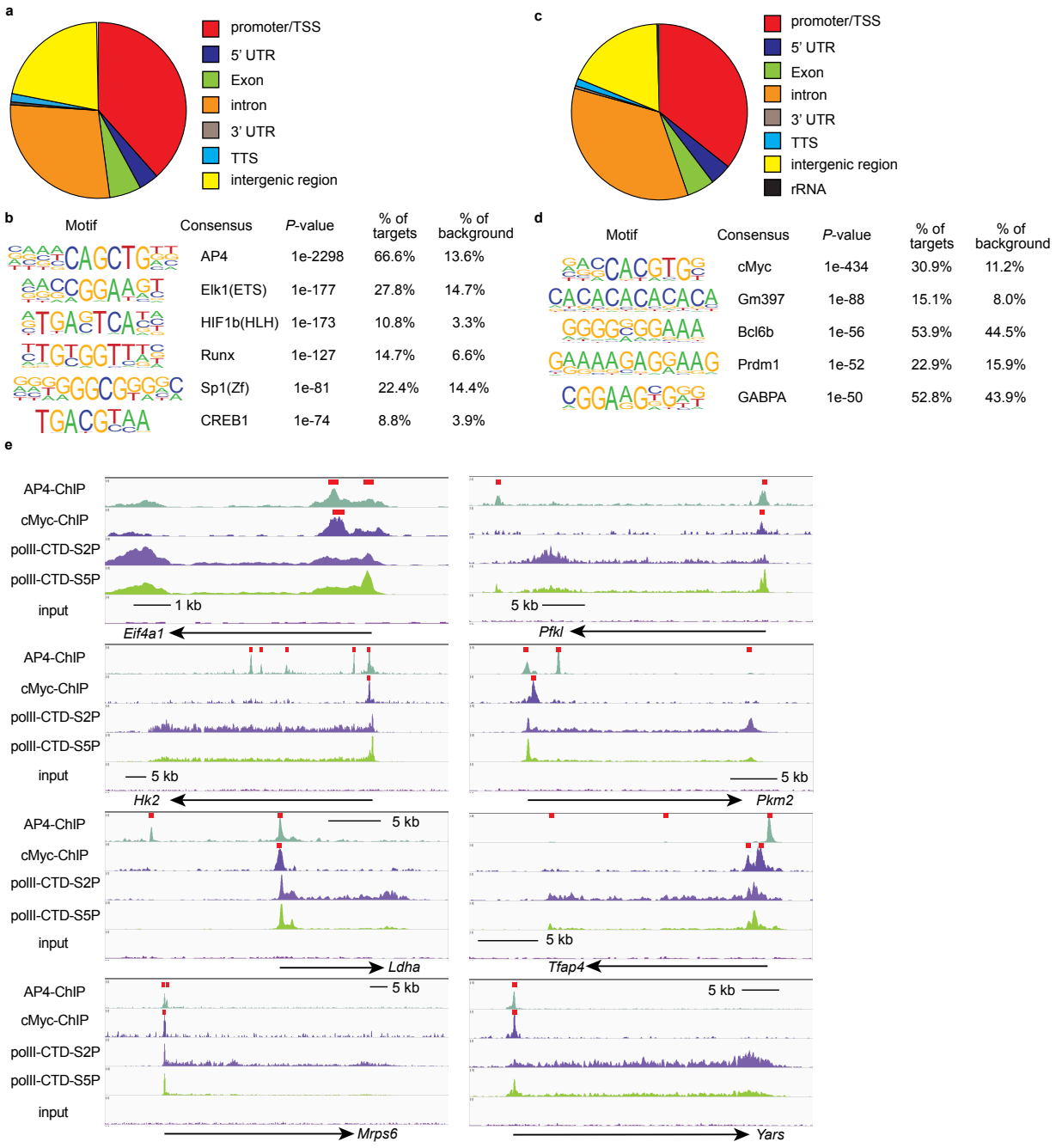

Figure 2.22. ChIP-sequencing analysis identifies AP4 and c-Myc target genes in CD8$^+$ T cells. (a-d) Annotation and motif analysis of genomic sequences bound by AP4 **(a,b)** or c-Myc **(c,d)** in activated C57BL/6 CD8$^+$ T cells. **(e)** Examples of AP4 and c-Myc binding to genes that are differently expressed between *Tfap4*$^{-/-}$ and *Tfap4*$^{+/+}$ OT-I T cells in vivo. BedGraph histograms are shown with statistically significant peaks as red rectangles. P < 1 × 10-10 for anti-AP4 ChIP, P < 5 × 10-9 for anti-c-Myc ChIP by Poisson distribution. ChIP-seq data for RNA polymerase II C-terminal domain (polII-CTD) serine phosphorylations (S2P and S5P) are shown as reference to transcribed regions. Data are from one experiment.

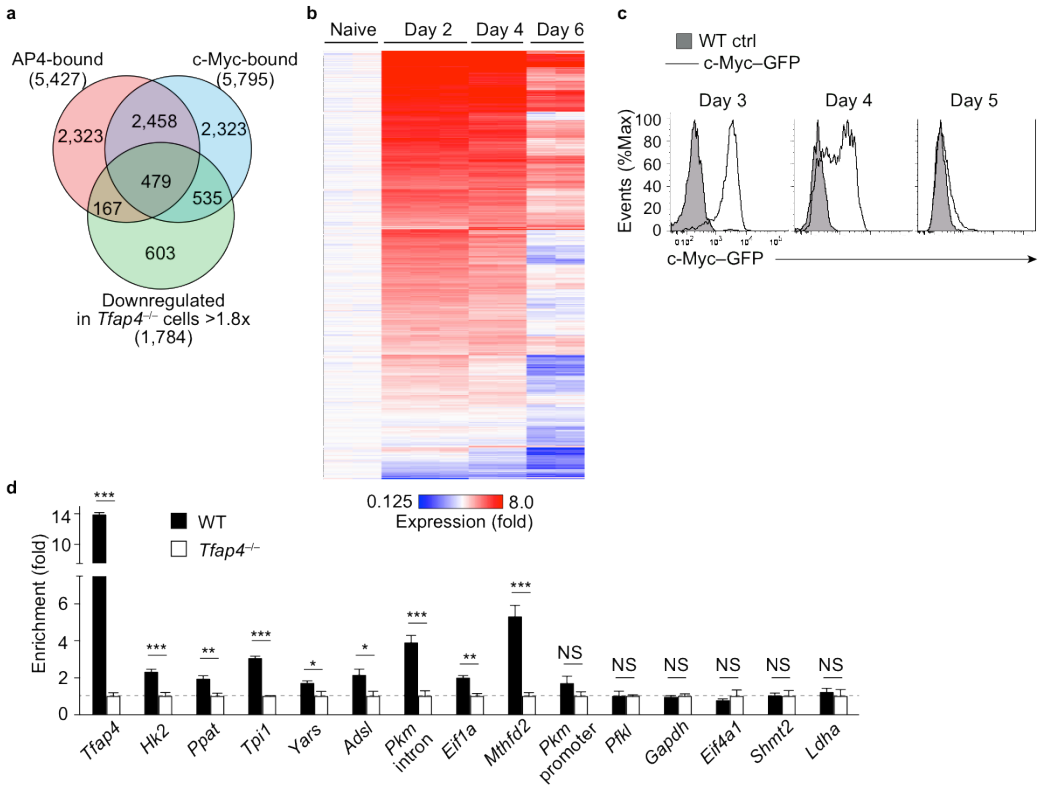

Figure 2.23. AP4 is essential for the sustained expression of genes that are targets of c-Myc. **(a)** Overlap of AP4-bound genes, c-Myc-bound genes and genes expressed differently in *Tfap4*$^{-/-}$ cells relative to their expression in *Tfap4*$^{+/+}$ cells. **(b)** Kinetics of expression of the 479 genes identified in d (middle) in *Tfap4*$^{+/+}$ OT-I T cells adoptively transferred into host mice and assessed before (Naive) and on days 2, 4 and 6 after infection of the host with LM-OVA; results are presented relative to those of naive cells, set as 1. **(c)** Fluorescence of GFP in *Tfap4*$^{+/+}$ P14 T cells (WT ctrl) and P14 T cells carrying a knock-in allele encoding c-Myc−GFP (c-Myc−GFP), adoptively transferred together into host mice and assessed by flow cytometry on days 3−5 after infection of the host with LCMV-Arm. **(d)** ChIP and quantitative PCR analysis of the binding of AP4 to genes targeted by both AP4 and c-Myc in *Tfap4*$^{+/+}$ P14 T cells adoptively transferred into host mice and assessed on day 5 after infection with LCMV-Arm; results are presented as 'enrichment' relative to the binding in their *Tfap4*$^{-/-}$ counterparts, set as 1 (dashed line). *P < 0.05, **P < 0.01 and ***P < 0.001 (unpaired *t*-test).

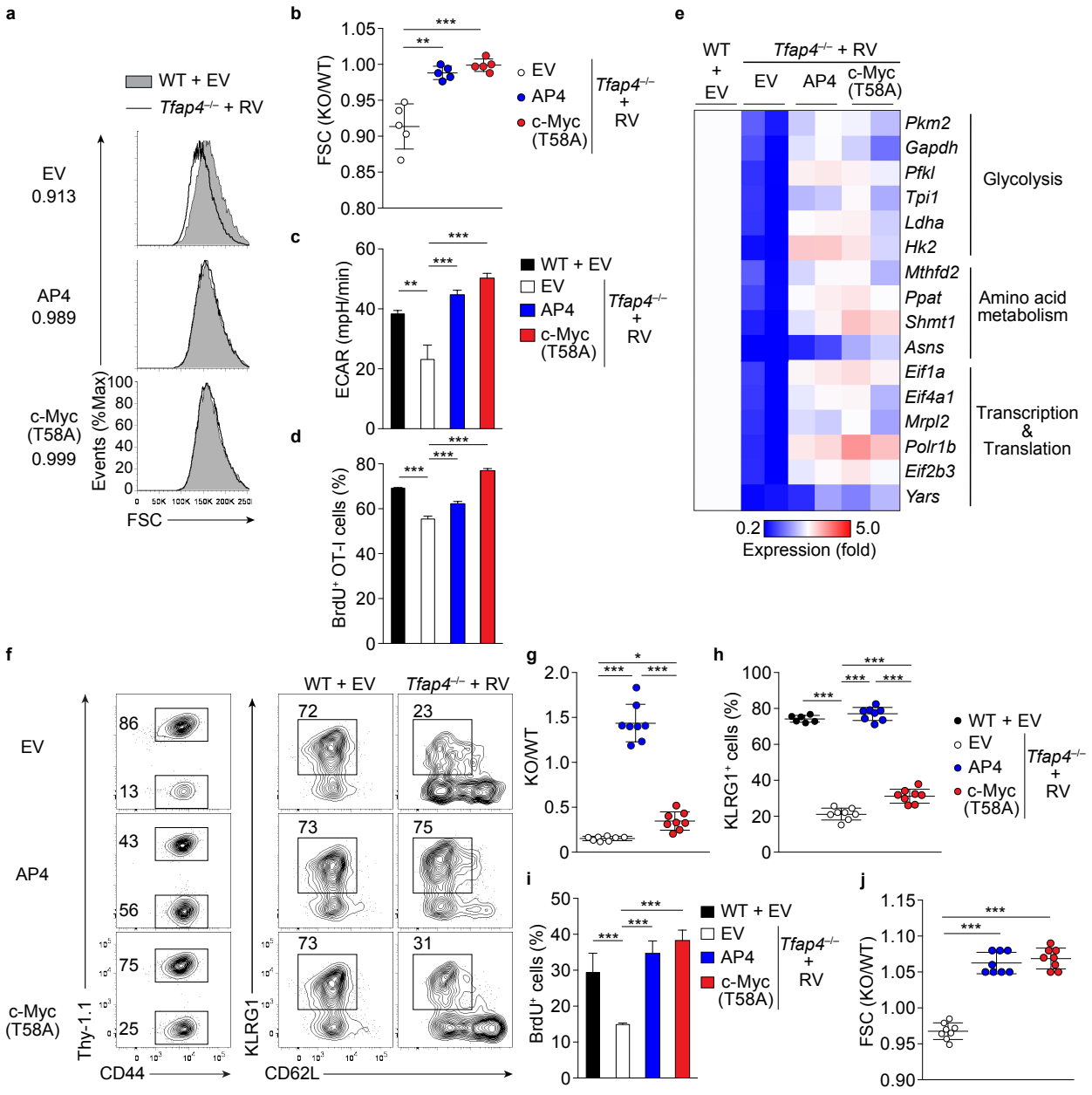

Figure 2.24. Sustained c-Myc expression 'rescues' defects of *Tfap4*$^{-/-}$ CD8^{+} T cells. (a) Flow cytometry of *Tfap4*$^{+/+}$ OT-I (control) T cells transduced with retrovirus containing an empty vector (WT $^{+}$ EV) cultured with *Tfap4*$^{-/-}$ OT-I T cells (KO + RV) transduced with that retrovirus or retrovirus containing a vector for the expression of AP4 or c-Myc(T58A) (left margin). Numbers along left margin indicate ratio of the forward scatter of *Tfap4*$^{-/-}$ OT-I T cells to that of *Tfap4*$^{+/+}$ OT-I T cells. **(b)** Ratio of the forward scatter of *Tfap4*$^{-/-}$ OT-I T cells to that of *Tfap4*$^{+/+}$ OT-I T cells (all transduced as in a). **(c,d)** ECAR **(c)** and incorporation of BrdU **(d)** of *Tfap4*$^{+/+}$ and *Tfap4*$^{-/-}$ OT-I T cells transduced as in a. **(e)** Quantitative RT-PCR analysis of genes targeted by both AP4 and c-Myc (encoding molecules in various pathways (right margin)) in *Tfap4*$^{+/+}$ and *Tfap4*$^{-/-}$ OT-I T cells transduced as in **(a)**; results were normalized to those of 'spiked-in' RNA ERCC-108 and are presented relative to average results for the *Tfap4*$^{+/+}$ OT-I T cells. **(f)** Expression of Thy-1.1 and CD44 (left) and of KLRG1 and CD62L (right) in *Tfap4*$^{+/+}$ (Thy-1.1^{+})

and *Tfap4*$^{-/-}$ (Thy-1.1^{-}) OT-I T cells transduced as in **(a)** and adoptively transferred into congenic wild-type host mice, assessed by on day 6 after infection of the host with LM-OVA. Numbers adjacent to outlined areas indicate percent cells in each. **(g–j)** Ratio of *Tfap4*$^{-/-}$ OT-I T cells to *Tfap4*$^{+/+}$ OT-I T cells (KO/WT), all transduced as in **(a) (g)**, and frequency of KLRG1^{+} cells **(h)**, incorporation of BrdU **(i)** and FSC ratio (as in b) **(j)** among *Tfap4*$^{+/+}$ and *Tfap4*$^{-/-}$ OT-I T cells transduced as in **(a)**. Each symbol **(b,g,h,j)** represents an individual mouse; small horizontal lines indicate the mean (± s.d.). *$P < 0.05$, *$P < 0.01$ and ***$P < 0.001$ (one-way ANOVA). Data are representative of five **(a)**, three **(c)** or two (d,f) experiments or are pooled from three **(b)** or two **(e,g–j)** experiments (error bars **(c,d,i)**, s.d.).

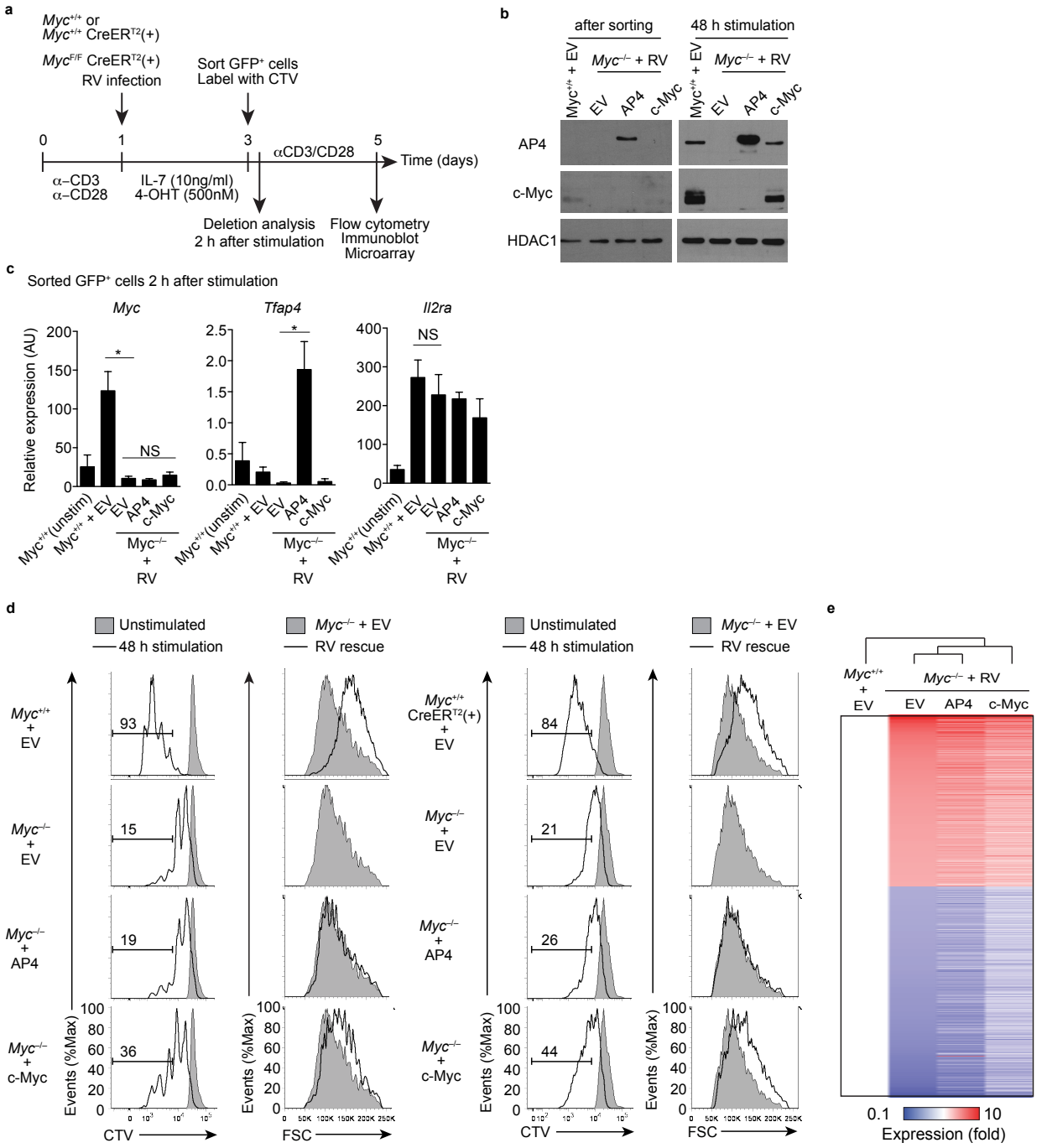

Figure 2.25. AP4 and c-Myc have distinct biological functions. (a) An experimental scheme to retrovirally express AP4 in Myc-deficient CD8$^+$ T cells. Myc$^{F/+}$Cre$^-$ (Myc$^{+/+}$) or Myc$^{+/+}$Rosa26-Cre-ERT2 and Myc$^{F/F}$Rosa26-Cre-ERT2 (Myc$^{-/-}$ after 4OHT treatment) CD8$^+$ T cells were transduced with empty-, FLAG-tagged AP4-, or Myc-expressing RV after activation with anti-CD3 and anti-CD28 for 24 h, and subsequently cultured in media containing IL-7 (10 ng/ml) and 4-hydroxytamoxifen (4OHT, 500 nM) for 2 days. Transduced cells (GFP$^+$) were sorted, labeled with the division-tracking dye CellTraceTM Violet (CTV), and restimulated with anti-CD3 and anti-CD28 for two days. **(b)** Immunoblot showing c-Myc and AP4 expression 48 h after re-stimulation under the same conditions. n = 2. **(c)** Quantitative RT-PCR analysis showing

the abundance of transcripts encoding Myc, *Tfap4*, or *Il2ra* after re-stimulation for 2 h. (n = 3). **(d)** Flow cytometry showing CTV fluorescence and FSC of RV-transduced $Myc^{+/+}$, $Myc^{+/+}$ Cre-ERT2($^{+}$) and $Myc^{-/-}$ CD8 T cells shown as histogram overlays. (n = 3). **(e)** Microarray analysis of $Myc^{+/+}$ and $Myc^{-/-}$ $CD8^{+}$ T cells transduced with AP4- or c-Myc-expressing RV shown as a heat map. Genes that were differently expressed by >2-fold between EV-transduced $Myc^{+/+}$ and $Myc^{-/-}$ cells are shown with the abundance normalized to $Myc^{+/+\ +}$ EV samples. Datasets were analyzed by hierarchical clustering using Euclidean distance matrix with average linkage. (n = 2). Error bars, s.d. * $P < 0.0001$, NS: not significant by one-way ANOVA. Data are representative of two experiments.

CHAPTER 3:

AP4 mediates resolution of chronic viral infection through amplification of germinal center B cell responses.

The contents of this chapter have been previously published in *Immunity*.

Chou C, Verbaro DJ, Tonc E, Holmgrem M, Cella M, Colonna M, Bhattacharya D, Egawa T. AP4 mediates resolution of chronic viral infection through amplification of germinal center B cell responses. *Immunity*. Manuscript accepted.

3.1 ABSTRACT

B cells diversify and affinity-mature their antigen receptor repertoire in germinal centers (GC). GC B cells receive help signals during transient interaction with T cells, yet it remains unknown how these transient T-B interactions sustain the subsequent proliferative program of selected B cells that occurs in an anatomically distant area. Here we show that the transcription factor AP4 is required for sustained GC B cell proliferation and subsequent establishment of a diverse and protective antibody repertoire. AP4 is induced by c-MYC during the T-B interactions, maintained by T cell derived IL-21 and promotes repeated rounds of divisions of selected GC B cells. B cell specific deletion of AP4 resulted in reduced GC sizes and somatic hypermutation and a failure to control chronic viral infection. These results indicate that AP4 integrates T cell mediated selection and sustained expansion of GC B cells for humoral immunity.

3.2 INTRODUCTION

Upon infection or vaccination, antigen (Ag)-specific lymphocytes that are present at low frequencies under steady-state conditions undergo rapid clonal expansion to increase the magnitude of adaptive immune responses. While expansion of Ag-specific B cells ensures that sufficient quantities of antibodies are made, it also serves as a template for somatic hypermutation (SHM), affinity maturation, and the subsequent generation of protective humoral memory for long-term immunity [1, 2]. These proliferating Ag-specific B cells form a specialized compartment in peripheral lymphoid organs, the germinal centers (GCs), in which B cells cyclically migrate between the light zone (LZ) and the dark zone (DZ) for selection and subsequent clonal expansion, respectively [1, 2, 3, 4, 5]. In the LZ, signals from T_{FH} cells facilitate the selection of clones that express B cell receptors (BCRs) with higher affinity for their cognate Ag relative to neighboring clones [2, 3, 6, 7, 8]. The important cues for clonal selection in the LZ include ligation of CD40 on B cells by CD40L on T_{FH} cells, as well as cytokines, especially IL-21 [1, 2, 9, 10, 11, 12, 13, 14]. GC B cells that receive these signals migrate to the DZ, where they rapidly divide multiple times and accumulate somatic mutations in their immunoglobulin (*Ig*) genes [15]. GC B cells can then re-enter the LZ for additional rounds of selection followed by clonal expansion for further affinity maturation [5]. This process allows for the emergence of B cell clones expressing high affinity antibodies that carry multiple *Ig* mutations [16].

The magnitude of expansion of selected B cell clones is programmed by T cell help that B cells receive during their transient interaction with T_{FH} cells in the LZ. Increased amounts of the cognate peptide Ags presented by B cells to T_{FH} cells in the context of MHC class II induce elevated production of cytokines, IL-4 and IL-21 by T_{FH}

cells [17], and facilitate rapid expansion of selected B cells in the DZ and affinity maturation [15, 18]. Thus, the transient T-B interaction in the LZ induces gene expression programs that allow selected B cells to sustain their proliferation in the DZ and establish a diverse BCR repertoire. The transcription factor c-MYC regulates proliferation of both pre-GC B cells and GC B cells, while mutations or translocations of the *Myc* gene are causally linked to GC-derived B cell lymphomas [1, 19, 20]. Although T cell help controls cell cycle progression of selected B cells by inducing c-MYC, expression of this proto-oncogene is detected only transiently in LZ B cells prior to their proliferation in the DZ [5, 18, 19, 20]. Thus, the identity of nuclear factors that are induced during the T-B interaction in the LZ and continue to be expressed in the DZ to potentiate proliferation of selected B cells remains unknown.

In this study, we dissected the genetic program that is activated in selected B cells during their transient interaction with T_{FH} cells in the LZ and supports sustained expansion of B cells in the DZ. Our data demonstrated that the transcription factor AP4 is essential for amplification of GC responses. AP4 is induced by c-MYC in B cells that receive T cell help through the CD40-CD40L interaction and maintained by IL-21 as they migrate toward the DZ. Although AP4 is dispensable for selection of B cells and their cell cycle progression in the LZ, it is essential for DZ B cells to re-enter additional division cycles after completing the one initiated in the LZ. This AP4-dependent proliferation of DZ B cells amplifies the magnitude of GC responses and suffices antibody diversification for protection against chronic viral infection. These results demonstrate that AP4 connects selection and enhanced expansion of Ag-specific B cells that occur in distinct locations in the GC.

3.3 RESULTS

The c-MYC inducible factor AP4 is expressed in both LZ and DZ GC B cells.

A number of transcription factors are upregulated in GC B cells during clonal selection. The expression of one such factor, AP4 (encoded by *Tfap4*), is significantly elevated in GC B cells expressing c-MYC compared to those lacking c-MYC based on previously reported gene expression data **(Figure 1A)** [20]. Indeed, AP4 was induced in CD40-stimulated B cells *in vitro*, but this induction required c-MYC (**Figures 1B and 1C**). c-MYC binds to an intronic region enriched for the H3K27ac enhancer mark in the *Tfap4* locus, suggesting that c-MYC directly regulates *Tfap4* expression (**Figure 1D**). Therefore, we hypothesized that AP4 lies downstream of c-MYC and controls GC B cell proliferation. AP4 protein was detected in splenic GCs, but not in follicular B cells, following immunization with sheep red blood cells (SRBCs) (**Figure 2A**, left), whereas this staining was absent following B cell-specific deletion of *Tfap4* (**Figure 2A**, middle). The majority of $AP4^{+}$ cells were also stained for AID (**Figure 2A**, right), which is expressed in both the LZ and DZ cells in mouse GCs [21]. Within GC, the LZ is marked by the presence of CD23- and CD35-expressing follicular dendritic cells (FDCs) [19, 20, 22]. As reported previously [5, 19, 20], c-MYC-expressing cells were detected exclusively in the LZ (**Figure 2B**, left). In contrast, AP4-expressing cells were distributed in both the LZ and DZ (**Figure 2B**, right). This result was further confirmed by immunoblotting showing AP4 expression in both $CD86^{hi}CXCR4^{lo}$ LZ and $CD86^{lo}CXCR4^{hi}$ DZ GC B populations (**Figure 2C**). AP4 was also expressed in both LZ and DZ cells derived from human tonsillar GCs, while c-MYC expression was detected only in the LZ (**Figure 2D**). We next measured AP4 and c-MYC expression at the single cell level using mice harboring

c-MYC-GFP and AP4-mCherry fusion protein knock-in alleles (**Figures 3A and 3B**) [23]. In the latter strain, mCherry was fused to the C-terminus of AP4, allowing for detection of AP4 by fluorescence with similar kinetics to endogenous protein (**Figures 3C and 3D**). In GC B cells, AP4 protein was specifically detected in mCherry^{+}, but not in mCherry^{-} cells (**Figure 3E**). AP4 was expressed in both LZ and DZ with ~50% of c-MYC^{+} LZ cells being AP4^{+} (**Figures 3F, 4A and 4B**). This was further confirmed by intracellular staining for AP4 in GC B cells (**Figure 4C**). These results suggest that c-MYC induces AP4 in the LZ, and that its expression persists as GC B cells migrate towards the DZ.

AP4 is required for normal GC formation in a B cell-intrinsic manner.

To test whether AP4 is required for GC responses, we immunized *Tfap4*$^{-/-}$ mice with the *T*-dependent Ag 4-Hydroxy-3-nitrophenylacetyl-chicken gamma globulin (NP-CGG). Although AP4 is dispensable for normal B cell development in the bone marrow and spleen (**Figure 5**), the frequencies and numbers of B220^{+}GL7^{+}Fas^{+} GC B cells were reduced in *Tfap4*$^{-/-}$ mice following immunization (**Figures 6A-6C**). This defect was also observed in mixed bone marrow chimeras reconstituted with a mixture of WT and *Tfap4*$^{-/-}$ bone marrow cells (**Figures 6D and 6E**), indicating that diminished GC response was a cell-intrinsic defect. Consistently, a comparable reduction of GC B cell numbers was seen in *Tfap4*$^{F/F}$ Mb1-iCre mice lacking AP4 specifically in B cells [24] (**Figures 6A-6C**). In the absence of AP4, individual splenic GC sizes were smaller (**Figures 6F and 6G**). GC B cell frequencies in Peyer's patches were similarly reduced in the absence of AP4 (**Figures 6H and 6I**). Following immunization with *T*-dependent Ag, c-MYC is expressed in activated B cells in a biphasic manner in pre-GC and GC B cells, and

essential for both initiation and maintenance of GCs [19, 20]. AP4 was also expressed in pre-GC B cells (**Figure 7A**), and B cell expansion was reduced at the pre-GC stage (**Figures 7B and 7C**). However, numbers of total and Ag-binding GC B cells were significantly reduced when AP4 was deleted in ongoing GCs following immunization using Cγ1-Cre [25] (**Figures 8A and 8B**), indicating that AP4 is cell-intrinsically required for the maintenance of GCs. This conclusion was further validated by a similar result observed when AP4 was deleted in GC B cells by Tamoxifen with the majority of T_{FH} cells retaining intact AP4 (**Figures 8C-8F**). In contrast, AP4 was dispensable for a *T*-independent response to NP-Ficoll (**Figure 9**), the formation of memory B cells (**Figure 10A**) and bone marrow antibody secreting cells (**Figure 10B**). These results indicate that AP4 cell-autonomously regulates both GC initiation and maintenance.

AP4 deficiency results in reduced proliferation of DZ B cells.

GC B cells induce c-MYC upon selection in the LZ [19]. The c-MYC induction was unimpaired in *Tfap4*$^{-/-}$ mice compared to control WT mice (**Figure 11A**), indicating that AP4 is dispensable for selection of LZ GC B cells. AP4 expression marked actively cycling cells both in the LZ and DZ B cell populations (**Figure 11B**). A considerable fraction of AP4^{+} LZ cells were in the S-phase with a reciprocal reduction of cells in the G1-phase, consistent with previous reports that c-MYC^{+} cells are actively cycling [19, 20]. AP4^{+} DZ cells, which no longer expressed c-MYC, were also enriched for cells in S and G2/M phases of cell cycle, suggesting that continued expression of AP4 supports proliferation of selected GC B cells in the DZ. To assess whether AP4 is required for selected GC B cells to re-enter additional division cycles in the DZ after completing a

cycle initiated in the LZ, we examined sequential incorporation of EdU and BrdU [15] by *Tfap4*$^{-/-}$ and control *Tfap4*$^{+/+}$ GC B cells in mixed bone marrow chimeras (**Figure 11C**). In the LZ, similar proportions of *Tfap4*$^{-/-}$ and *Tfap4*$^{+/+}$ cells were distributed in distinct cell cycle phases. In contrast, frequencies of DZ cells in the early and mid/late S-phases were significantly reduced in the absence of AP4. These results indicate that AP4 is dispensable for cell cycle progression initiated in the LZ and an initial division in the DZ, but is necessary to promote subsequent divisions. As EdU and BrdU incorporation by CD45.1 WT GC B cells was comparable between *Tfap4*$^{-/-}$ and control mixed chimeras (**Figure 11D**), the requirement for AP4 in the cell cycle re-entry was cell-intrinsic. AP4 thus amplifies proliferation of DZ B cells by promoting their re-entry to additional division cycles. Paradoxically, however, LZ to DZ cell number ratios were unaltered in the absence of AP4 (**Figure 12**) presumably because impaired expansion of DZ cells may reduce DZ to LZ trafficking of GC B cells, affecting cellularity in both zones.

AP4 sustains GC B cell activation in the DZ.

We next defined AP4-dependent gene regulatory programs for GC B cell expansion by profiling gene expression in c-MYC^{+}AP4^{+} LZ cells and AP4^{+} DZ cells along with c-MYC^{-}AP4^{-} LZ cells (pre-selection LZ cells) and AP4^{-} DZ cells (post-mitotic DZ cells) (**Figure 13A**). Since AP4 was expressed in a small fraction of GC B cells, this method would better define AP4-dependent gene expression than directly comparing AP4-sufficient and -deficient GC B cells. A similar approach was used to determine c-MYC target genes [20]. Consistent with their active cell cycle status (**Figure 11B**), c-MYC^{+}AP4^{+} LZ and AP4^{+} DZ cells were larger in size compared to total LZ and

DZ cells, respectively (**Figures 13A and 13B**). Gene expression profiling by RNAseq identified ~1,200 genes upregulated in c-MYC^{+}AP4^{+} relative to c-MYC^{-}AP4^{-} LZ cells by more than 1.8-fold, which were clustered into three groups (**Figure 13C**). Among these genes, those in Cluster I were more highly expressed in AP4^{+} than AP4^{-} DZ B cells and thus predicted to be relevant to AP4-dependent GC B cell expansion. Genes in Clusters II and III were expressed similarly in AP4^{+} and AP4^{-} DZ B cells and included *Myc* and known c-MYC-target genes, such as *Batf*, *Irf4*, and *Ccnd2* [20]. Genes in Cluster I were enriched for those in pathways related to protein translation and metabolism (**Figure 13D**). ChIPseq analysis for AP4 and c-MYC binding using purified GC B cells and activated B cells *in vitro*, respectively, revealed that ~75% and ~60% of genes in the ribosome and metabolic pathways were directly bound by c-MYC and AP4, respectively, with ~50% and ~20% of those being common direct targets of c-MYC and AP4 (**Figures 13E and 14**). These data suggest that c-MYC and AP4 sequentially sustain transcription of genes in ribosome biogenesis and metabolic pathways in selected GC B cells. Interestingly, however, AP4 overexpression was insufficient to fully compensate for c-MYC deficiency in B cells cultured in a condition mimicking GC differentiation [26] (**Figure 15**). This result suggests that AP4-dependent proliferation program requires prior c-MYC expression.

AP4 is required for accumulation of somatic mutations.

Since expansion of GC B cells is essential for accumulation of somatic mutations and diversification of *Ig* repertoires, we next determined the frequencies of mutations in the J_H4-adjacent intronic region of *Igh* [27]. The overall frequencies of mutations and the

frequencies of clones carrying multiple mutations following NP-CGG immunization were substantially decreased in the absence of AP4 (**Figures 16A and 16B**). The mutation frequency in the V_H186.2 BCR, which is over-represented in NP-reactive B cell clones [28, 29], was also reduced (**Figure 16C**). However, *Aicda* mRNA expression was unaltered and frequencies of class switched IgG_1^+ GC B cells were increased in the absence of AP4 (**Figures 16D and 16E**), suggesting that reduced somatic mutation unlikely resulted from impaired AID activity. The binding avidity of BCR to NP and the surrogate Ag 4-hydroxy-3-iodo-5-nitrophenylacetic acid (NIP) and the frequencies of NP- and NIP-binding clones expressing an Igλ light chain [28], as well as NP-specific Igλ antibody titers in serum, were modestly reduced in the absence of AP4 (**Figures 17A-17C and 18A-18K**). However, the frequencies of V_H186 BCR clones carrying the affinity-enhancing W33L mutation and the ratio of titers between high-affinity anti-NP_4 to low-affinity anti-NP_{15} IgG_1 were comparable between *Tfap4*$^{-/-}$ and control GC B cells (**Figures 17D and 18L**). These results suggest that AP4 promotes expansion of selected GC B cells, thus diversifying BCR repertoires through somatic hypermutation, although it is dispensable for the selection of high-affinity clones and affinity maturation of anti-NP antibodies.

AP4 is required for control of chronic viral infection.

Our results demonstrate that AP4 contributes to diversification of BCR repertoire by promoting expansion of DZ GC B cells. Antibody diversification and accumulation of somatic mutations are critical for the generation of protective antibodies against chronic viral infections in mammals, as exemplified by broadly neutralizing antibodies (bnAbs) against HIV that harbor high frequencies of mutations [30, 31]. These bnAbs against HIV

emerge years after the initial infection, raising the possibility that maximal diversification of the BCR repertoire by GCs as the virus mutates is essential for their emergence [32]. In mice, the generation of high affinity antibodies during GC responses is required for control of chronic LCMV infection [33, 34]. LCMV clone 13 (LCMV-c13) infection of *Tfap4*$^{F/F}$ Mb1-iCre mice induced GC formation; however, the numbers and frequencies of GC B cells were significantly reduced compared to control *Tfap4*$^{F/F}$ Cre(–) mice (**Figures 19A and 19B**) despite normal numbers of CXCR5^{+}PD-1^{+} T_{FH} cells in the mutants (**Figures 20**). Consistent with previous studies [33, 35], the serum viral titers in control mice started to decline 30 days after infection, and viremia was mostly resolved by day 100 (**Figure 21A**). In *Tfap4*$^{F/F}$ Mb1-iCre mice, despite comparable viremia 7 days post-infection, viral loads remained high until day 100 (**Figure 21A**). Similarly defective control of viremia was seen in *Tfap4*$^{F/–}$ AID-Cre compared to *Tfap4*$^{F/+}$ AID-Cre mice (**Figure 21B**). These results indicate that AP4 expression in B cells is essential for control of chronic LCMV infection. Consistent with the presence of GCs in *Tfap4*$^{F/F}$ Mb1-iCre mice, AP4 was dispensable for the production of class switched anti-LCMV antibodies (**Figure 22**). However, AP4-deficient GC B cells accumulated reduced numbers of mutations (**Figure 23A**). Consequently, heat-inactivated immune sera from *Tfap4*$^{F/F}$ Mb1-iCre mice were minimally able to neutralize LCMV *in vitro*, in sharp contrast to their WT counterparts (**Figures 23B and 23C**). These results demonstrate that induced and sustained AP4 expression in Ag-specific B cells is required for maximizing the magnitude of GC responses and for generating protective antibodies against viral infections.

AP4 is sustained by IL-21R signals following induction by c-MYC.

The finding that AP4 is induced by c-MYC in selected GC B cells, but is maintained longer than c-MYC, suggests that help signals derived from T_{FH} cells may sustain AP4 expression during migration of LZ B cells towards the DZ. To test this, we first induced c-MYC-dependent AP4 expression in B cells by co-culturing them on NIH3T3 feeders engineered to express CD40L at a level comparable to activated $CD4^+$ T cells (**Figure 24A**). Under these conditions, both c-MYC and AP4 protein levels increased rapidly (**Figure 24B**). During GC reactions, selected B cells contact T_{FH} cells and receive survival and proliferative signals through a CD40-CD40L ligation, and subsequently lose this contact as they migrate to the DZ [2, 5, 6, 11, 12, 13, 14, 36]. Indeed, deprivation of CD40 stimulation reduced AP4 expression at both transcript and protein levels (**Figures 24B and 24C**). Importantly, subsequent stimulation of the CD40-primed cultured B cells with IL-21 sustained AP4 expression despite the absence of c-MYC protein, while T_{FH}-derived cytokines, IL-4 and IFN-g, showed only a modest and no effect, respectively (**Figure 24B**). IL-21 increased the level of AP4 in a dose-dependent manner (**Figures 24D and 24E**). IL-21 was also sufficient to sustain AP4 expression in cultured GC B cells *ex vivo* following stimulation with CD40L (**Figure 24F**). However, IL-21 was insufficient to increase the AP4 level without priming of B cells with CD40L (**Figure 25A**). Furthermore, co-stimulation of B cells with IL-21 and CD40L reduced AP4 mRNA levels compared to CD40L stimulation alone, although its protein levels were not changed possibly due to compensation by IL-21-mediated elevation of protein translation (**Figure 25B and 25C**). Thus, IL-21 can maintain AP4 expression after c-MYC expression is downregulated in B cells *in vitro*. In addition to upregulation of AP4

mRNA (**Figure 24C**), global protein translation as measured by a puromycin pulse labeling [37] was markedly elevated by IL-21 (**Figure 24B**). Interestingly, IL-21-mediated increase of protein translation was reduced in AP4-deficient B cells (**Figure 26A**). Therefore, prior expression of AP4 induced by CD40 signals and c-MYC amplifies the effect of IL-21 on protein translation, including accumulation of its own protein, which may be retained in a subset of DZ cells passively or post-transcriptionally. IL-21 is also necessary for upregulation of *Bcl6* and *Aicda* transcripts [9, 38]. However, expression of these genes were not affected in IL-21 stimulated *Tfap4*$^{-/-}$ B cells *in vitro* (**Figures 26B and 26C**), indicating that AP4 plays a targeted role in controlling the IL-21-dependent GC B cell program.

To validate this finding *in vivo*, we generated bone marrow chimeras by reconstituting mice with a mixture of bone marrow cells from *Igh*$^{-/-}$ (75%) and *Il21r*$^{-/-}$ (25%) mice (**Figure 27A**). In the resulting chimeras, all B cells were exclusively derived from *Il21r*$^{-/-}$ bone marrow cells, while a large proportion of non-B cells, including T_{FH} cells, were sufficient for *Il21r* (**Figures 27B-27E**). Consistent with previous reports [9, 10], GC responses were blunted in bone marrow chimeras with *Il21r*$^{-/-}$ B cells following NP-CGG immunization, with a significant reduction in the levels of *Bcl6* and *Aicda* transcripts compared to control chimera with *Il21r*$^{+/+}$ B cells (**Figure 28**). In these chimeras, *Il21r*$^{-/-}$ LZ B cells expressed significantly reduced *Tfap4*, but not *Myc* transcripts compared to *Il21r*$^{+/+}$ LZ B cells (**Figure 29**). *Ccnd3*, a direct AP4 target in GC B cells (**Figures 13E and 14**), was also downregulated in *Il21r*$^{-/-}$ GC B cells (**Figure 29A**). While frequencies of c-MYC^{+} cells were similar between *Il21r*$^{-/-}$ and *Il21r*$^{+/+}$ GCs, frequencies of AP4^{+} cells as well as AP4 protein levels were markedly diminished in both

LZ and DZ of *Il21r*$^{-/-}$ GCs (**Figures 29B-29D**). Furthermore, early and mid/late S-phase cells in the DZ, but not in the LZ, were reduced in the absence of IL-21R signals, which is similar to the phenotype observed in AP4-deficient GCs (**Figures 30A and 30B**). Thus, IL-21 amplifies GC response through sustaining AP4 expression.

3.4 DISCUSSION

In the present work, we have defined a molecular mechanism by which T cell help signals received in the LZ programs repeated rounds of proliferation of selected GC B cells in the anatomically distant DZ. Studies using a DEC205-targeted Ag-delivery demonstrated that amounts of cognate Ag that GC B cells capture and present to T_{FH} cells in the LZ regulate the magnitude of expansion of the selected B cells in the DZ through upregulation of c-MYC target genes [15, 18]. However, expression of c-MYC is restricted to a small subset of LZ GC B cells, and it thus remains unknown how GC B cell proliferation initiated in the LZ is sustained in the DZ after they lose contact with T_{FH} cells and expression of c-MYC. Our results indicate that AP4 connects the selection in the LZ to sustained proliferation in the DZ. AP4 is induced by CD40 signals in a c-MYC-dependent manner and its expression is maintained after the c-MYC decay. AP4 is maintained by the cytokine IL-21, which is upregulated in T_{FH} cells during their transient interaction with Ag-presenting GC B cells [17]. IL-21 may continue to provide T cell help to selected B cells during the T-B interaction and during their migration towards the DZ to express important genes for GC reactions, including AP4. This effect is mediated at the transcriptional level, and also at the translational level in part in an AP4-dependent manner. Thus, IL-21 may specifically act on selected B cells that have upregulated AP4. However, it may not reach the DZ B cells since IL-21R-dependent upregulation of AP4 at the transcript level was observed only in the LZ B cells.

GCs are essential for the generation of protective antibodies that accumulate multiple somatic mutations in their *Ig* genes. Recent studies identified bnAbs against HIV that are characterized by substantially high quantities of somatic hypermutations [32],

suggesting that enhanced BCR diversification by sustained GC responses is critical for the generation of these antibodies. Strains of LCMV have been used to study both humoral and cellular immune responses against chronic viral infection in mice. GC responses and expression of AID are essential for the control of chronic LCMV infection [33, 34]. Our data indicate that AP4-mediated durable GC response is required for the control of chronic LCMV infection in a B cell-intrinsic manner. This was evidenced by reduced accumulation of somatic mutations and the impaired development of antibodies with neutralizing activities in the absence of AP4. Although these results indicate that AP4 is required for diversification of antibody repertoire and subsequent affinity maturation, AP4 deficiency had no substantial impact on antibody affinity maturation to NP. This can be explained by recent reports that anti-hapten antibody affinity is robustly increased by a few dominant mutations, whereas affinity maturation against complex protein Ag requires sequential accumulation of many mutations during GC reaction [39, 40].

We previously demonstrated that AP4 maximizes acute $CD8^+$ T cell responses by sustaining c-MYC-initiated gene expression program [41]. Together with our current study, both T and B cells seem to be dependent on restricted c-MYC expression and subsequently utilize its downstream factor AP4 to achieve the maximal magnitude of adaptive immune response. After induction by c-MYC, expression of AP4 is sustained in an IL-2 or IL-21-dependent manner in $CD8^+$ T or GC B cells, respectively, and compensates for the early termination of c-MYC expression [41]. It is unclear why activated lymphocytes utilize c-MYC only for a brief window and terminate its expression prematurely before the completion of their clonal expansion. Although c-MYC is critical for the establishment of highly proliferative states of lymphocytes upon Ag receptor

stimulation, prolonged expression of c-MYC may make the cells prone to apoptosis [42] or increase the risk of transformation in the presence of genotoxic stress during GC responses. Aberrant expression of c-MYC has been causally linked to increased incidence of pre-B cell leukemia and B cell lymphoma [43]. The *Myc* locus is also efficiently targeted by AID [44]. Therefore, restriction of c-MYC at both protein and transcript levels may be necessary to prevent transformation during GC responses, although extensive lymphocyte proliferation is critical for protection against virulent pathogens.

Collectively, our results demonstrate that direct T cell help during the T-B interaction and potential remote help mediated by IL-21 sequentially induce transient expression of c-MYC and sustained expression of AP4 to drive sufficient expansion of GC B cells following clonal selection by T_{FH} cells. Such sustained GC responses are necessary for the generation of mutated antibodies with protective activity against chronic viral infection in the mouse model and may also be important for the generation of the anti-HIV bnAbs in humans. In conjunction with our previous study, the current data suggest that activated B and T cells both utilize a transcription factor cascade in which c-MYC hands off its role to AP4, a relay that is required to maximize clonal expansion to drive effective antiviral immunity.

3.5 MATERIALS AND METHODS

Mice

C57BL/6N and B6-CD45.1 mice were purchased from Charles River Laboratory. *Rosa26*-CreER^{T2} mice [45], Cγ1-Cre mice [25], AID-Cre mice [46], *Igh*$^{-/-}$ (μMT) mice [47], and *Il21r*$^{-/-}$ mice [48] were purchased from the Jackson Laboratory. *Tfap4*^{F} [41], *Tfap4*$^{-}$ [49], *Myc*^{F} [50], Mb1-iCre [24] and *Myc*^{GFP} [23] alleles have been described. A *Tfap4*^{mCherry} allele was generated by inserting a sequence encoding the mCherry fluorescence protein to the carboxyl terminus of AP4. A targeting vector was constructed with 5-kb 5' homologous and 5-kb 3' homologous arms cloned into a targeting cassette containing HSVtk and loxP-flanked *Pgk* Neo^{r} selection cassettes. *Not*I linearized targeting vector DNA was electroporated into JM8.N4 ES cells (KOMP Repository), and G418/Gancyclovir double-resistant clones were screened for homologous recombination by Southern blotting. Targeted ES cells were injected into B6(Cg)-*Tyr*$^{c-2J}$ blastocysts, and chimeric males were crossed to EIIa-cre females [51] (Jackson Laboratory) to obtain germ-line transmission and to delete the selection cassette. For the experiments with bone marrow chimeras, B6-CD45.1 mice were lethally irradiated (10.5 Gy) and reconstituted with donor bone marrow cells for at least 8 weeks before experiments. All mice were maintained in the C57BL/6 (B6) background, were housed in a specific pathogen-free facility at Washington University in St. Louis, and were analyzed at 6–14 weeks of age unless stated otherwise. Both sexes were included without randomization or blinding. All experiments were performed according to a protocol approved by Washington University's Animal Studies Committee.

Human tissue samples

Tonsils were obtained from routine tonsillectomies performed at the Barnes-Jewish Hospital according to a protocol approved by an Internal Review Committee at Washington University School of Medicine.

LCMV Infection

Mice were infected with 2 x 10^6 plaque-forming units (PFU) of LCMV-c13 by intravenous injection. For the quantification of serum viral load, RNA was extracted from 10 μl of serum from LCMV-infected mice using Trizol. 1 μl of ERCC RNA Spike-In Control Mixes, at a concentration of 1:10,000, was added to the lysate before RNA extraction and reverse transcription. The level of the LCMV NP transcript relative to that of 'spiked-in' RNA was determined by real-time quantitative RT-PCR using the primers previously described [41, 52]. I*n vitro* neutralization assay was performed according to a previously described protocol with some modifications [53]. Vero cells were plated at 5 x 10^4 cells per well in a flaT-Bottom 96-well plate one day before infection. Hea*t*-inactivated (one hour at 55 °C) sera from LCMV-infected and control mice were serially diluted with media and incubated with an equal volume of viral supernatant containing 300 PFU of LCMV clone 13 at 37 °C for 90 min. Infectivity of the mixtures was determined by intracellular staining for LCMV NP of Vero cells that were incubated with the mixture for 48 hours [54]. For each dilution of serum samples, the percentage of LCMV NP^+ Vero cells treated with LCMV-immune serum was normalized to that treated with control serum. A neutralization curve and an EC_{50} value for each sample were obtained

using the non-linear fit equation "log (inhibitor) vs. normalized response -- variable slope" in Prism 6 software (Graphpad).

Immunization protocols and treatments

Mice were immunized with either ~8-10 x 10^8 SRBC (Lampire), 100 μg of NP-conjugated chicken gamma globulin (NP-CGG, Biosearch) precipitated in alum, or 100 μg of NP-Ficoll (Biosearch) in PBS by intraperitoneal injection. NP- and NIP-APC were prepared by conjugating allophycocyanin (Sigma-Aldrich) with NP or NIP ester (Biosearch) as previously described [55].

***In vitro* B cell culture**

CD40L-expressing feeders were generated by infecting NIH-3T3 cells with a retrovirus expressing CD40L and sor*t*-purified based on surface CD40L expression. The feeders were seeded in RPMI-1640 supplemented with 10% FBS (Gibco) at a density of 4 x 10^6 cells per 6-, or 12- well plate, or 100mm dish one day before adding splenic B cells purified from B6 mice using anti-CD19-microbeads (Miltenyi). B cells were removed from feeders by gentle shaking and pipetting. For liquid culture of B cells, CD40L-activated B cells were incubated in medium containing IL-4 (eBioscience), IL-21 (Peprotech), or IFN-γ (Peprotech) for additional 16-18 hours. To measure protein translation, B cells were treated with 10 μg/ml of puromycin (Sigma) for 10 min at 37°C before lysis. CD40L- and murine BAFF-expressing feeders [26] were used for culturing of GC B cells *ex vivo*.

Real-time quantitative RT-PCR

RNA was extracted with Trizol (Life Technologies) and was reverse-transcribed with qScript Supermix (Quanta Bio). DyNAmo ColorFlash SYBR green qPCR mix (Thermofisher) and a LightCycler 480 (Roche) were used for real-time quantitative RT-PCR. Quantities of transcripts were normalized to that of 18S ribosomal RNA unless specified otherwise. For quantification of gene expression normalized to that of 'spiked-in' RNA, 1 μl of ERCC (External RNA Controls Consortium) RNA Spike-In Control Mixes (Ambion) was added at a dilution of 1:10,000 to lysates from 1×10^6 cells prior to RNA extraction. Primers for 18S-rRNA, ERCC-00108, LCMV-NP, *Tfap4*, *Myc* and *Bcl6* were described previously (Chou et al., 2014). The following primers were used:

Aicda, CGTGGTGAAGAGGAGAGATAGTG and
CAGTCTGAGATGTAGCGTAGGAA;

Atic, CGTCTCTTGGTTTGAGTCTGGT and GGAACCCTGTTAGCTCAGACAC;

Cad, GTACGAAGATTGGGAGTTGCAT and CTACGCAGTTCTCATCGACCAT;

Ccnd2, CAGACCTTCATCGCTCTGTG and CGTGAGTGTGTTCACTTCATCA;

Ccnd3, GAAGATGCTGGCATACTGGAT and CCAGGTAGTTCATAGCCAGAGG;

Eif3b, AGGATTTCGTAGACGACGTGAG and CCGATCTTTGAGTACATCACCA;

Eif4g1, CCTACCGAGTTTGGGACCTAT and ACTAGCAGGAAACTGCTGCAC;

Gar1, TGTCAGAAAACATGAAGGCATC and GCAGCAGCTTGTATGGGTCTAT;

Gart, AGTCTCCTCAGGTCAAGCAAGT and GCACTGTGATCATTGACAGAGAC;

Il21r, TCTGAGAAAGACCCTGAAGGAG and CATGGAGAATCAGCAGGAGTAA

Lap3, AGTGAGAGGTCTCTGGGATCG and TTGTAAATTGTGGCAGGTCATC;

Lsm2, GGAACTCAAGAATGACCTGAGC and TGAGGGTATTTCTCAGGGTCTG;

Nme1, CGGTAAAGCCTTGTCATCTGAA and CTCGAACCGCTTGATGATCT;

Ran, CAGCACAGTACGAGCATGATTT and CCAGCTTCACTTTCTCACAGGT;

Rpl23, CCACAGTTAAGAAAGGCAAACC and CTATGACCCCTGCGTTATCTTC;

Rpl27, TCCAAGATCAAGTCCTTTGTGA and AACAGTCTTGTCCAAGGGGATA;

Rpl35a, AAAGGCCATTGGACACAGAAT and TAGTTTAAATCCGGGATGGGTA;

Rplp0, TGGAAGTCCAACTACTTCCTCAA and GTTGTCTGCTCCCACAATGAAG;

Rplp2, AATACTAGACAGCGTGGGCATC and TTTCCATTCAGCTCACTGATGA;

Rps10, GGAGGCTGACAGAGACACCTAC and CCTCTAAACTGGAACTCAGTGG;

Rps16, GTCCCCTGGAGATGATCGAG and AGAAGCAAAACAGGCTCCAGTA;

Rps29, ACAGAAATGGCATCAAGAAACC and ATTGTTGGCCTGCATCTTCTT;

Snrpd1, GTGGATGTTGAACCTAAGGTGA and ACCACGTCCTCTTCCTCTACC;

Snrpe, CAAAAGGTGCAGAAGGTGATG and TTCACTTGTTCATACAGCCACA;

Xpot, GCGAGGAAGAGATATTGGAGTG and ATCACAACAGACGTGGCTTCTA.

Flow cytometry

Single-cell suspensions were prepared as described [41]. The following monoclonal antibodies were used in this study: For sorting of GC B cells, splenocytes were stained

with monoclonal antibodies (identified above) before being sorted as $B220^{+}IgD^{-}GL7^{+}Fas^{+}$ cells or $B220^{+}IgD^{-}CD38^{-}GL7^{+}$ on a FACSAria II (BD). For analysis, cells were stained with monoclonal antibodies and were analyzed with an LSRII (BD) or LSR Fortessa (BD), with staining with DAPI (4, 6-diamidino-2-phenylindole; Sigma) or Aqua Live/Dead (L34957, Life Technologies) for the exclusion of dead cells. Intracellular staining of AP4 was performed as previously described [41]. For cell cycle analysis, mice were injected intravenously 1 mg EdU (Sigma-Aldrich), followed by 2 mg BrdU (Sigma-Aldrich) in PBS one hour later as described [15]. Cells were harvested 30 minutes after BrdU injection and processed using an APC BrdU Flow Kit (BD Pharmingen) and a Click-iT Plus EdU Pacific Blue Flow Cytometry Kit (Invitrogen). BrdU was detected using an AF647-conjugated anti-BrdU antibody (MoBU-1, Invitrogen). Data were analyzed with FlowJo software (TreeStar).

Immunofluorescence microscopy

For the detection of AP4 and c-MYC, tissues were fixed in 4% paraformaldehyde at 4 °C over night before embedding in OCT compound (Sakura Finetek). 8 μm sections were cut on a cryostat (Microm HM 550), fixed in ice-cold acetone, and stained. Sections were mounted with ProLong Gold Antifade Mountant with DAPI (P36935, Life Technologies). For the detection of AID, a Tyramide Signal Amplification System (T30955, Life Technologies) was used. Images were acquired with Zeiss AxioCam MRn microscope equipped with an AX10 camera. Subsequent color balancing, overlaying, and area measurements were performed in an ImageJ software (NIH) and Photoshop (Adobe).

Antibodies

The following antibodies were used in Immunofluorescence microscopy: Alexa Fluor (AF) 488-conjugated anti-IgD (11-26c.2a, Biolegend), AF647-conjugated anti-GL7 (GL-7, Biolegend), anti-Rabbit IgG (4414S, Cell Signaling), biotinylated anti-TCRb (H57-597, Biolegend), anti-CD35 (8C12, BD), unconjugated anti-AID (MAID-2, eBioscience), anti-human CD23 (NCL-L-CD23-1B12, Leica), anti-Myc (ab32072, Abcam), anti-AP4 [49]. Secondary reagents: Streptavidin-conjugated AF555 (S32355, Life Technologies), biotinylated anti-Rat IgG (6430-08, Southern Biotech), anti-Mouse IgG_1 (A85-1, BD). The following antibodies were used in Flow cytometry: AF488-conjugated anti-CD86 (GL-1, Biolegend), anti-IgD (11-26c.2a, Biolegend), anti-CD45.1 (A20, Biolegend), anti-CD23 (B3B4, Biolegend); FITC-conjugated anti-GL7 (GL-7, Biolegend); PE-conjugated anti-GL7 (GL-7, BD), anti-CD40L (MR1, Biolegend), anti-Igl (RML-42, Biolegend), anti-CD43 (S7, Biolegend), anti-CD5 (53-7.3, BD), anti-CD93 (AA4.1, Biolegend); PerCP-Cy5.5-conjugated anti-CXCR4 (L276F12, Biolegend), anti-IgG_1 (RMG1-1, Biolegend), anti-IgD (11-26c.2a, Biolegend), anti-B220 (RA3-6B2, Biolegend); PE-Cy7-conjugated anti-Fas (Jo2, BD), anti-B220 (RA3-6B2, Biolegend), anti-CD24 (M1/69, Biolegend); APC-conjugated anti-CD19 (6D5, Biolegend), anti-PD1 (29F.1A12, Biolegend); AF647-conjugated anti-CD45.2 (104, Biolegend), anti-GL7 (GL-7, Biolegend), anti-CD86 (GL-1, Biolegend), anti-IgM (RMM1, Biolegend), anti-CD38 (90, Biolegend); AF700-conjugated anti-CD19 (6D5, Biolegend); APC-Cy7-conjugated anti-CD45.2 (104, Biolegend), anti-B220 (RA3-6B2, Biolegend); Pacific Blue-conjugated anti-IgD (11-26c.2a, Biolegend), anti-B220 (RA3-6B2, Biolegend), anti-CD21/35 (7E9, Biolegend), anti-CD19 (6D5, in house); Brilliant Violet (BV) 510-conjugated anti-B220

(RA3-6B2, Biolegend); BV605-conjguated anti-CD45.1 (A20, Biolegend); and biotinylated anti-CXCR5 (2G8, BD), anti-BP-1 (6C3, Biolegend).

Enzyme-linked immunosorbent assay (ELISA)

Anti-NP antibody titers were assessed using NP_4-BSA (Biosearch), NP_{15}-BSA (Biosearch), biotinylated anti-mouse IgG_1 (A85-1, BD), anti-mouse Igl (1175-08, Southern Biotech), and horseradish peroxidase-conjugated Streptavidin (554066, BD), which was developed with TMB substrate (S1599, Dako). Anti-LCMV antibody titers were measured as previously described using LCMV virion purified on a 20% sucrose cushion, biotinylated anti-mouse IgG_1 antibody and anti-mouse IgG_{2c} antibody (1077-08, SouthernBiotech) [56, 57]. Endpoint titers were calculated by a one-phase exponential decay curve using a Prism 6 software (Graphpad) [58].

Immunoglobulin sequence analysis

An intronic sequence 3' to the J_H4 exon of *Igh* and the $V_H186.2$ sequences were PCR amplified from genomic DNA extracted from 3,000-5,000 GC B cells using Phusion HF (Thermo) and oligonucleotide primes described previously [15]. PCR products were gel extracted, cloned into a pCR2.1-TOPO vector (Life Technologies), and sequenced. Obtained J_H4 intronic sequences were aligned to the mm9 assembly of the mouse genomic sequence. $V_H186.2$ sequences were analyzed with ImMunoGeneTics (IMGT) V-QUEST (http://www.imgt.org/) [59, 60]. Mutation frequencies in the J_H4 intronic region were calculated by dividing the total number of mutations from all clones with the total number of base pairs analyzed for each group. For mutation analysis of the

immunoglobulin heavy chain gene, 5,000-20,000 GC B cells were purified from spleens 30 days after LCMV clone 13-infection. Total RNA was extracted using TRIzol and cDNA was synthesized using the SuperScript III firs*t*-strand synthesis system (Invitrogen) with a Cγ2c (Outer) primer [61], followed by a semi-nested PCR using Phusion HF. An adaptor-tagged promiscuous V_H (MsVHE) primer (5'-TCTTTCCCTACACGACGCTCTTCCGATCTGGGAATTC GAGGTGCAGCTGCAGGAGTCTGG-3') and an adaptor-tagged Cγ2c primer (5'-GTGACTGGAGTTCAGACGTGTGCTCTTCCGAGCTCAGG GAAATAACCCTTGAC-3') were used for the first round PCR [61]. The following primers were used for the second round PCR: 5'-AATGATACGGCGACCACCGA GATCTACACTCTTTCCCTACACGAC-3' and 5'-CAAGCAGAAGACGGCATACG AGAT*NNNNNNN*GTGACTGGAGTTCA GACG-3' (*NNNNNNN*: sample-specific bar codes). The PCR products were quantitated using Qubit (Invitrogen) and pooled in equimolar ratios for paired-end 2x250 bp sequencing on an Illumina MiSeq DNA sequencer. To determine the mutation frequency in the VDJ coding regions, only reads longer than 400 bp and with an average qscore > 30 were analyzed with IMGT HighV-QUEST [59, 60]. All sequences with >90% identity to the reference sequences from the IMGT database were used for mutation analysis. Only mutations with a qscore > 22 were counted.

Chromatin Immunoprecipitation Assay

For anti-c-MYC ChIP, splenic naive B cells, purified with anti-CD19 microbeads (Miltenyi), were activated with 10 μg/ml of anti-IgM (115-005-020, Jackson

ImmunoResearch) for two days, and further cultured on CD40L-expressing NIH 3T3 feeder cells for 24 hours. For anti-AP4 ChIP, splenic LZ and DZ GC B cells eight days after immunization with SRBCs were purified by sorting on a FACS AriaII. Anti-c-MYC, anti-AP4 and anti-H3K27ac (ab4729, Abcam) ChIPs were performed as previously described [41]. Sequence tags were mapped onto the NCBI37 mm9 with Bowtie2 [62]. The Homer software package [63] was used for peak calling with a Poisson *P*-value cutoff of 1×10^{-40} for AP4 and 1×10^{-6} for c-MYC for extraction of the 4758 and 4046 peaks with the highest statistical significance, respectively.

RNAseq Analysis

Total RNA was purified from 3,000 – 10,000 sorted $MYC^{-}AP4^{-}$ LZ, $MYC^{+}AP4^{+}$ LZ, $AP4^{+}$ DZ, and $AP4^{-}$ DZ GC cells from AP4-mCherry/c-MYC-GFP reporter mice eight days after immunization with SRBCs (Figure 4A) using a Nucleospin RNA XS extraction kit (Macherey-Nagel) according to the manufacturer's instructions. The purified RNA was reverse-transcribed and amplified using a SMAR*T*-Seq v4 Ultra Low Input RNA Kit (Clonetech), followed by library construction using a Nextera DNA Library Prep Kit (Illumina). High throughput sequencing was performed using a HiSeq 2500 sequencer (Illumina) with a 50 bp single read option. Sequence tags were mapped onto the NCBI37 mm9 with TopHat [64], followed by transcript assembly and RPKM estimation using Cufflinks [65, 66, 67, 68] on the Galaxy platform (https://usegalaxy.org/). Analysis was done with three biological replicates and genes upregulated in $MYC^{+}AP4^{+}$ relative to MYC^{-} $AP4^{-}$ LZ cells by more than 1.8-fold with a Student's *t*-test *P*-value less than 0.1 were analyzed by hierarchical clustering using Euclidean distance matrix with centroid

linkage. Pathway analysis was performed using a web-based gene set analysis toolkit (http://bioinfo.vanderbilt.edu/webgestalt/).

Immunoblot analysis

Whole cell extracts were prepared by lysis of cells in Laemmli buffer containing 1% SDS and 2% 2-mercaptoethanol. Lysates from equal numbers of cells were separated by 8% or 10% SDS PAGE and transferred to PVDF membranes (Roche). Membranes were incubated with primary antibodies (identified below), followed by detection with horseradish peroxidase–conjugated species-specific antibody to immunoglobulin light chain (115-035-174, 211-032-171; Jackson ImmunoResearch) and a Luminata HRP substrate (Millipore). Anti-AP4 was described [41]. The following antibodies were purchased: anti-Puromycin (MABE343; Millipore), anti-c-MYC (9402S; Cell Signaling), anti-phospho-STAT3 (Tyr705) (9145; Cell Signaling) and anti-BCL6 (4242S, Cell Signaling). Anti-HDAC1 (ab7028; Abcam) was used as loading controls.

Statistical analysis

P values were calculated with an unpaired two-tailed Student's *t*-test for two-group comparisons and by one-way ANOVA for multiple-group comparisons with the Tukey post-hoc test using Prism 6 software (Graphpad) unless specified otherwise. For the comparison of cumulative frequencies between two datasets and the frequency of $W33L^+$ clones between two groups, the Kolmogorov-Smirnov test and χ^2 test with Yates correction were used, respectively. *P* values of <0.05 were considered significant. N.S., not significant; *P<0.05; **P<0.01; ***P<0.001; ****P<0.0001.

3.6 ACKNOLEDGEMENTS

We thank Barry Sleckman for c-MYC-GFP mice, Fred Alt for *Myc*^{F} mice, Eugene Oltz for Mb1-iCre mice, J. Michael White for ES cell microinjection, Sunnie Hsiung, Yinan Wang, Rachel Wong and Sidonia Faragasan for technical support, Chyi-Song Hsieh, Kenneth Murphy and Eugene Oltz for discussion. Supported by the Lucille P. Markey Pathway Program (C.C.), the National Institutes of Health (P30 AR048335 to the Rheumatic Diseases Core Center; R01 AI097244 and R56 AI114593 to T.E.; R01 AI099108 to D.B.; UL1 TR000448 to the Washington University Institute of Clinical and Translational Sciences; P30 CA91842 to the Siteman Cancer Center), and the Edward Mallinckrodt Jr. Foundation (T.E.). D.B. is a New York Stem Cell Foundation-Robertson Investigator. The authors declare no competing financial conflict of interest related to this study.

3.7 AUTHOR CONTRIBUTIONS

C.C. and T.E. designed experiments. C.C., D.J.V., E.T., and M.H. performed experiments. M. Ce. and M.Co provided critical reagents, C.C., D.B. and T.E. analyzed data. C.C. and T.E. wrote manuscript with editorial comments from the other coauthors.

3.8 REFERENCES

1. Basso, K. & Dalla-Favera, R. Germinal centres and B cell lymphomagenesis. *Nat Rev Immunol* **15**, 172-184 (2015).
2. Victora, G.D. & Nussenzweig, M.C. Germinal centers. *Annual review of immunology* **30**, 429-457 (2012).
3. Allen, C.D., Okada, T. & Cyster, J.G. Germinal-center organization and cellular dynamics. *Immunity* **27**, 190-202 (2007).
4. Corcoran, L.M. & Tarlinton, D.M. Regulation of germinal center responses, memory B cells and plasma cell formation-an update. *Curr Opin Immunol* **39**, 59-67 (2016).
5. Victora, G.D. *et al.* Germinal center dynamics revealed by multiphoton microscopy with a photoactivatable fluorescent reporter. *Cell* **143**, 592-605 (2010).
6. MacLennan, I.C. Germinal centers. *Annual review of immunology* **12**, 117-139 (1994).
7. Rajewsky, K. Clonal selection and learning in the antibody system. *Nature* **381**, 751-758 (1996).
8. Shih, T.A., Meffre, E., Roederer, M. & Nussenzweig, M.C. Role of BCR affinity in T cell dependent antibody responses in vivo. *Nat Immunol* **3**, 570-575 (2002).
9. Linterman, M.A. *et al.* IL-21 acts directly on B cells to regulate Bcl-6 expression and germinal center responses. *J Exp Med* **207**, 353-363 (2010).

10. Zotos, D. *et al.* IL-21 regulates germinal center B cell differentiation and proliferation through a B cell-intrinsic mechanism. *J Exp Med* **207**, 365-378 (2010).

11. Castigli, E. *et al.* CD40-deficient mice generated by recombination-activating gene-2-deficient blastocyst complementation. *Proc Natl Acad Sci U S A* **91**, 12135-12139 (1994).

12. Kawabe, T. *et al.* The immune responses in CD40-deficient mice: impaired immunoglobulin class switching and germinal center formation. *Immunity* **1**, 167-178 (1994).

13. Renshaw, B.R. *et al.* Humoral immune responses in CD40 ligand-deficient mice. *J Exp Med* **180**, 1889-1900 (1994).

14. Xu, J. *et al.* Mice deficient for the CD40 ligand. *Immunity* **1**, 423-431 (1994).

15. Gitlin, A.D., Shulman, Z. & Nussenzweig, M.C. Clonal selection in the germinal centre by regulated proliferation and hypermutation. *Nature* **509**, 637-640 (2014).

16. Kocks, C. & Rajewsky, K. Stepwise intraclonal maturation of antibody affinity through somatic hypermutation. *Proc Natl Acad Sci U S A* **85**, 8206-8210 (1988).

17. Shulman, Z. *et al.* Dynamic signaling by T follicular helper cells during germinal center B cell selection. *Science* **345**, 1058-1062 (2014).

18. Gitlin, A.D. *et al.* HUMORAL IMMUNITY. T cell help controls the speed of the cell cycle in germinal center B cells. *Science* **349**, 643-646 (2015).

19. Calado, D.P. *et al.* The cell-cycle regulator c-Myc is essential for the formation and maintenance of germinal centers. *Nat Immunol* **13**, 1092-1100 (2012).

20. Dominguez-Sola, D. *et al.* The proto-oncogene MYC is required for selection in the germinal center and cyclic reentry. *Nat Immunol* **13**, 1083-1091 (2012).

21. Victora, G.D. *et al.* Identification of human germinal center light and dark zone cells and their relationship to human B-cell lymphomas. *Blood* **120**, 2240-2248 (2012).

22. Hardie, D.L., Johnson, G.D., Khan, M. & MacLennan, I.C. Quantitative analysis of molecules which distinguish functional compartments within germinal centers. *Eur J Immunol* **23**, 997-1004 (1993).

23. Huang, C.Y.B., A. L.; Walker, L. M.; Bassing, C. H.; Sleckman, B. P. Dynamic regulation of c-Myc proto-oncogene expression during lymphocyte development revealed by a GFP-c-Myc knock-in mouse. *Eur J Immunol* **38**, 342-349 (2008).

24. Hobeika, E. *et al.* Testing gene function early in the B cell lineage in mb1-cre mice. *Proc Natl Acad Sci U S A* **103**, 13789-13794 (2006).

25. Casola, S. *et al.* Tracking germinal center B cells expressing germ-line immunoglobulin gamma1 transcripts by conditional gene targeting. *Proc Natl Acad Sci U S A* **103**, 7396-7401 (2006).

26. Nojima, T. *et al.* In-vitro derived germinal centre B cells differentially generate memory B or plasma cells in vivo. *Nat Commun* **2**, 465 (2011).

27. Jolly, C.J., Klix, N. & Neuberger, M.S. Rapid methods for the analysis of immunoglobulin gene hypermutation: application to transgenic and gene targeted mice. *Nucleic Acids Res* **25**, 1913-1919 (1997).

28. Allen, D. *et al.* Timing, genetic requirements and functional consequences of somatic hypermutation during B-cell development. *Immunol Rev* **96**, 5-22 (1987).

29. Allen, D., Simon, T., Sablitzky, F., Rajewsky, K. & Cumano, A. Antibody engineering for the analysis of affinity maturation of an anti-hapten response. *EMBO J* **7**, 1995-2001 (1988).

30. Halper-Stromberg, A. *et al.* Broadly neutralizing antibodies and viral inducers decrease rebound from HIV-1 latent reservoirs in humanized mice. *Cell* **158**, 989-999 (2014).

31. Klein, F. *et al.* Somatic mutations of the immunoglobulin framework are generally required for broad and potent HIV-1 neutralization. *Cell* **153**, 126-138 (2013).

32. Mascola, J.R. & Haynes, B.F. HIV-1 neutralizing antibodies: understanding nature's pathways. *Immunol Rev* **254**, 225-244 (2013).

33. Harker, J.A., Lewis, G.M., Mack, L. & Zuniga, E.I. Late interleukin-6 escalates T follicular helper cell responses and controls a chronic viral infection. *Science* **334**, 825-829 (2011).

34. Bergthaler, A. *et al.* Impaired antibody response causes persistence of prototypic T cell-contained virus. *PLoS Biol* **7**, e1000080 (2009).

35. Wherry, E.J., Blattman, J.N., Murali-Krishna, K., van der Most, R. & Ahmed, R. Viral persistence alters CD8 T-cell immunodominance and tissue distribution and results in distinct stages of functional impairment. *J Virol* **77**, 4911-4927 (2003).

36. Allen, C.D. *et al.* Germinal center dark and light zone organization is mediated by CXCR4 and CXCR5. *Nat Immunol* **5**, 943-952 (2004).

37. Nathans, D. Puromycin Inhibition of Protein Synthesis: Incorporation of Puromycin into Peptide Chains. *Proc Natl Acad Sci U S A* **51**, 585-592 (1964).

38. Ettinger, R. *et al.* IL-21 induces differentiation of human naive and memory B cells into antibody-secreting plasma cells. *J Immunol* **175**, 7867-7879 (2005).

39. Tas, J.M. *et al.* Visualizing antibody affinity maturation in germinal centers. *Science* **351**, 1048-1054 (2016).

40. Kuraoka, M. *et al.* Complex Antigens Drive Permissive Clonal Selection in Germinal Centers. *Immunity* **44**, 542-552 (2016).

41. Chou, C. *et al.* c-Myc-induced transcription factor AP4 is required for host protection mediated by CD8+ T cells. *Nat Immunol* **15**, 884-893 (2014).

42. Sander, S. *et al.* Synergy between PI3K signaling and MYC in Burkitt lymphomagenesis. *Cancer cell* **22**, 167-179 (2012).

43. Adams, J.M. *et al.* The c-myc oncogene driven by immunoglobulin enhancers induces lymphoid malignancy in transgenic mice. *Nature* **318**, 533-538 (1985).

44. Kato, L. *et al.* Nonimmunoglobulin target loci of activation-induced cytidine deaminase (AID) share unique features with immunoglobulin genes. *Proc Natl Acad Sci U S A* **109**, 2479-2484 (2012).

45. Ventura, A. *et al.* Restoration of p53 function leads to tumour regression in vivo. *Nature* **445**, 661-665 (2007).

46. Robbiani, D.F. *et al.* AID is required for the chromosomal breaks in c-myc that lead to c-myc/IgH translocations. *Cell* **135**, 1028-1038 (2008).

47. Kitamura, D., Roes, J., Kuhn, R. & Rajewsky, K. A B cell-deficient mouse by targeted disruption of the membrane exon of the immunoglobulin mu chain gene. *Nature* **350**, 423-426 (1991).

48. Frohlich, A. *et al.* IL-21 receptor signaling is integral to the development of Th2 effector responses in vivo. *Blood* **109**, 2023-2031 (2007).

49. Egawa, T. & Littman, D.R. Transcription factor AP4 modulates reversible and epigenetic silencing of the Cd4 gene. *Proc Natl Acad Sci U S A* **108**, 14873-14878 (2011).

50. de Alboran, I.M. *et al.* Analysis of C-MYC function in normal cells via conditional gene-targeted mutation. *Immunity* **14**, 45-55 (2001).

51. Lakso, M. *et al.* Efficient in vivo manipulation of mouse genomic sequences at the zygote stage. *Proc Natl Acad Sci U S A* **93**, 5860-5865 (1996).

52. McCausland, M.M. & Crotty, S. Quantitative PCR technique for detecting lymphocytic choriomeningitis virus in vivo. *Journal of virological methods* **147**, 167-176 (2008).

53. Seiler, P. *et al.* Enhanced virus clearance by early inducible lymphocytic choriomeningitis virus-neutralizing antibodies in immunoglobulin-transgenic mice. *J Virol* **72**, 2253-2258 (1998).

54. Korns Johnson, D. & Homann, D. Accelerated and improved quantification of lymphocytic choriomeningitis virus (LCMV) titers by flow cytometry. *PloS one* **7**, e37337 (2012).

55. McHeyzer-Williams, L.J. & McHeyzer-Williams, M.G. Analysis of antigen-specific B-cell memory directly ex vivo. *Methods Mol Biol* **271**, 173-188 (2004).

56. Ahmed, R., Salmi, A., Butler, L.D., Chiller, J.M. & Oldstone, M.B. Selection of genetic variants of lymphocytic choriomeningitis virus in spleens of persistently

infected mice. Role in suppression of cytotoxic T lymphocyte response and viral persistence. *J Exp Med* **160**, 521-540 (1984).

57. Kunz, S., Edelmann, K.H., de la Torre, J.C., Gorney, R. & Oldstone, M.B. Mechanisms for lymphocytic choriomeningitis virus glycoprotein cleavage, transport, and incorporation into virions. *Virology* **314**, 168-178 (2003).

58. Purtha, W.E., Tedder, T.F., Johnson, S., Bhattacharya, D. & Diamond, M.S. Memory B cells, but not long-lived plasma cells, possess antigen specificities for viral escape mutants. *The Journal of experimental medicine* **208**, 2599-2606 (2011).

59. Lefranc, M.P. *et al.* IMGT, the international ImMunoGeneTics information system. *Nucleic acids research* **37**, D1006-1012 (2009).

60. Brochet, X., Lefranc, M.P. & Giudicelli, V. IMGT/V-QUEST: the highly customized and integrated system for IG and TR standardized V-J and V-D-J sequence analysis. *Nucleic acids research* **36**, W503-508 (2008).

61. Tiller, T., Busse, C.E. & Wardemann, H. Cloning and expression of murine Ig genes from single B cells. *J Immunol Methods* **350**, 183-193 (2009).

62. Langmead, B. & Salzberg, S.L. Fast gapped-read alignment with Bowtie 2. *Nat Methods* **9**, 357-359 (2012).

63. Heinz, S. *et al.* Simple combinations of lineage-determining transcription factors prime cis-regulatory elements required for macrophage and B cell identities. *Molecular cell* **38**, 576-589 (2010).

64. Trapnell, C., Pachter, L. & Salzberg, S.L. TopHat: discovering splice junctions with RNA-Seq. *Bioinformatics* **25**, 1105-1111 (2009).

65. Trapnell, C. *et al.* Transcript assembly and quantification by RNA-Seq reveals unannotated transcripts and isoform switching during cell differentiation. *Nat Biotechnol* **28**, 511-515 (2010).

66. Roberts, A., Trapnell, C., Donaghey, J., Rinn, J.L. & Pachter, L. Improving RNA-Seq expression estimates by correcting for fragment bias. *Genome Biol* **12**, R22 (2011).

67. Roberts, A., Pimentel, H., Trapnell, C. & Pachter, L. Identification of novel transcripts in annotated genomes using RNA-Seq. *Bioinformatics* **27**, 2325-2329 (2011).

68. Trapnell, C. *et al.* Differential analysis of gene regulation at transcript resolution with RNA-seq. *Nat Biotechnol* **31**, 46-53 (2013).

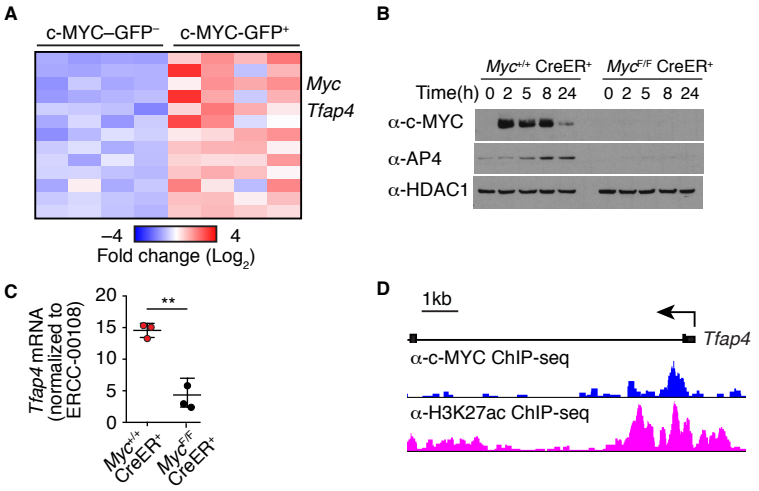

Figure 3.1. MYC is required for AP4 induction after B cell activation. (A) Expression levels of transcription factors upregulated in MYC^+ relative to MYC^- GC B cells 12 days after immunization with SRBC shown as a heat map. **(B and C)** AP4 protein expression and *Tfap4* mRNA levels (2 hours) in B cells that were harvested from Tamoxifen-treated *Myc*$^{F/F}$ *Rosa26*-CreER^{T2} or *Rosa26*-CreER^{T2} mice and co-cultured with CD40L-expressing feeders. Data are representative of three experiments. **(D)** Binding of c-MYC to the *Tfap4* locus in CD40L-activated B cells. Histograms of sequence tags pulled down with anti-c-MYC or anti-H3K27ac antibody are shown. Data are shown by means ± SD. Unpaired Student's *t* test. $n = 3$ per group (B and C).

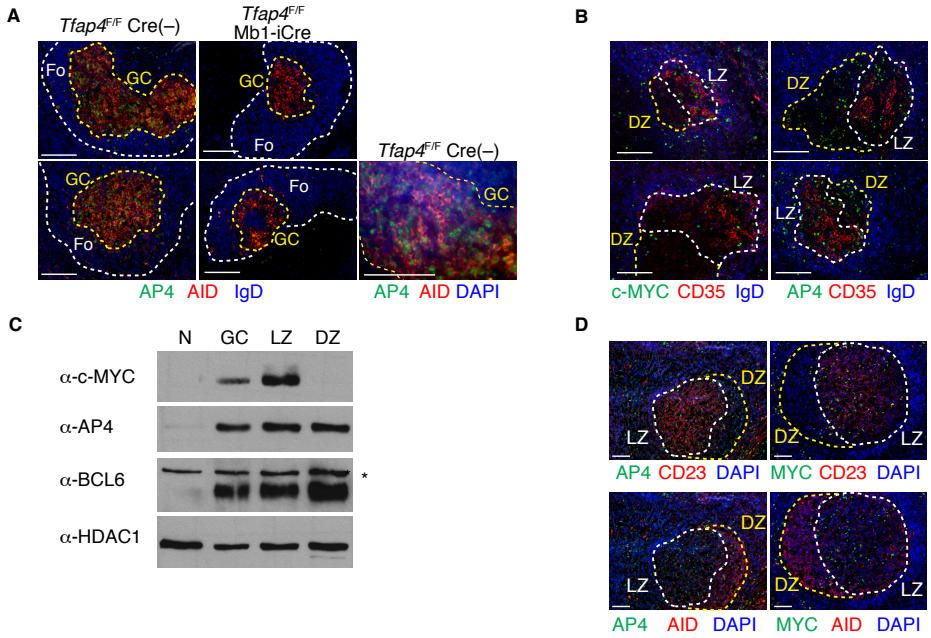

Figure 3.2. AP4 is expressed in both LZ and DZ GC B cells. (A) Staining for AP4, AID and IgD of spleen sections eight days after SRBC immunization. B cell follicles (Fo) and GCs are marked by white and yellow dashed lines, respectively. Data are representative of two experiments. **(B)** Staining for AP4 and c-MYC of spleen sections eight days after SRBC immunization. LZ and DZ of GCs defined by the presence of $CD35^{+}$ FDCs are shown with white and yellow dashed lines, respectively. Data are representative of two experiments. **(C)** AP4, c-MYC, and BCL6 protein levels in naive (N), total $B220^{+}GL7^{+}Fas^{+}$ GC, $CD86^{hi}CXCR4^{lo}$ LZ and $CD86^{lo}CXCR4^{hi}$ DZ B cells eight days after SRBC immunization. (D) Immunofluorescence microscopy showing expression of AP4, c-MYC, AID, and CD23 in human tonsils. LZ and DZ are surrounded by white and yellow dashed lines, respectively. Data are representative of three independent experiments. Data are representative of three experiments. *: non-specific band. Scale bar, 100 μm. $n = 4$ (A and B); $n = 3$ (C); $n = 2$ (D)

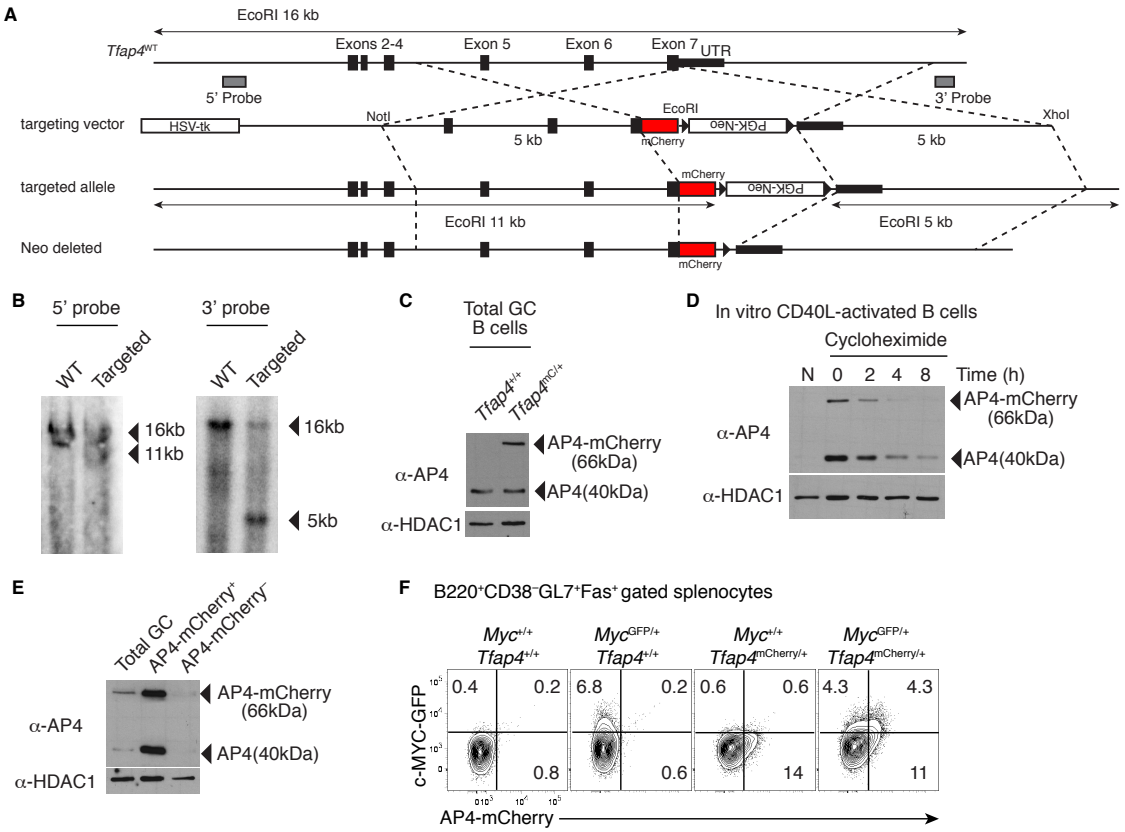

Figure 3.3. Generation of *Tfap4*^{mCherry} protein reporter allele. (A) A targeting strategy to generate the AP4-mCherry fusion protein reporter allele. **(B)** Southern blot analysis of targeted ES clones. Genomic DNA from WT and one representative targeted ES clone was digested with EcoRI and probed with the 5' probe (left panel) and 3' probe (right panel). **(C and D)** Immunoblot analysis showing AP4 and AP4-mCherry expression in GC B cells from *Tfap4*$^{mCherry/+}$ mice eight days after immunization with SRBCs (C), or splenic B cells from the same strain activated with CD40L followed by treatment with cycloheximide (D). Data are representative of two independent experiments. **(E)** AP4 and AP4-mCherry protein expression in total, AP4-mCherry^{+}, and AP4-mCherry^{-} GC B cells in (C). Data are representative of three independent experiments. **(F)** Flow cytometric analysis showing mCherry and GFP expression in GC B cells from the indicated mice eight days after immunization with SRBCs. Data are representative of two independent experiments.

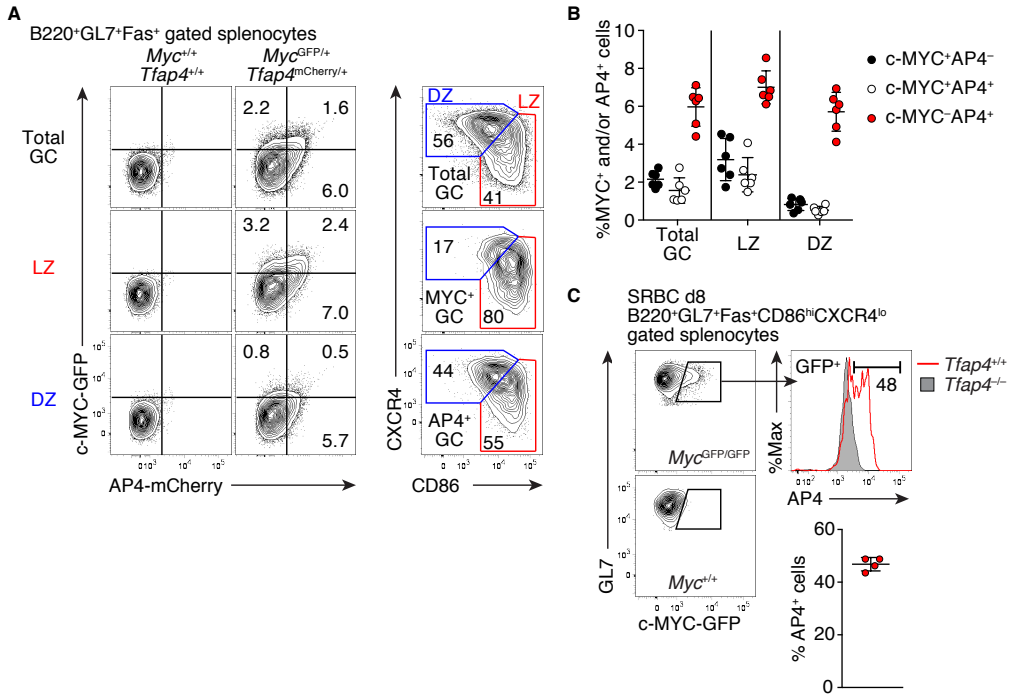

Figure 3.4. MYC^{+} GC B cells co-express AP4. (A and B) Expression of GFP and mCherry in GC B cells of *Myc*$^{GFP/+}$ *Tfap4*$^{mCherry/+}$ mice eight days after SRBC immunization (A). Distribution of AP4-mCherry^{+} or c-MYC-GFP^{+} cells in the LZ and DZ defined by CD86 and CXCR4 expression is shown in the right panels (A). Frequencies of AP4- or c-MYC-expressing cells in total GC, LZ and DZ GC B cells from two independent experiments are shown in (B). **(C)** Intracellular staining for AP4 in c-MYC-GFP^{+} LZ GC B cells eight days after SRBC immunization. Staining for AP4 in *Tfap4*$^{-/-}$ LZ cells is shown as control. Data are pooled from two experiments. Data are shown by means ± SD. *n* = 6 for (A and B); *n* = 4 for *Myc*^{GFP}*Tfap4*$^{+/+}$ and *n* = 2 for *Tfap4*$^{-/-}$ mice (C)

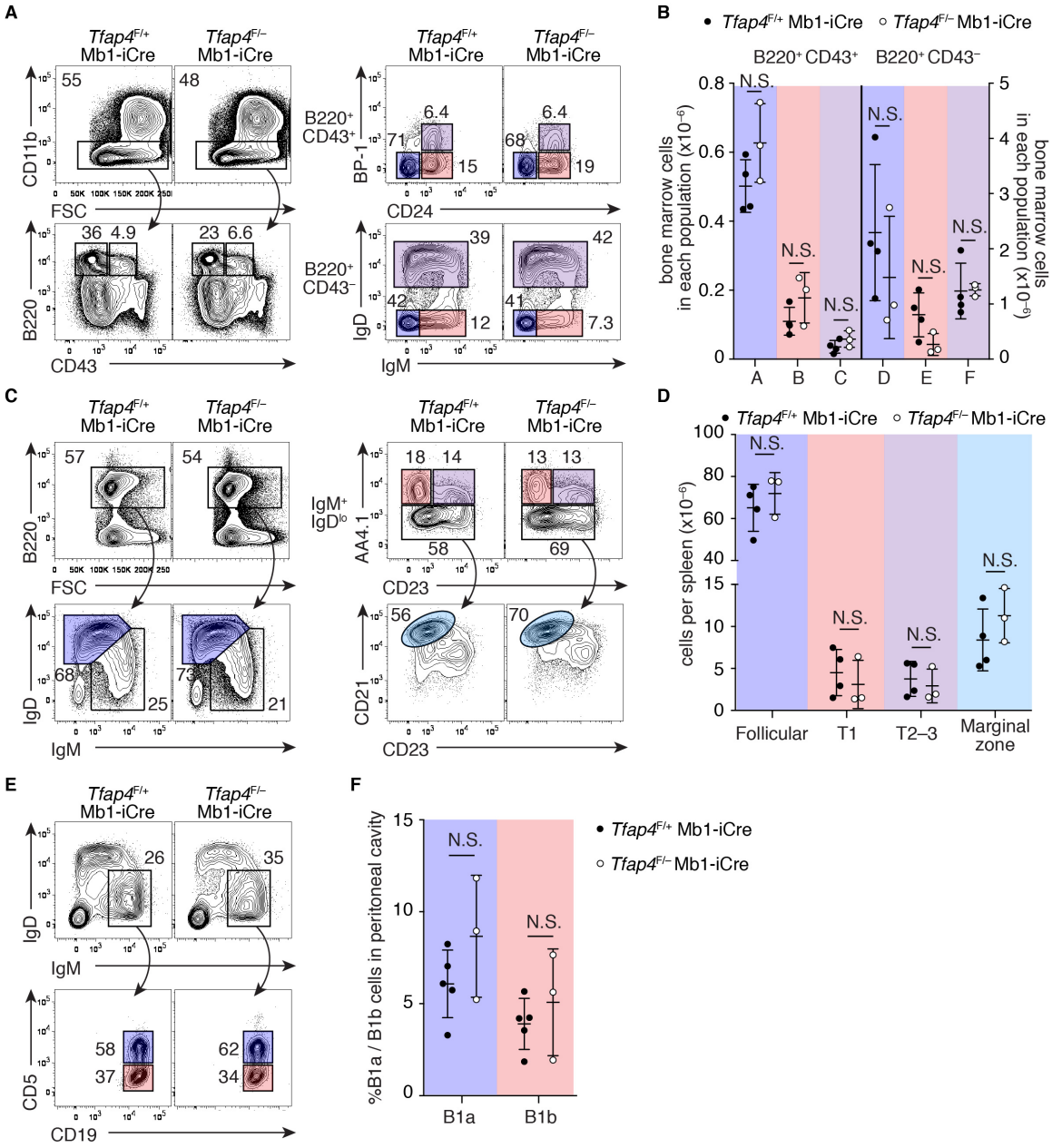

Figure 3.5. AP4 is dispensable for B cell development and homeostasis. (A) Flow cytometric analysis showing expression of CD11b, B220, CD43, BP-1, CD24, IgM and IgD in bone marrow cells from *Tfap4*$^{F/–}$ Mb1-iCre (N=4) and control *Tfap4*$^{F/+}$ Mb1-iCre mice (N=3). **(B)** Absolute numbers of B220^{+}CD43^{+} and B220^{+}CD43$^{–}$ bone marrow cells per femur in each developmental stage as color-coded in (A). **(C)** Expression of B220, IgD, IgM, AA4.1, CD23, and CD21 in splenocytes from *Tfap4*$^{F/–}$ Mb1-iCre and control *Tfap4*$^{F/+}$ Mb1-iCre mice. **(D)** Absolute number of B220^{+} splenocytes in each developmental stage as color-coded in (C). **(E)** Expression of IgD, IgM, CD5 and CD19 in cells in peritoneal cavity lavage from *Tfap4*$^{F/–}$ Mb1-iCre and control *Tfap4*$^{F/+}$ Mb1-iCre mice. **(F)** Frequencies of B1a and B1b cells in (E). Data are pooled from two independent experiments, and shown by means ± SD in (B, D and F). Unpaired Student's *t* test.

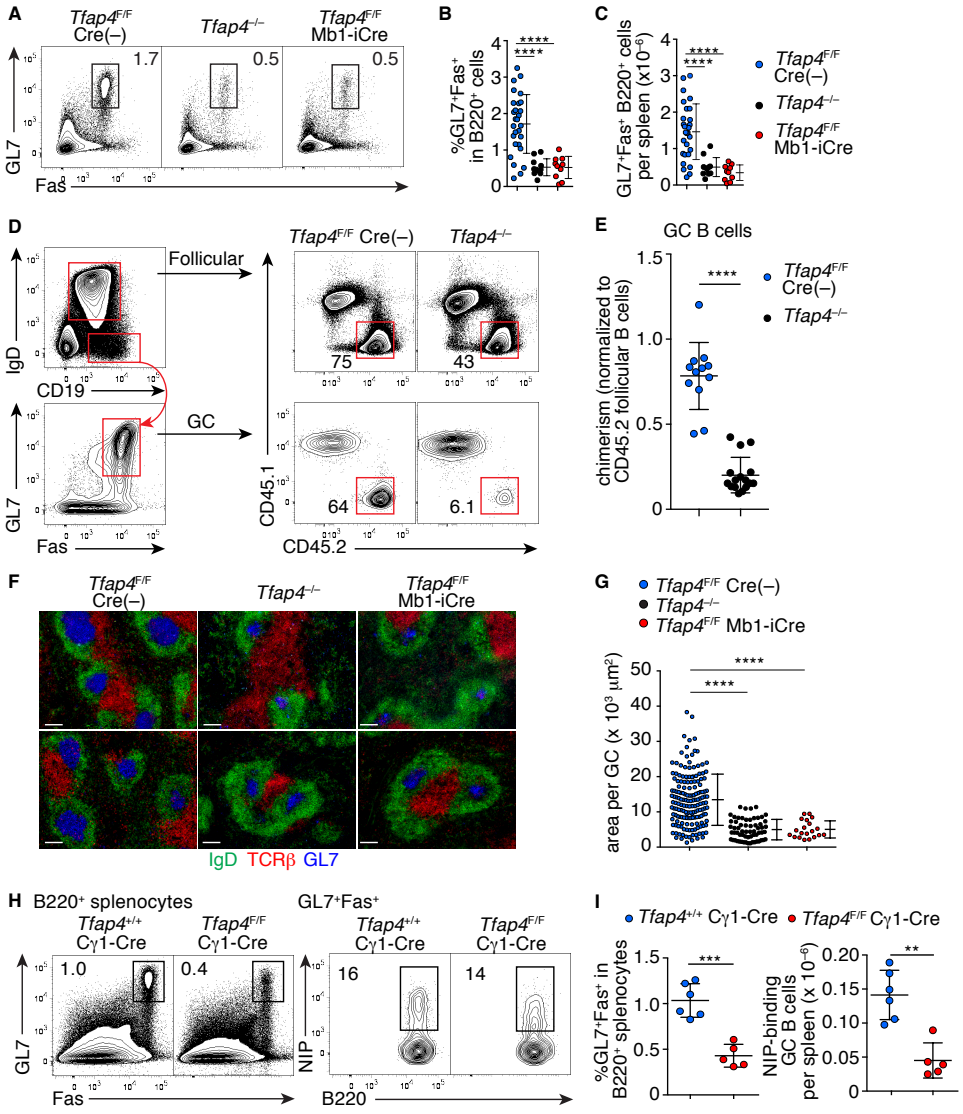

Figure 3.6. AP4 is required for normal GC formation in a B cell-intrinsic manner
(A-C) Expression of GL7 and Fas in B220$^+$ splenocytes ten days after NP-CGG immunization (A). Statistical analysis of frequencies (B) and absolute numbers (C) of GL7$^+$Fas$^+$ cells in B220$^+$ splenocytes from four independent experiments is shown. **(D and E)** Flow cytometric analysis of CD45.2 donor cell contribution to the follicular (IgD$^+$CD19$^+$) and GC (IgD$^-$CD19$^+$GL7$^+$Fas$^+$) B cell compartments in mixed bone marrow chimeras 12 days after NP-CGG immunization (D). Statistical analysis of CD45.2 donor cell contribution to GC normalized to that of follicular B cells from five independent experiments is shown in (E). **(F)** Staining for GL7, IgD and TCRβ of spleen sections from mice with indicated genotypes ten days after NP-CGG immunization. Representative data from four independent experiments are shown. Scale bar: 100 µm. **(G)** Statistical analysis of the size of each GC in (F). Data are pooled from four independent experiments. **(H and I)** Flow cytometric analysis showing expression of GL7 and Fas on B220$^+$-gated cells in Peyer's patches from *Tfap4*$^{-/-}$ (N=6), *Tfap4*$^{F/F}$ Mb1-

iCre (N=7) and control *Tfap4*$^{F/F}$ Cre(–) (N=7) mice (H). Statistical analysis of data from two independent experiments is shown in (I). Data in (B, C, E, G and I) are shown by means ± SD. One-way ANOVA for (B, C and G). Unpaired Student's *t* test for (E and I). $n = 10$ for *Tfap4*$^{-/-}$ and *Tfap4*$^{F/F}$ Mb1-iCre, and $n = 28$ for *Tfap4*$^{F/F}$ Cre(–) (A-C, F and G); $n = 12$ for *Tfap4*$^{F/F}$ Cre(–) and $n = 16$ for *Tfap4*$^{-/-}$ (D and E).

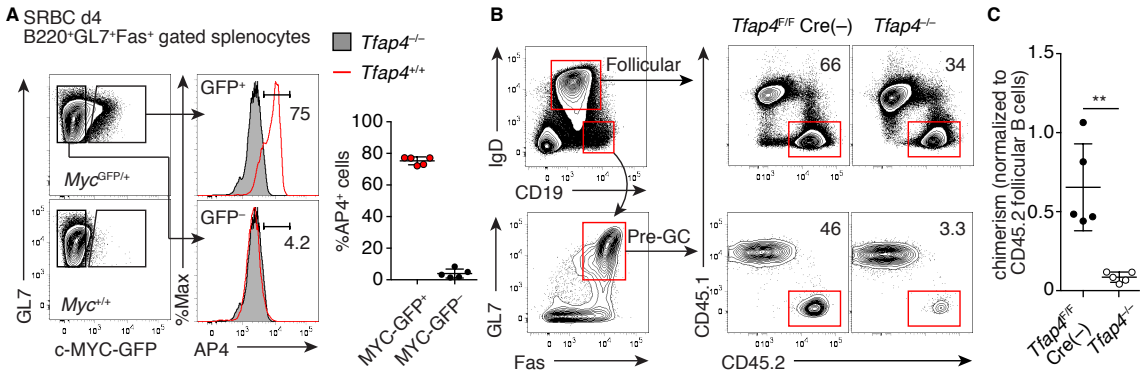

Figure 3.7. AP4 is essential for expansion of pre-GC B cells. (A) Intracellular staining for AP4 in c-MYC-GFP^{+} pre-GC B cells four days after immunization with SRBCs (N=5). AP4 staining in *Tfap4*$^{-/-}$ cells is shown as negative control. Data are pooled from two experiments. **(B and C)** Flow cytometric and statistical analysis showing the contribution of CD45.2 donor cells to the follicular (IgD^{+}CD19^{+}) and pre-GC (IgD^{-} CD19^{+}GL7^{+}Fas^{+}) B cell compartments in mixed bone marrow chimeras (N=5 per group) five days after NP-CGG immunization. Donor cell contribution to the pre-GC compartment was normalized to that of follicular B cells. Data are pooled from three independent experiments. Data are shown by means ± SD. Unpaired Student's *t* test.

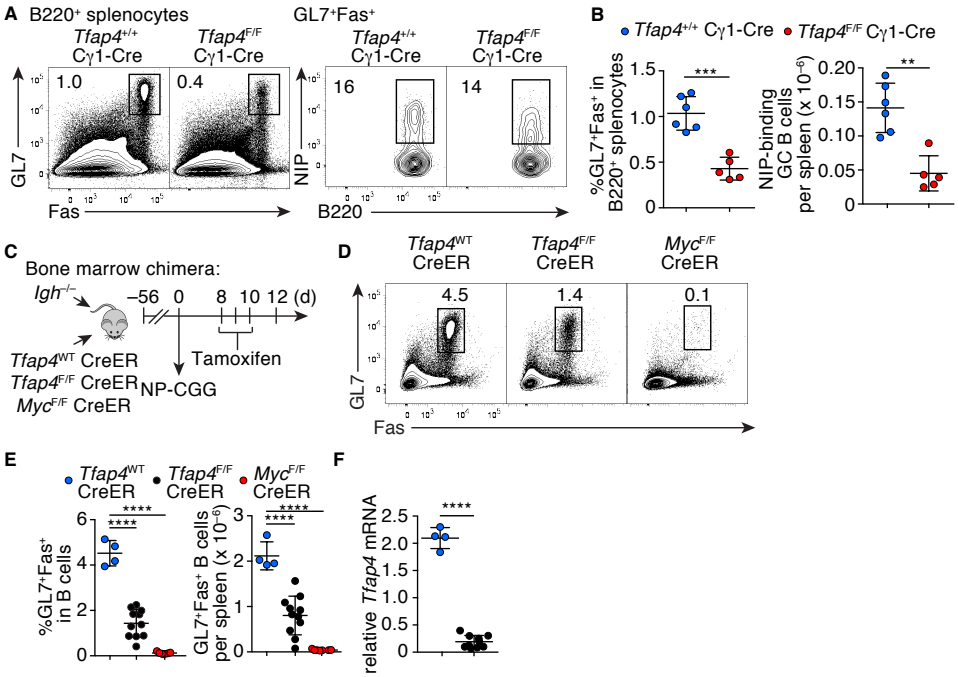

Figure 3.8. AP4 is necessary for GC maintenance. (A and B) Expression of GL7 and Fas in B220^{+} splenocytes and NIP-allophycocyanin (APC)- binding by B220^{+}GL7^{+}Fas^{+} cells from *Tfap4*$^{F/F}$ Cγ1-Cre and control *Tfap4*$^{+/+}$ Cγ1-Cre mice ten days after NP-CGG immunization. Statistical analysis from two independent experiments is shown in (F). **(C)** Experimental scheme for the generation of mixed bone marrow chimeras used in (B-D). A three to one mixture of bone marrow cells from *Igh*$^{-/-}$ mice and *Tfap4*$^{+/+}$ *Rosa26*-CreER^{T2}, *Tfap4*$^{F/F}$ *Rosa26*-CreER^{T2}, or *Myc*$^{F/F}$ *Rosa26*-CreER^{T2} mice were transplanted into lethally irradiated B6-CD45.1 hosts. Tamoxifen was administered on days eight, nine, and ten after immunization with NP-CGG, followed by analysis of GC responses on day 12. **(D)** Expression of GL7 and Fas on donor-derived B220^{+} splenocytes from the indicated mixed bone marrow chimeras (N=4-11). Data are representative of four independent experiments. **(E)** Frequencies of GL7^{+}Fas^{+} in B220^{+} cells (left panel) and absolute numbers of B220^{+}GL7^{+}Fas^{+} cells in the spleens (right panel) from indicated mixed bone marrow chimeras. Data are pooled from four independent experiments. **(F)** *Tfap4* mRNA levels in B220^{+}GL7^{+}Fas^{+} splenocytes from the bone marrow chimeras. Data are pooled from two independent experiments. Data are shown by means ± SD. Unpaired Student's *t* test for (B and F). One-way ANOVA for (E).

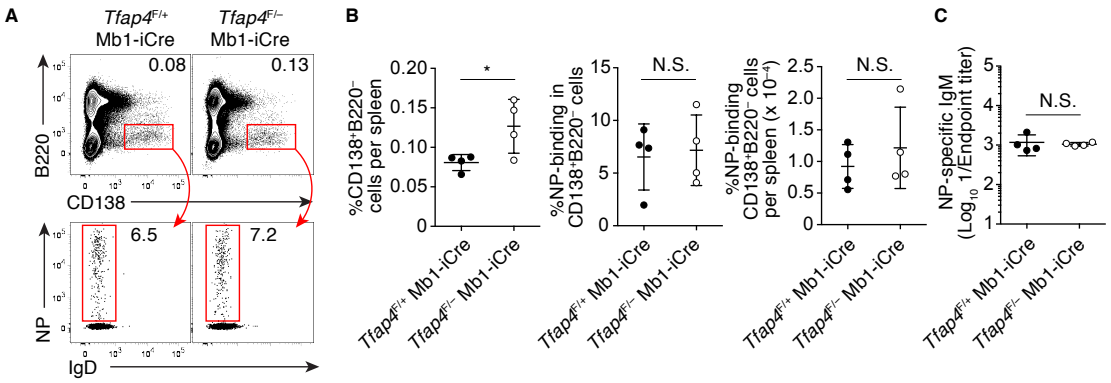

Figure 3.9. AP4 is dispensable for responses to T-independent antigen. (A) Expression of B220, CD138, and IgD in splenocytes and intracellular NP-binding in $CD138^{+}B220^{-}$ splenocytes from *Tfap4*$^{F/-}$ Mb1-iCre (N=4) and control *Tfap4*$^{F/+}$ Mb1-iCre (N=4) mice seven days after immunization with NP-Ficoll. Data are representative of two independent experiments. **(B)** Frequencies and absolute numbers of $CD138^{+}B220^{-}$ cells per spleen and the frequency of NP-binding cells in $CD138^{+}B220^{-}$ splenocytes in (A). Data are pooled from two independent experiments. **(C)** Serum NP-specific IgM titers seven days after NP-Ficoll immunization in (A). Data are shown by means ± SD. Unpaired Student's *t* test.

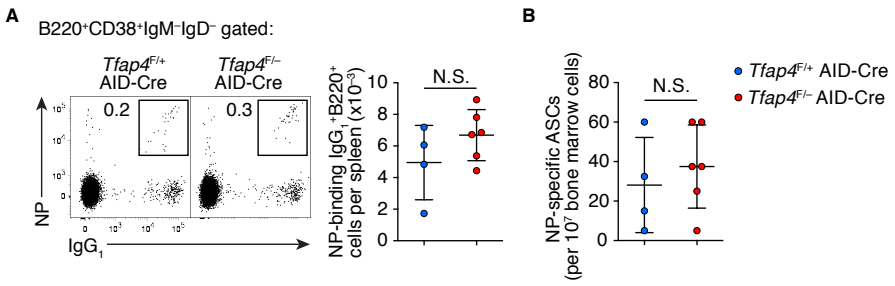

Figure 3.10. AP4 is dispensable for the formation of memory B cells and bone marrow antibody secreting cells (ASCs). (A) Binding to APC-NP and expression of IgG_1 in $B220^+CD38^+IgM^-IgD^-$ splenocytes from *Tfap4*$^{F/-}$ AID-Cre (N=6) and *Tfap4*$^{F/+}$ AID-Cre (N=4) mice eight weeks after immunization. **(B)** Statistical analysis of the number of NP-specific bone marrow ASCs in (A). Data are pooled from two experiments and shown by means ± SD. Unpaired Student's *t* test.

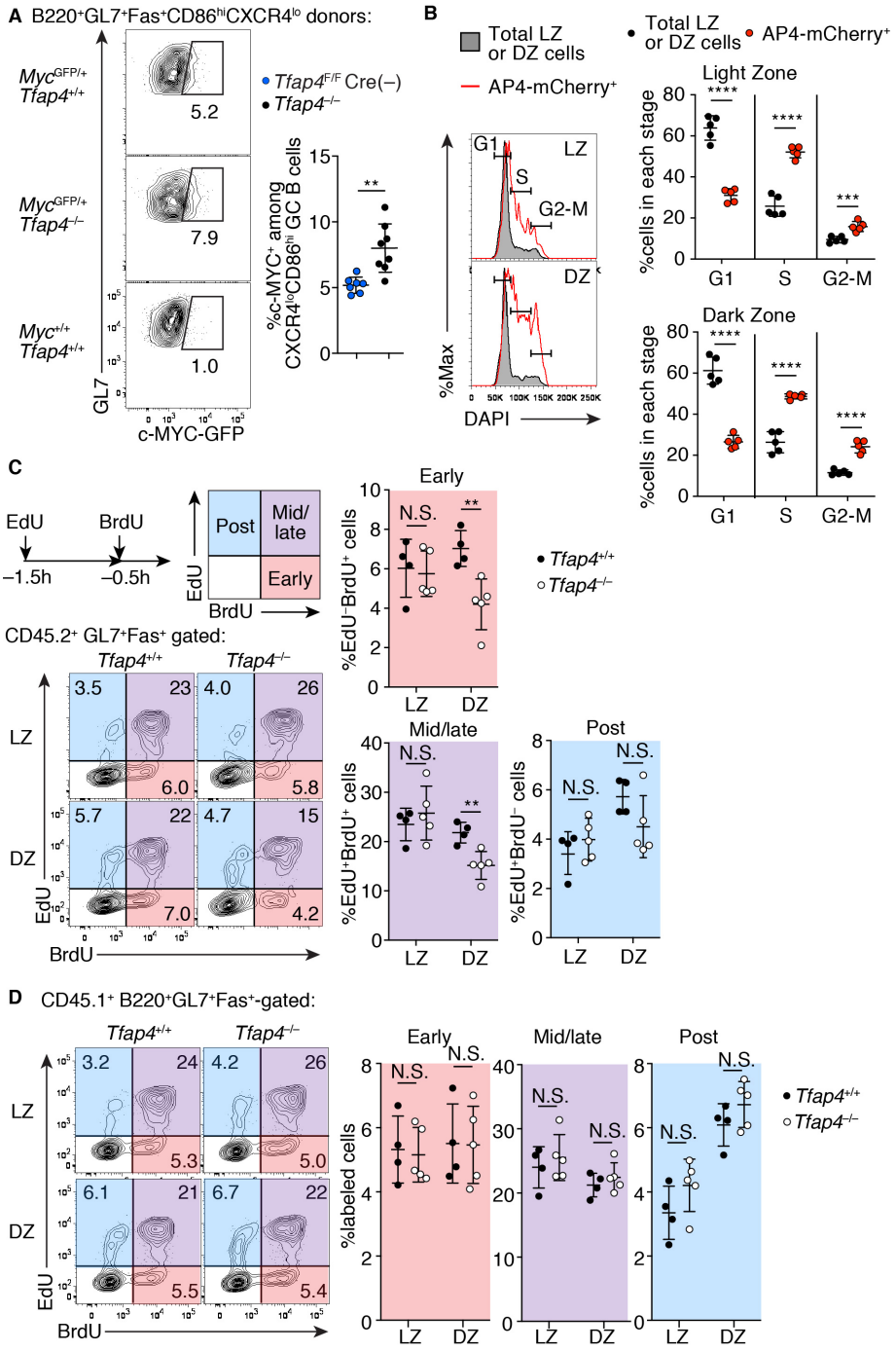

Figure 3.11. AP4 enhances GC B cell proliferation through the regulation of cell cycle re-entry in the DZ. (A) Flow cytometric analysis showing c-MYC-GFP expression in *Tfap4*$^{-/-}$ and control *Tfap4*$^{F/F}$ Cre(–) LZ GC B cells eight days after NP-CGG immunization (N=7-8 per group). Data are pooled from three independent experiments. **(B)** Cell cycle analysis by DNA content measurement of AP4-mCherry^{+} LZ and DZ cells compared to total LZ and DZ cells from *Tfap4*^{mCherry} reporter mice eight days after SRBC immunization. Data are pooled from two independent experiments. **(C)** Cell cycle analysis by sequential EdU and BrdU labeling of CD45.2 *Tfap4*$^{-/-}$ and control *Tfap4*$^{F/F}$ Cre(–) donor LZ and DZ GC B cells in mixed bone marrow chimeras eight days after

NP-CGG immunization. Early-, mid/late-, and post-S phases of the cell cycle were defined as previously described. Representative plots and statistical analysis from two independent experiments are shown. **(D)** EdU and BrdU incorporation by LZ and DZ GC B cells derived from WT CD45.1 donor cells in mixed bone marrow chimeras following sequential pulse labeling with EdU and BrdU as described in (C). Data are pooled from two independent experiments. Unpaired Student's *t* test.

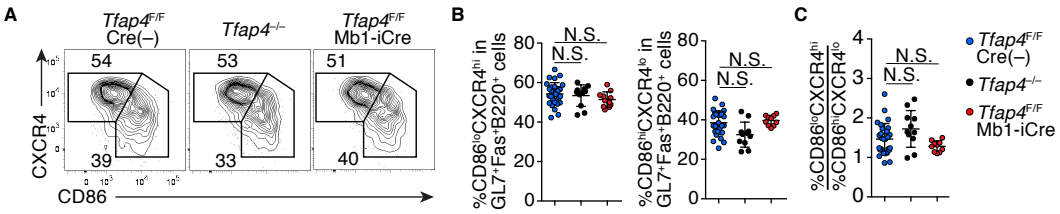

Figure 3.12. AP4-defieincy does not alter LZ-DZ segregation. (A-C) Expression of CD86 and CXCR4 in $B220^{+}GL7^{+}Fas^{+}$ GC B cells from mice with indicated genotypes ten days after NP-CGG immunization. Representative plots (A) and statistical analysis of frequencies of LZ ($CD86^{hi}CXCR4^{lo}$) and DZ ($CD86^{lo}CXCR4^{hi}$) cells in the GC B cell compartment (B) and DZ to LZ ratios (C) from four independent experiments are shown. One-way ANOVA.

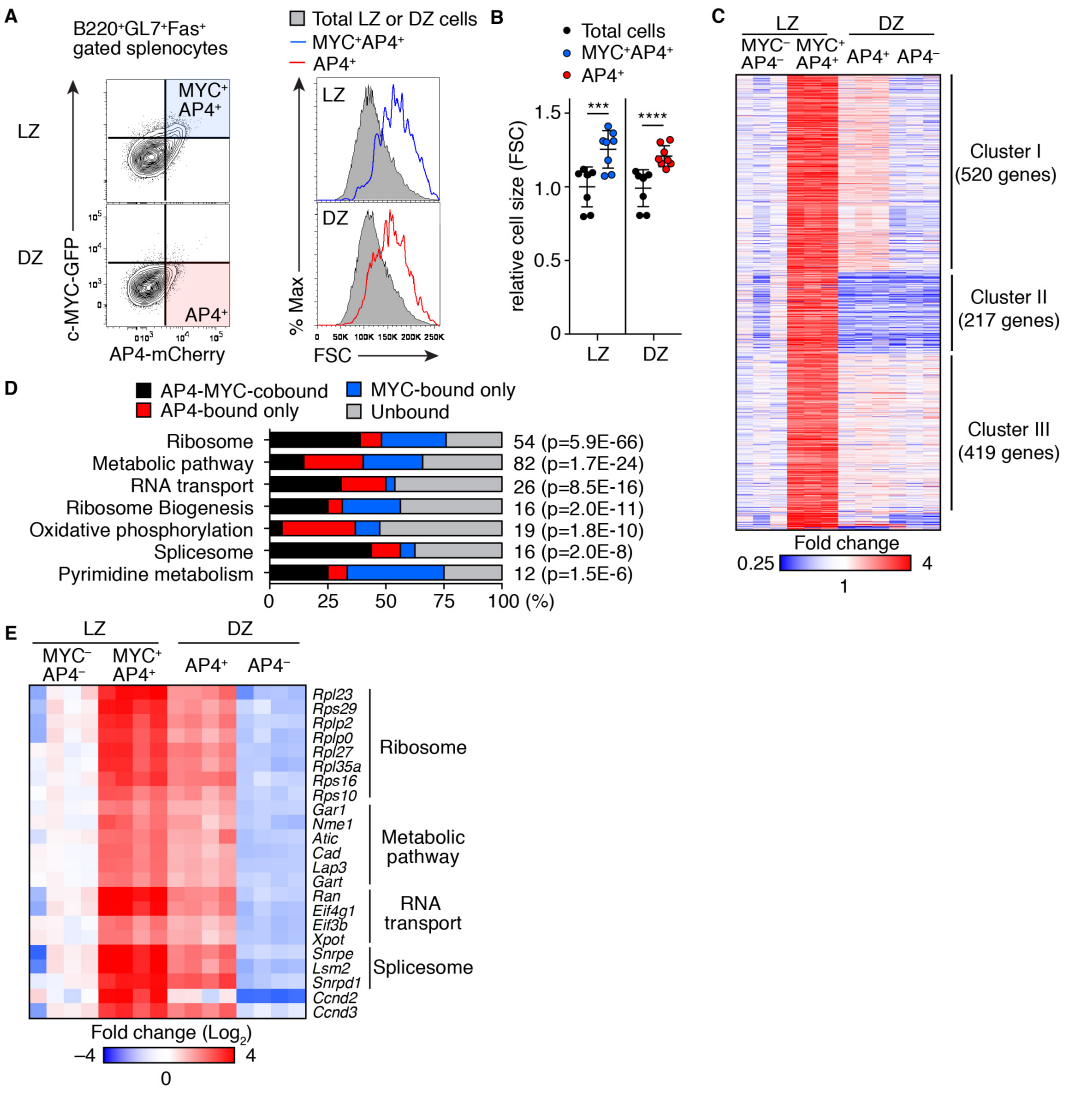

Figure 3.13. AP4-expressing DZ cells maintain activation signatures following c-MYC downregulation. (A and B) Relative cell sizes (forward scatter) of MYC^+AP4^+ LZ and DZ B cells from AP4-mCherry/c-MYC-GFP knock-in mice eight days after SRBC immunization (A). Statistical analysis from three independent experiments is shown in (B). **(C)** RNAseq analysis of MYC^-AP4^- LZ, MYC^+AP4^+ LZ, $AP4^+$ DZ and $AP4^-$ DZ cells. Expression of genes which were expressed higher by >1.8-fold in MYC^+AP4^+ LZ cells than MYC^-AP4^- LZ cells is shown as a heat map following unsupervised clustering analysis that yielded three major clusters. **(D)** Pathway analysis of Cluster I genes in (C) combined with ChIPseq analysis showing the frequencies of genes directly bound by AP4, c-MYC, or both in each pathway. The number of genes in each pathway is shown to the right of the bar with *P*-values for enrichment. **(E)** Spike-in qPCR validation of representative AP4-MYC-cobound genes in (D). Expression levels in four independent samples from two experiments are shown as a heatmap. Data are shown by mean ± SD. Unpaired Student's *t* test.

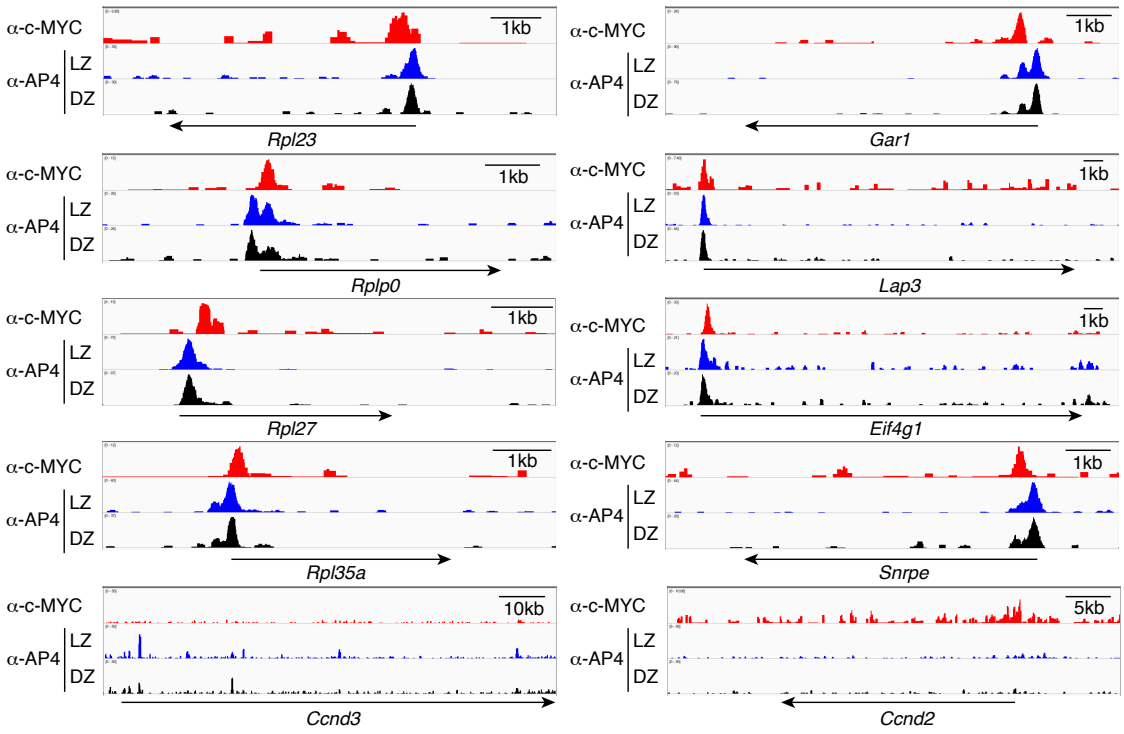

Figure 3.14. Identification of AP4 and c-MYC co-target genes. Examples of c-MYC and AP4 binding to genes shown in Figure 14E determined by ChIPseq using sorted LZ or DZ GC B cells or *in vitro* activated B cells.

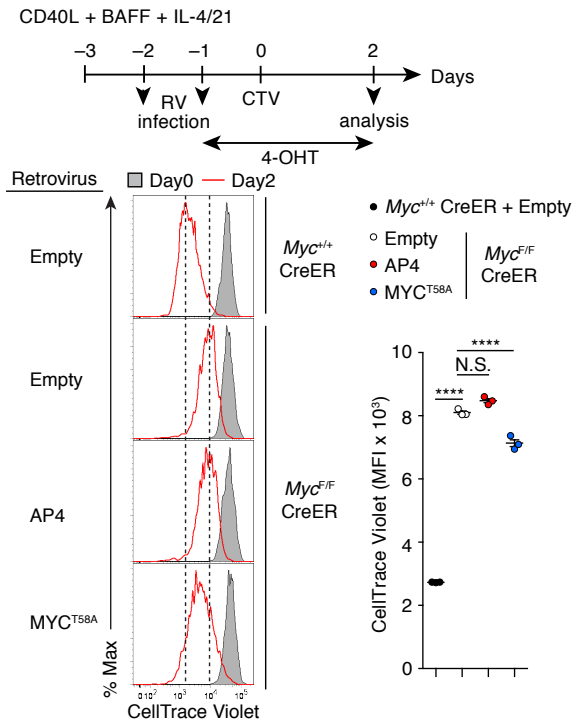

Figure 3.15. Overexpression of AP4 does not rescue defects of *Myc*$^{-/-}$ B cells. Flow cytometric analysis showing CellTrace Violet dilution of *Myc*-deficient B cells infected with a control retrovirus (RV) or one expressing AP4 or MYC^{T58A}. CD40L-primed *Myc*$^{F/F}$ *Rosa26*-CreER^{T2} or *Myc*$^{+/+}$ *Rosa26*-CreER^{T2} splenic B cells were infected with indicated RV, followed by treatment with 4-hydroxytamoxifen (4-OHT), and proliferation was analyzed. Data are representative of two independent experiments. One-way ANOVA.

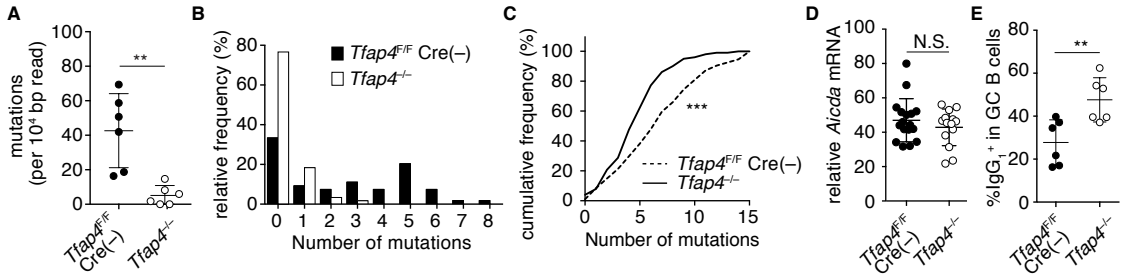

Figure 3.16. AP4 is necessary for the accumulation of somatic mutations. (A) Frequencies of mutations in an J_H4 adjacent intronic region in *Tfap4*$^{-/-}$ and control *Tfap4*$^{F/F}$ Cre(–) donor GC B cells from mixed bone marrow chimeras 12 days after NP-CGG immunization. Data are pooled from three independent experiments. **(B)** Frequencies of clones carrying multiple mutations in (A). **(C)** Cumulative frequency distribution of $V_H186.2$ somatic mutations in CD45.2 donor GC B cells in (A). Data are pooled from three independent experiments. **(D and E)** Expression of *Aicda* mRNA and frequencies of CD45.2 donor-derived IgG_1^+ GC B cells in (A). Data are pooled from three independent experiments. Data in (A, D, E) are shown by means ± SD, with unpaired Student's *t* test. Kolmogorov-Smirnov test for (C). $n = 6$ for each group (A-C); $n = 17$ for *Tfap4*$^{F/F}$ Cre(–) and $n = 14$ for *Tfap4*$^{-/-}$ (D).

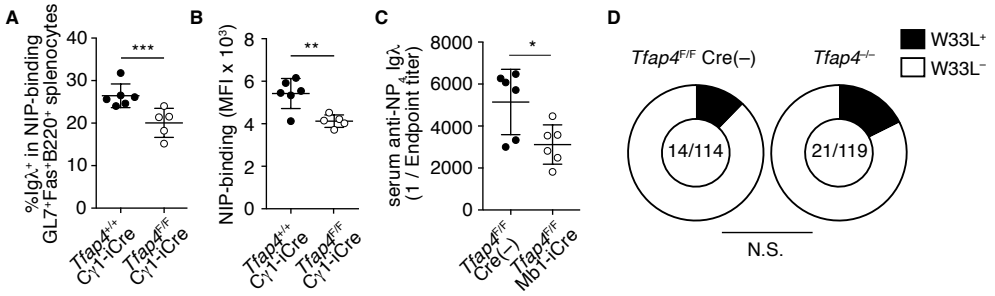

Figure 3.17. AP4 is dispensable for accumulation of W33L mutations. (A) Frequencies of Igλ$^+$ cells in NIP-APC-binding GC B cells from *Tfap4*$^{F/F}$ Cγ1-Cre and control *Tfap4*$^{+/+}$ Cγ1-Cre mice ten days after NP-CGG immunization. Data are pooled from two independent experiments. **(B)** NIP-APC-binding by GC B cells in (F). Data are pooled from two independent experiments. **(C)** NP_4-specific serum Igλ titers in *Tfap4*$^{F/F}$ Mb1-iCre and control *Tfap4*$^{F/F}$ Cre(–) mice 56 days after NP-CGG immunization. Data are pooled from two independent experiments. **(D)** Frequencies of the W33L mutation in V_H186.2 BCR$^+$ clones in CD45.2 GC B cells. Numbers of W33L bearing clones and total number of clones sequenced are shown. Data are pooled from four independent experiments. Data in (A-D) are shown by means ± SD, with unpaired Student's *t* test. χ^2 test with Yates correction for (D). $n = 6$ for each group.

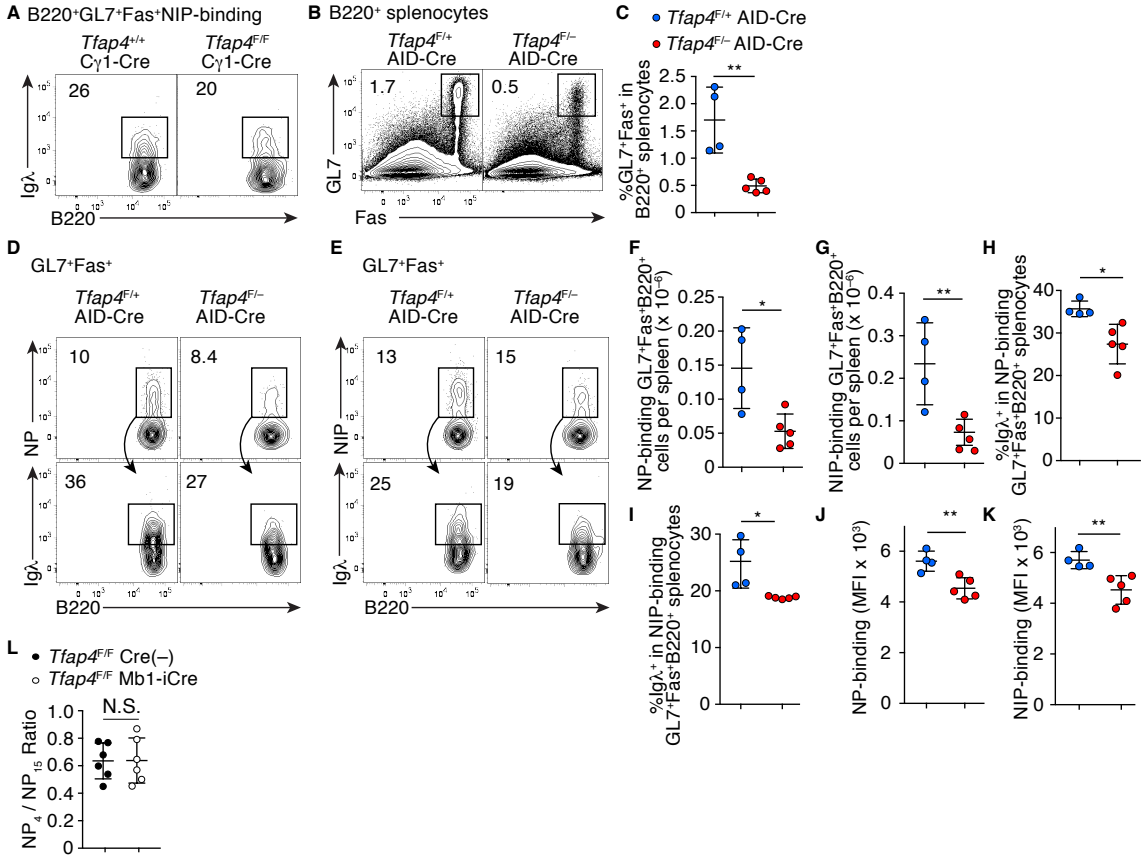

Figure 3.18. Antibody responses in GC B cell- and activated B cell-specific AP4 conditional knockout mice following immunization with NP-CGG in Alum. (A) Flow cytometric analysis showing Igλ expression in NIP-Allophycocyanin (APC) binding $GL7^+Fas^+B220^+$ splenocytes from *Tfap4*$^{F/F}$ Cγ1-Cre (N=5) and control *Tfap4*$^{+/+}$ Cγ1-Cre (N=6) mice ten days after NP-CGG immunization. **(B)** Expression of GL7 and Fas in $B220^+$ splenocytes from *Tfap4*$^{F/–}$ AID-Cre (N=5) and control *Tfap4*$^{F/+}$ AID-Cre (N=4) mice ten days after NP-CGG immunization. **(C)** Statistical analysis of frequencies of $GL7^+Fas^+$ cells in $B220^+$ splenocytes in (B). **(D and E)** NP- and NIP-conjugate APC binding by $B220^+GL7^+Fas^+$ splenocytes and Igλ expression in NP-APC- or NIP-APC-binding GC B cells in (B). **(F-K)** Absolute numbers of and Igλ expression in NP-APC- (F and H) and NIP-APC-binding $B220^+GL7^+Fas^+$ splenocytes (G and I), as well as NP-APC- (J) and NIP-APC-binding (K) by $B220^+GL7^+Fas^+$ splenocytes in (B). **(L)** Ratio of NP_4- to NP_{15}-specific serum IgG_1 titers from *Tfap4*$^{F/F}$ Mb1-iCre (N=6) and control *Tfap4*$^{F/F}$ Cre(–) (N=6) mice 56 days after NP-CGG immunization. Data are representative of (A, B, D and E) or pooled from (C and F-L) two independent experiments. Data are shown by means ± SD. Unpaired Student's *t* test.

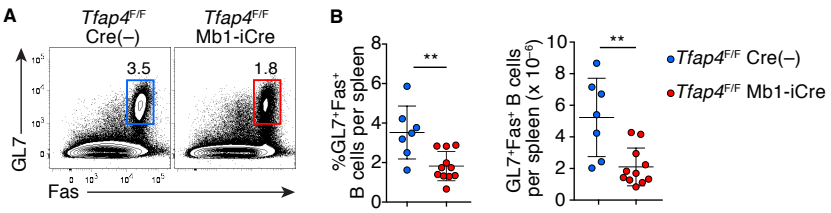

Figure 3.19. AP4 maximizes GC expansion against LCMV clone 13 infection. (A and B) Frequencies and absolute numbers of $B220^{+}GL7^{+}Fas^{+}$ cells in the spleens of *Tfap4*$^{F/F}$ Mb1-iCre and control *Tfap4*$^{F/F}$ Cre(–) mice 30 days after infection with LCMV-c13. Data are pooled from two independent experiments. Unpaired Student's *t* test. $n = 7$ for *Tfap4*$^{F/F}$ Cre(–) and $n = 11$ for *Tfap4*$^{F/F}$ Mb1-iCre.

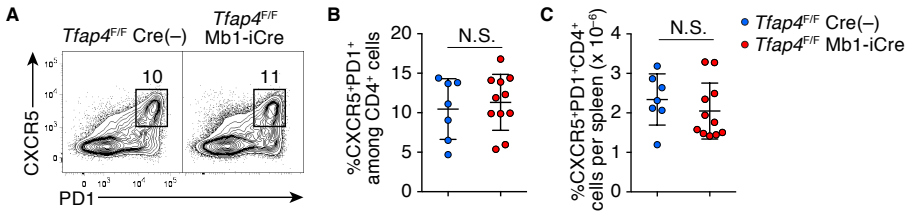

Figure 3.20. AP4 is dispensable for the expansion of T_{FH} cells. (A-C) Flow cytometric analysis showing CXCR5 and PD1 expression in $CD4^+$ splenocytes from *Tfap4*$^{F/F}$ Mb1-iCre (N=11) and control *Tfap4*$^{F/F}$ Cre(–) (N=7) mice 30 days after infection with LCMV-c13. Statistical analysis from two independent experiments is shown by means ± SD in (B and C). Unpaired Student's *t* test.

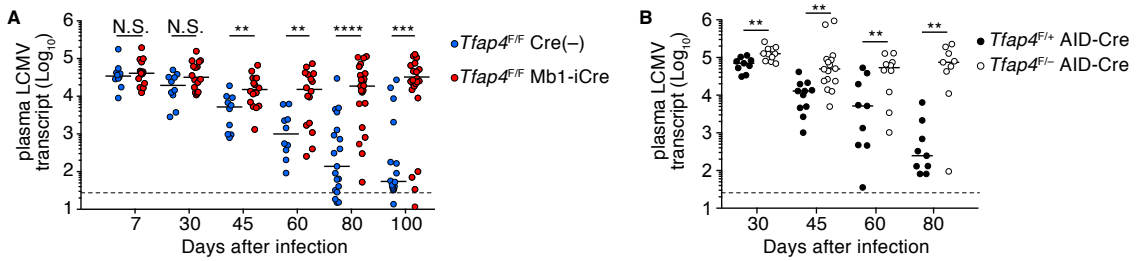

Figure 3.21. AP4 is required for B cell-dependent clearance of LCMV clone 13. (A and B) Analysis of plasma LCMV loads in *Tfap4*$^{F/F}$ Mb1-iCre and control *Tfap4*$^{F/F}$ Cre(–) mice (A) and *Tfap4*$^{F/–}$ AID-Cre and control *Tfap4*$^{F/+}$ AID-Cre mice (B) after infection. Data are pooled from six (A) and three (B) independent experiments. Lines in represent medians. Mann-Whitney's ranked test. For each time point n = 10–19 for *Tfap4*$^{F/F}$ Cre(–) and n = 16–25 for *Tfap4*$^{F/F}$ Mb1-iCre (A); for each time point n = 9–11 per group (B)

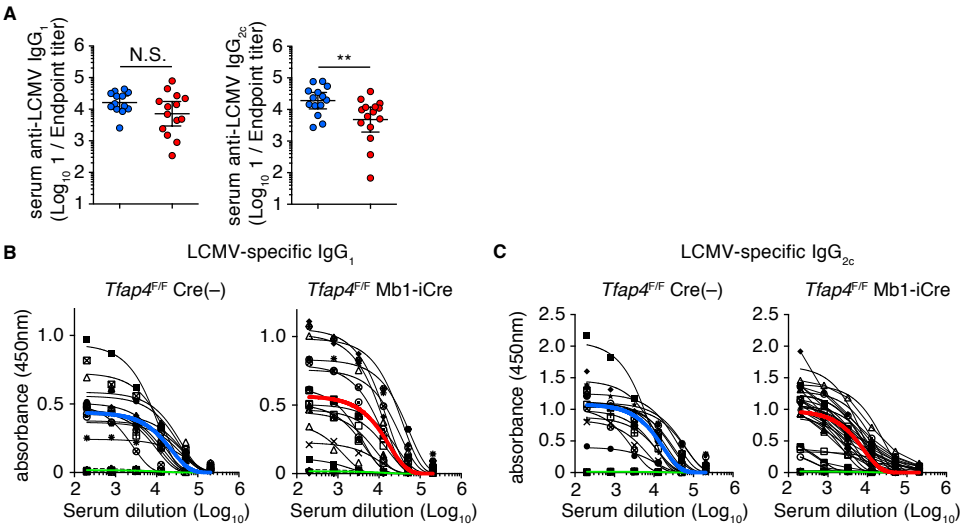

Figure 3.22. AP4 is dispensable for the development of LCMV-specific isotype switched antibodies. (A) Titers of LCMV-binding serum IgG in *Tfap4*$^{F/F}$ Mb1-iCre and control *Tfap4*$^{F/F}$ Cre(–) mice 80 days after infection. Data are pooled from six independent experiments. Data in are show by means ± SD. **(B and C)** Binding curves showing the reactivity of serum IgG_1 and IgG_{2c} from mice infected with LCMV-c13 to LCMV virion, as determined by ELISA. The thick curves in each group represent the average reactivity to LCMV virion. Green curves, showing reactivity of West Nile Virus vaccine-induced serum IgG to LCMV virion, serve as background controls. Each character symbol represents an individual mouse. Data are pooled from six independent experiments. $n = 12$ for *Tfap4*$^{F/F}$ Cre(–) and $n = 14$ for *Tfap4*$^{F/F}$ Mb1-iCre

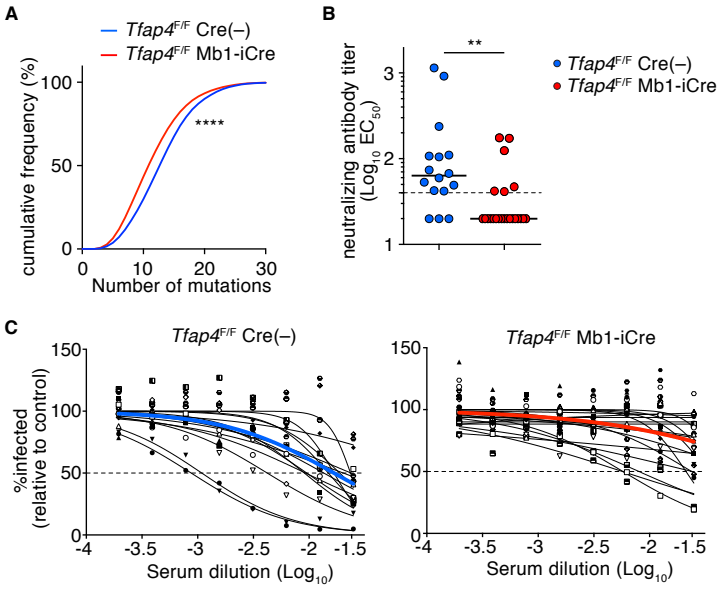

Figure 3.23. AP4 is necessary for the development of LCMV-neutralizing antibodies. (A) Cumulative frequency distribution of somatic mutations of the *Igh* variable regions in GC B cells 30 days after infection. Data are pooled from two independent experiments. **(B)** Neutralizing serum antibody titers from *Tfap4*$^{F/F}$ Mb1-iCre and control *Tfap4*$^{F/F}$ Cre(–) mice 80 days after LCMV infection. Neutralizing titers were shown as $1/EC_{50}$. Data are pooled from six independent experiments. Lines in (B) represent medians. **(C)** Inhibition of LCMV infection of Vero cells by heat-inactivated sera collected from *Tfap4*$^{F/F}$ Mb1-iCre (N=25) and control *Tfap4*$^{F/F}$ Cre(–) (N=14) mice 80 days after infection. Data are pooled from six independent experiments. Kolmogorov-Smirnov test for (A). Mann-Whitney's ranked test for (B). $n = 6$ per group (A); $n = 14$ for *Tfap4*$^{F/F}$ Cre(–) and $n = 25$ for *Tfap4*$^{F/F}$ Mb1-iCre (B).

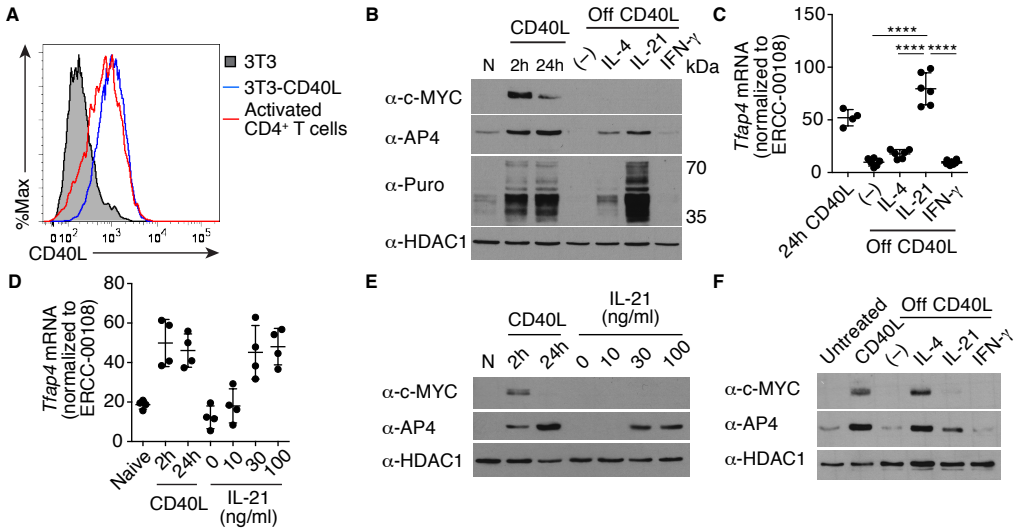

Figure 3.24. IL-21 sustains AP4 expression after CD40 stimulation is withdrawn. (A) Flow cytometric analysis showing expression of CD40L on NIH-3T3 cells infected with a CD40L-expressing retrovirus compared to that in CD4$^+$ T cells polarized *in vitro* for 2 days. **(B)** AP4 and c-MYC protein levels and puromycin (Puro) incorporation in naive (N), stimulated B cells with CD40L, and those subsequently stimulated with cytokines without CD40L (off CD40L). (–) denotes no cytokines added. Data are representative of three independent experiments. **(C)** Cell-number normalized *Tfap4* mRNA levels in activated B cells from (B). Data are pooled from two independent experiments. **(D and E)** Cell-number normalized *Tfap4* mRNA and protein levels in B cells stimulated with CD40L and those subsequently stimulated with IL-21. Data are pooled from three independent experiments. **(F)** AP4 and c-MYC protein levels in GC B cells *ex vivo* that were untreated, CD40L-stimulated, and those subsequently stimulated with cytokines without CD40L signals (off CD40L). (–) denotes no cytokine added. GC B cells were purified eight days after SRBC immunization. Data are representative of two independent experiments. Data in are shown by means ± SD. One-way ANOVA. n = 4–6 (B-E); n = 2 (F).

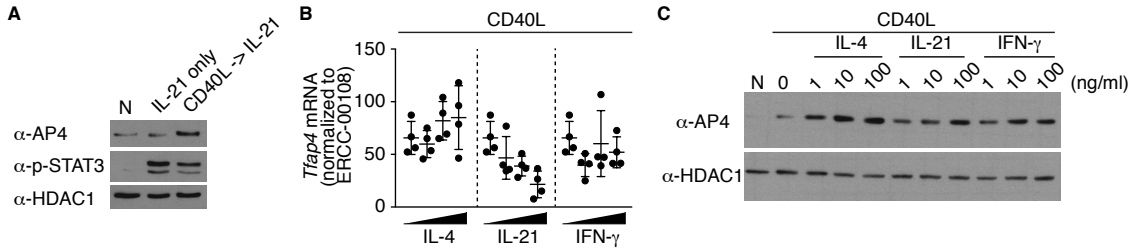

Figure 3.25. IL-21 does not increase AP4 expression when CD40L is engaged. (A) Immunoblot analysis showing AP4 and phosphorylated STAT3 protein levels in naive B cells (N), naive B cells cultured in the presence of IL-21 (IL-21 alone) for 24 hours, and CD40-primed B cells subsequently cultured in the presence of IL-21 (CD40L -> IL-21). **(B and C)** *Tfap4* mRNA levels (B) and AP4 protein levels (C) in B cells co-stimulated with CD40L and each cytokine (0, 10, 30, 100 ng/ml). Cell number normalized transcript levels are shown. Data are representative (A and C) of or pooled (B) from two independent.

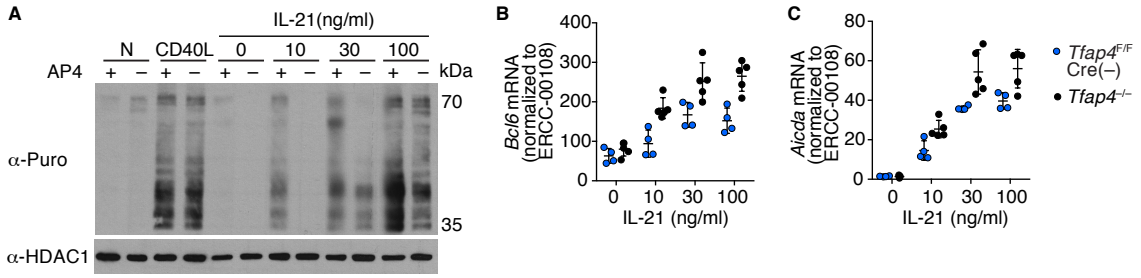

Figure 3.26. AP4 is specifically required for increased protein translation by IL-21 signal. (A) Puromycin incorporation by *Tfap4*$^{F/-}$ Mb1-iCre and control *Tfap4*$^{F/+}$ Mb1-iCre naive B cells (N), CD40L-stimulated B cells, and those subsequently stimulated with different concentrations of IL-21 without CD40L. Data are representative of two independent experiments. **(B and C)** *Bcl6* and *Aicda* mRNA levels in *Tfap4*$^{-/-}$ (N=5) and control *Tfap4*$^{+/+}$ (N=4) B cells that were sequentially stimulated by CD40 ligation and IL-21. Cell number normalized transcript levels are shown. Data representative (A) or pooled (B and C) from two independent experiments are shown by means ± SD.

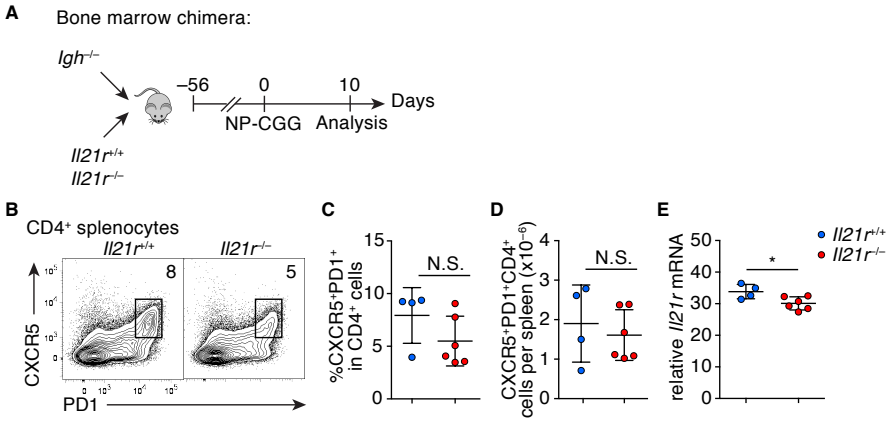

Figure 3.27. *Il21r* is dispensable for expansion of T_{FH} cells. (A) A schematic showing the generation of mixed bone marrow chimeras, in which *Il21r* is deficient in all B cells. A three to one mixture of bone marrow cells from $Igh^{-/-}$ mice and $Il21r^{-/-}$ or $Il21r^{+/+}$ mice were transplanted into lethally irradiated B6-CD45.1 hosts, followed by NP-CGG immunization and analysis of GC responses on day ten. **(B)** Flow cytometric analysis showing CXCR5 and PD1 expression in $CD4^+$ splenocytes from mixed bone marrow chimeras (N=4-6 per group) in (A). **(C and D)** Frequencies (C) and absolute numbers (D) of $CXCR5^+PD1^+$ cells in $CD4^+$ cells in (B). **(E)** *Il21r* mRNA levels in $CXCR5^+PD1^+CD4^+$ splenocytes in (B). Data representative (B) or pooled (C-E) from two independent experiments are shown by means ± SD. Unpaired Student's *t* test.

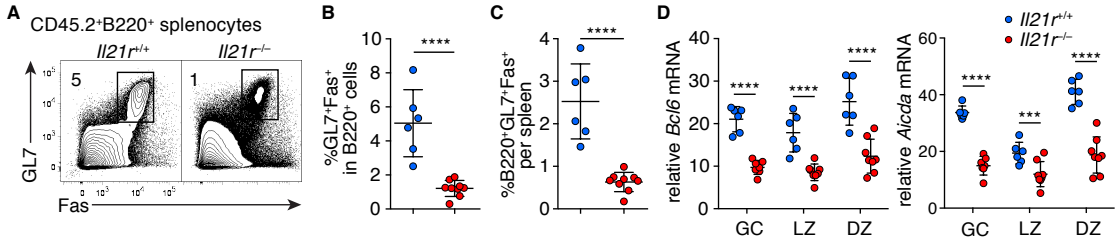

Figure 3.28. *Il21r* is required for GC response. (A) GL7 and Fas expression in donor-derived $B220^+$ splenocytes (N=6-9 per group) in Figure 27. **(B and C)** Frequencies of $GL7^+Fas^+$ cells in donor-derived $B220^+$ splenocytes (B) and absolute numbers of $B220^+GL7^+Fas^+$ cells per spleen (C) in (A). **(D)** *Bcl6* and *Aicda* mRNA levels in total GC, LZ, and DZ cells in (A). Data representative (A) or pooled (B-D) from two independent experiments are shown by means ± SD. Unpaired Student's *t* test.

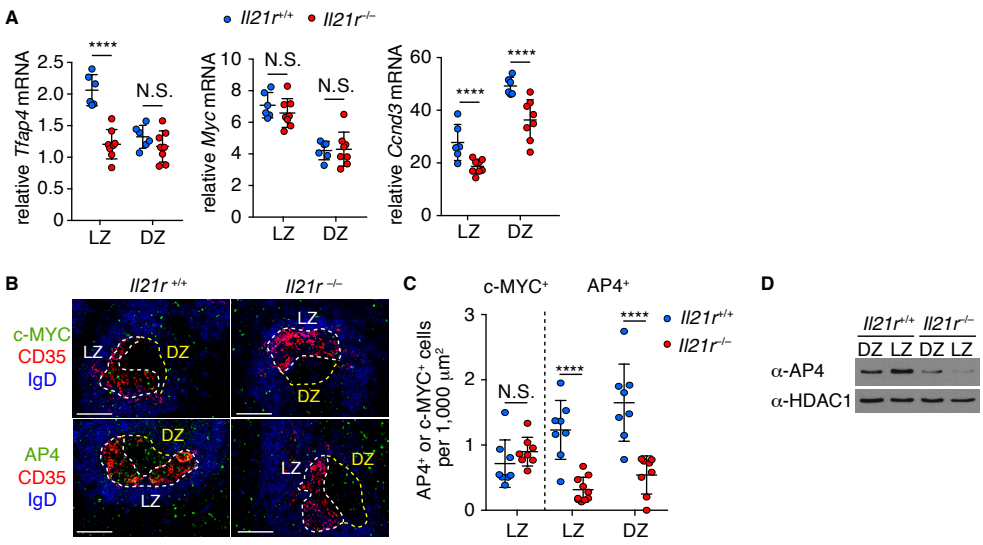

Figure 3.29. *Il21r* is required for maximal AP4 expression in GC B cells. (A) *Tfap4*, *Myc*, *Ccnd3* mRNA levels in *Il21r*$^{+/+}$ and *Il21r*$^{-/-}$ CD86^{hi}CXCR4^{lo} LZ and CD86^{lo}CXCR4^{hi} DZ GC B cells from mixed bone marrow chimeras (Figure 27) ten days after NP-CGG immunization. Data are pooled from three independent experiments. **(B and C)** Staining for c-MYC and AP4 expression of spleen sections from mice in (A). LZ and DZ defined as in Figure 2. Data are representative of three independent experiments. Scale bar, 100 μm. Statistical analysis of c-MYC- and AP4-expressing cell frequencies per 1,000 μm^2 of LZ or DZ is shown in (C). Data are pooled from three independent experiments. **(D)** AP4 protein levels in LZ and DZ GC B cells in (A). Data are representative of three independent experiments. Data in are shown by means ± SD. unpaired Student's *t* test. $n = 6$ for *Il21r*$^{+/+}$ and $n = 8$ for *Il21r*$^{-/-}$ (A); $n = 4$ for *Il21r*$^{+/+}$ and $n = 6$ for *Il21r*$^{-/-}$ (B-D).

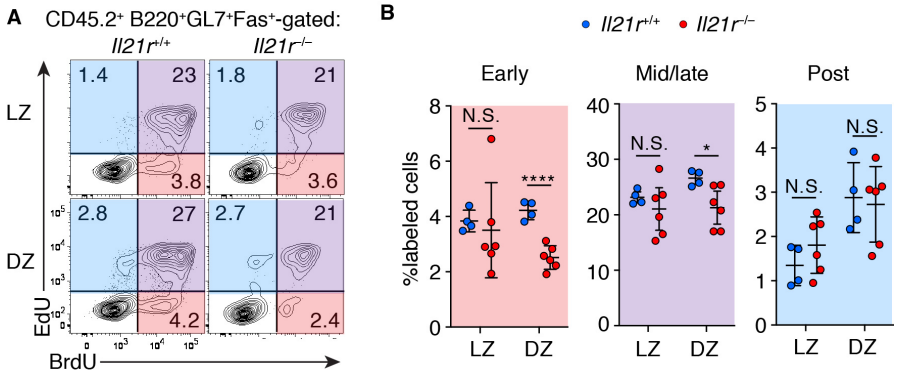

Figure 3.30. *Il21r* promotes cell-cycle re-entry of DZ GC B cells. (A and B) Cell cycle analysis by sequential EdU and BrdU labeling of CD45.2 *Il21r*$^{-/-}$ and control *Il21r*$^{+/+}$ donor LZ and DZ GC B cells from mixed bone marrow chimeras in Figure 27. Data are pooled from two independent experiments and shown by means ± SD. unpaired Student's *t* test. $n = 4$ for *Il21r*$^{+/+}$ and $n = 6$ for *Il21r*$^{-/-}$

CHAPTER 4:

Discussion

In the study, we have demonstrated that for both CD8 T cells and GC B cells, c-MYC initiates the activation and proliferation program that are later on maintained by AP4 (**Figure 1**). Sustained AP4 expression after c-MYC downregulation is necessary for the continued proliferation of lymphocytes. In CD8 T cell responses, full-blown clonal expansion provides sufficient tissue infiltration and subsequent protection of host from certain neurotropic viruses. For GC B cells response, sustained proliferation in the DZ after selection by T_{FH} is required for diversification of BCR repertoire to increase the probability of generating rare affinity enhancing mutations critical for the protective activities of antibodies. Thus, both CD8 T cells and GC B cells utilize the c-MYC-AP4 hand-off mechanism to maximize their responses.

Our conclusion that AP4 sustains c-MYC's function after c-MYC is downregulated is primarily based on the observation that the appearance of defective cell growth, metabolism and proliferation in *Tfap4*$^{-/-}$ CD8 T cells coincided with the downregulation of c-MYC after the priming phase. Although gene expression and ChIP-seq analyses, as well as rescue experiments support this conclusion, we did not completely rule out the possibility that AP4 is required during CD8 T cell priming to program a durable response later in the infection. This can be tested by reconstituting AP4 protein in *Tfap4*$^{-/-}$ CD8 T cell only after c-MYC is downregulated, using the *Rosa26*-sAP4 mice generated in our lab (see **Appendix**). Likewise, we also did not rule out the possibility that residual c-MYC expression, which falls below detection limit, contributes to driving continued expansion of CD8 T cells. This can be tested by genetically ablating *Myc* at various time points after infection. These experiments will be difficult to conduct in the context of GC reaction, however, due to the cyclic nature of the

response and asynchrony of selection events. But nevertheless, our data indicate that c-MYC and AP4 regulate overlapping target genes that are involved in lymphocyte activation.

How does AP4 maintain transcription of thousands of target genes? Recent studies on the mechanisms by which c-MYC amplifies the transcription of activated genes in lymphocytes may provide some insights[1]. Binding of c-MYC to genomic loci can be sequence specific and promiscuous, depending on the level of its expression [2]. c-MYC activates the gene transcription by regulating the 'pause-release' of RNA polymerase II. Several studies demonstrated that RNA polymerase II "pauses" at a short distance downstream of transcriptional start sites (TSS) across the metazoan genome, yielding abortive transcripts of 20 – 65 nucleotides in length [3, 4, 5, 6]. The establishment of pausing generates accessible chromatin configuration, likely through the recruitment of DNA-binding transcription factors [7]. RNA polymerase II then initiates RNA synthesis but is stalled by two pause-inducing factors: negative elongation factor complex (NELF) and DRB sensitivity-inducing factor (DSIF) [8]. The "release" from elongation inhibition requires phosphorylation of NELF by the kinase positive elongation factor b (pTEF-b) [9], which is recruited by a distinct class of transcription factors, exemplified by c-MYC and NFκB [6, 10, 11]. Thus, the ability to interact with pTEF-b allows c-MYC to "amplify" transcription. However, to activate transcription of a large number of genes, c-MYC must also exhibit promiscuity in DNA binding. In a recent study using human cancer cell lines, c-MYC was reported to interact with sequences containing E-box motifs other than the consensus "CACGTG" [12]. In support of this, our ChIP-seq analysis also shows that only 30% of the c-MYC-bound genes contain the consensus c-MYC-binding motif (**Chapter**

2). Our evidence that AP4 binds to and regulates over 50% of c-MYC targets leads us to hypothesize that AP4 is also able to stimulate transcription through triggering the release of RNA polymerase II. Whether AP4 also interacts with the two components of pTEF-b: Cdk9 and cyclin T1 in activated primary CD8 T and B cells remains to be tested.

Why did two distinct transcription factors evolve to have significantly overlapping functions? Why is it necessary for c-MYC expression to be rapidly terminated? The evolutionary pressure that drove the development of this "hand-off" mechanism remains an outstanding question. Chromosomal translocation involving the immunoglobulin loci and *Myc* is causally linked to GC-derived lymphomas[13, 14, 15], likely a result of AID activity on actively transcribed *Myc* locus[16]. In addition, enforced Myc expression is sufficient to drive GC lymphomagenesis in the presence of constitutive PI3K signaling[12]. Thus, it is possible that *Myc* is transcriptionally silenced in the DZ where AID-mediated SHM takes place, to minimize deleterious chromosomal translocation, and post-transcriptionally restricted to suppress malignant transformation in the presence of other oncogenic mutations. The maintenance of cellular activation and rapid proliferation in the absence of *Myc* requires a second factor, AP4. Long-term studies that define functional differences between c-MYC and AP4 in cancer models will further clarify the biological role of the MYC-AP4 hand off in sustaining lymphocyte proliferation, while staving off their transformation.

It is hardly convincing that the sole function of AP4 is to sustain gene expression programs initiated by c-MYC. While the majority of AP4-bound genes are indeed bound by c-MYC, a significant number of genes are bound only by AP4. One of these genes, *Il2ra* (which encodes the high affinity IL-2 receptor alpha subunit, also known as CD25)

was in fact downregulated in the absence of AP4 in the later, but not early, phase of the acute infection (**Figure 2a**). Consistent with the lack of c-MYC binding in the locus, ectopic c-MYC expression failed to rescue *Il2ra* levels in *Tfap4*$^{-/-}$ CD8 T cells (**Figure 2b,c**). Signaling through CD25 is required for granzyme B expression and differentiation into KLRG1^{+} effector cells[17, 18, 19, 20, 21]. Consistent with premature downregulation of CD25, *Tfap4*$^{-/-}$ CD8 T cells expressed reduced amount of Granzyme B on day 4 after infection (data not shown) and failed to express the KLRG1 marker at the peak of response (**Chapter 2**). So far, our preliminary data suggest that prolonged CD25 expression failed to rescue the blasting defect of *Tfap4*$^{-/-}$ CD8 T cells in vitro (data not shown). Given the mild defect in proliferation seen in *Il2ra*$^{-/-}$ CD8 T cells during acute infection, we found it unlikely that the severely impaired clonal expansion of *Tfap4*$^{-/-}$ CD8 T cells was caused by their failure to sustain CD25 expression. Further experiments need to be done to distinguish between CD25- and AP4-dependent programs in controlling CD8 T cell expansion and effector differentiation. Rescue experiments by CD25 overexpression in *Tfap4*$^{-/-}$ CD8 T cells or vice versa will address these issues.

Signaling through the IL-2R is required for sustained expression of both c-MYC [22, 23] and AP4 [24]. However, AP4, but not c-MYC, promotes the expression of CD25 (data now shown). These data suggest a feed-forward loop in which IL-2 signals promote the accumulation of AP4, which in turn sustains CD25 expression, thus increasing sensitivity to decreasing amount of IL-2 present in the later phase of immune response. Such a mechanism may ensure acquisition of effector functions, including Gzmb expression, especially in non-lymphoid tissues where IL-2 is limiting. As an anti-tumor therapy,

ectopic expression of AP4 may allow autologous T cells to efficiently compete against T_{reg} for IL-2, thereby enhancing the efficacy of IL-2-based therapies.

Are there other transcription factors that relay the effects of AP4 after AP4 is downregulated? Our data on expansion kinetics and BrdU incorporation indicate that both CD8 T cells and GC B cells continue to proliferate, albeit at a significantly slower rate than earlier time points, after AP4 is downregulated. It is possible that AP4 is the terminal factor in the cascade and allows the cells to build up enough energy and building blocks for the last couple rounds of cell divisions. Alternatively, other transcription factors, induced by AP4, promote CD8 T cell proliferation late in the infection. Further analyses on AP4 target genes in both CD8 T cells and GC B cells are instrumental to addressing this question.

CD8 T cell response is regulated by the sequential activation of regulatory modules [25]. The mechanism by which each module is temporally induced still remains unknown. Our study uncovers a transcription factor cascade between c-MYC and AP4 utilized by lymphocytes to maximize their responses. Along the same line, Kaech and colleagues recently identified a cascade between Tbet (encoded by *Tbx21*) and Zeb2 that promotes effector differentiation of CD8 T cells [26]. Not unlike CD8 T cell response, GC response is likely regulated in a modular fashion as well. However, the cyclic nature and asynchronous selection events make it difficult to define each module. Studies that dissect the underlying regulatory networks connecting individual module to allow for their sequential activation will provide significant insights into how adaptive immune response is regulated and create opportunities to manipulate the response for therapeutic purposes.

REFERENCES

1. Nie, Z. *et al.* c-Myc is a universal amplifier of expressed genes in lymphocytes and embryonic stem cells. *Cell* **151**, 68-79 (2012).
2. Kress, T.R., Sabo, A. & Amati, B. MYC: connecting selective transcriptional control to global RNA production. *Nat Rev Cancer* **15**, 593-607 (2015).
3. Muse, G.W. *et al.* RNA polymerase is poised for activation across the genome. *Nat Genet* **39**, 1507-1511 (2007).
4. Core, L.J., Waterfall, J.J. & Lis, J.T. Nascent RNA Sequencing Reveals Widespread Pausing and Divergent Initiation at Human Promoters. *Science* **322**, 1845-1848 (2008).
5. Nechaev, S. *et al.* Global Analysis of Short RNAs Reveals Widespread Promoter-Proximal Stalling and Arrest of Pol II in Drosophila. *Science* **327**, 335-338 (2010).
6. Rahl, P.B. *et al.* c-Myc regulates transcriptional pause release. *Cell* **141**, 432-445 (2010).
7. Adelman, K. & Lis, J.T. Promoter-proximal pausing of RNA polymerase II: emerging roles in metazoans. *Nat Rev Genet* **13**, 720-731 (2012).
8. Yamaguchi, Y., Shibata, H. & Handa, H. Transcription elongation factors DSIF and NELF: Promoter-proximal pausing and beyond. *Bba-Gene Regul Mech* **1829**, 98-104 (2013).
9. Peterlin, B.M. & Price, D.H. Controlling the elongation phase of transcription with P-TEFb. *Mol Cell* **23**, 297-305 (2006).
10. Blau, J. *et al.* Three functional classes of transcriptional activation domain. *Molecular and cellular biology* **16**, 2044-2055 (1996).

11. Barboric, M., Nissen, R.M., Kanazawa, S., Jabrane-Ferrat, N. & Peterlin, B.M. NF-kappaB binds P-TEFb to stimulate transcriptional elongation by RNA polymerase II. *Mol Cell* **8**, 327-337 (2001).

12. Sander, S. *et al.* Synergy between PI3K signaling and MYC in Burkitt lymphomagenesis. *Cancer cell* **22**, 167-179 (2012).

13. Cory, S. Activation of cellular oncogenes in hemopoietic cells by chromosome translocation. *Adv Cancer Res* **47**, 189-234 (1986).

14. Adams, J.M. *et al.* The c-myc oncogene driven by immunoglobulin enhancers induces lymphoid malignancy in transgenic mice. *Nature* **318**, 533-538 (1985).

15. Shiramizu, B. *et al.* Patterns of chromosomal breakpoint locations in Burkitt's lymphoma: relevance to geography and Epstein-Barr virus association. *Blood* **77**, 1516-1526 (1991).

16. Kato, L. *et al.* Nonimmunoglobulin target loci of activation-induced cytidine deaminase (AID) share unique features with immunoglobulin genes. *Proc Natl Acad Sci U S A* **109**, 2479-2484 (2012).

17. Williams, M.A., Tyznik, A.J. & Bevan, M.J. Interleukin-2 signals during priming are required for secondary expansion of CD8+ memory T cells. *Nature* **441**, 890-893 (2006).

18. Obar, J.J. *et al.* CD4+ T cell regulation of CD25 expression controls development of short-lived effector CD8+ T cells in primary and secondary responses. *Proceedings of the National Academy of Sciences of the United States of America* **107**, 193-198 (2010).

19. D'Souza, W.N. & Lefrancois, L. IL-2 is not required for the initiation of CD8 T cell cycling but sustains expansion. *Journal of immunology* **171**, 5727-5735 (2003).

20. Pipkin, M.E. *et al.* Interleukin-2 and inflammation induce distinct transcriptional programs that promote the differentiation of effector cytolytic T cells. *Immunity* **32**, 79-90 (2010).

21. Kalia, V. *et al.* Prolonged interleukin-2Ralpha expression on virus-specific CD8+ T cells favors terminal-effector differentiation in vivo. *Immunity* **32**, 91-103 (2010).

22. Preston, G.C. *et al.* Single cell tuning of Myc expression by antigen receptor signal strength and interleukin-2 in T lymphocytes. *EMBO J* **34**, 2008-2024 (2015).

23. Chou, C. & Egawa, T. Myc or no Myc, that is the question. *Embo Journal* **34**, 1990-1991 (2015).

24. Chou, C. *et al.* c-Myc-induced transcription factor AP4 is required for host protection mediated by CD8+ T cells. *Nat Immunol* **15**, 884-893 (2014).

25. Best, J.A. *et al.* Transcriptional insights into the CD8(+) T cell response to infection and memory T cell formation. *Nat Immunol* **14**, 404-412 (2013).

26. Dominguez, C.X. *et al.* The transcription factors ZEB2 and T-bet cooperate to program cytotoxic T cell terminal differentiation in response to LCMV viral infection. *J Exp Med* **212**, 2041-2056 (2015).

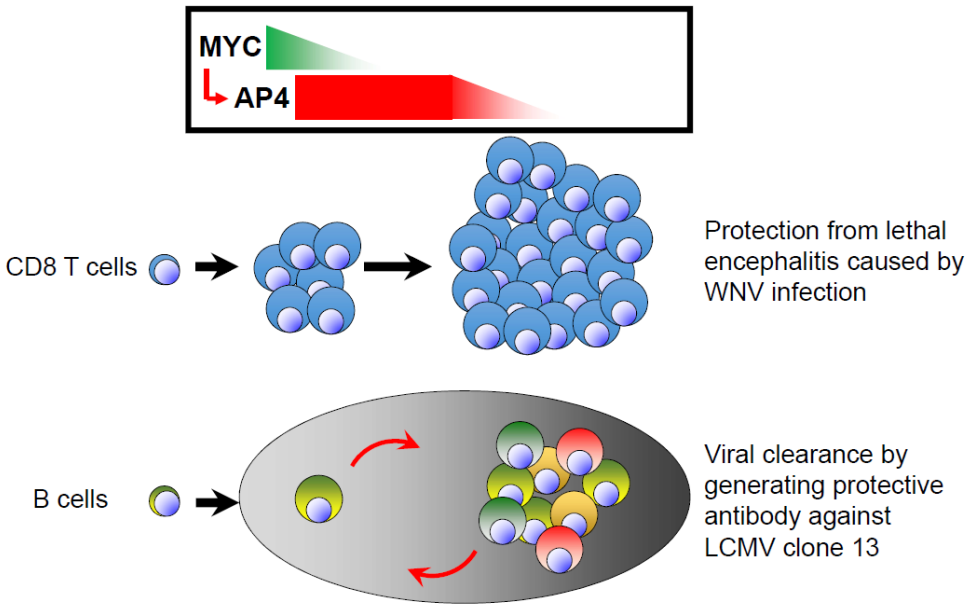

Figure 4.1. Lymphocytes utilize the c-MYC-AP4 hand-off to maximize adaptive immune responses. c-MYC induces AP4 during lymphocyte activation. While c-MYC is transient, AP4 sustains longer than c-MYC. Sustained AP4 expression promotes continued proliferation of activated lymphocytes. This conserved mechanism is required in CD8 T cells for maximal clonal expansion, and in GC B cells, to maximally diversify BCR repertoire.

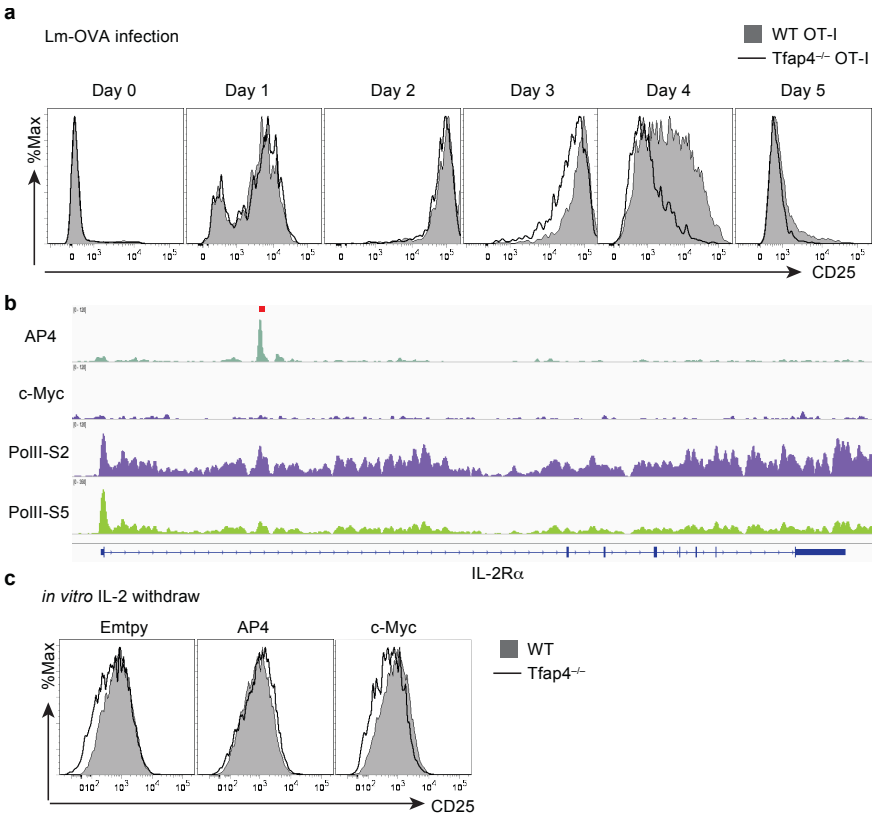

Figure 4.2. AP4 is required for sustained CD25 expression. a, Flow cytometric analysis showing CD25 expression of WT and *Tfap4*$^{-/-}$ OT-I cells at various time points after infection with LM-OVA. **b**, AP4 and c-MYC binding to the *Il2ra* locus determined by ChIP-seq analysis. c, Expression of CD25 on WT and *Tfap4*$^{-/-}$ CD8 T cells infected with an empty retrovirus, or retroviruses expressing AP4 or c-MYC.

.

Appendix:

Identification and use of a stabilized form of AP4 to enhance CD8 T cell activities.

A.1 BACKGROUND

The concept of "exhaustion" was first used to describe the observation that during chronic LCMV infection, antigen-specific, tetramer-binding CD8 T do not produce cytokines [1]. During "exhaustion", effector functions of CD8 T cells are gradually lost in a defined hierarchical order [2, 3]. Cytotoxic activity, high proliferative capacity, and IL-2 production are typically lost first, followed by the ability to produce tumor necrosis factor α (TNFα). Severe "exhaustion" leads to complete abolishment of IFNγ expression. The ultimate outcome of "exhaustion" is the physical deletion of antigen-specific CD8 T cells [3, 4]. The loss of effector function is partly a result of high level of inhibitory receptor expression, such as PD-1, Lag-3, 4-1BB, and CLTA4. PD-1 ligation is known to inhibit membrane-proximal T cell receptor signaling [5]. Consistently, Lag-3 has been shown to negatively affect cell cycle progression [6]. Over the past few years, several studies have reported complete or partial reversal of CD8 T cell "exhaustion" by blocking PD-1, Lag-3, CTLA-4, or combinations of the three [7, 8, 9].

Many attempts have been made to reverse CD8 T cell "exhaustion" induced by viral persistence [7, 10, 11], with most focusing on targeting the inhibitor receptor PD-1. Recently, whole genome microarray analysis on exhausted CD8 T cells revealed that several pathways involved in glucose metabolism and ribosome biogenesis were down-regulated compared to effector T cells [12, 13], a signature partly reminiscent of *Tfap4*$^{-/-}$ T cells during acute infection. These studies, together with the finding that AP4 protein was hardly detectable in exhausted P14 cells (data not shown), led us to hypothesize that forced expression of AP4 in antigen-specific CD8 T cells may restore expansion capacity and effector function lost during exhaustion.

The role of CD4 help to CD8 T cells during acute infection has been elegantly shown by Bevan's group [14]. CD4 T cells also play a vital role in controlling chronic infections. Using LCMV clone 13 infection model, several groups demonstrated exacerbation of chronic infection in the absence of CD4 T cells [3, 15]. In mice deficient for or depleted of CD4 T cells, antigen-specific CD8 T cells lost their effector functions and some were even deleted from the effector pool [1, 16]. However, it is unclear from these studies whether CD4 T cells contribute directly to control viral infection or indirectly through supporting B and CD8 T cells [17]. The most convincing data came from three back-to-back publications establishing IL-21 as a key factor produced by CD4 T cells to re-invigorate CD8 T cells [18, 19, 20]. These results were later on extended to HIV infection showing that the presence of IL-21-producing CD4 T cells was associated with improved control of infection and function of CD8 T cells in humans [21, 22]. In addition to functional CD8 T cell responses, antibody production by B cells were also required to control chronic LCMV infection [23]. Robust antibody response is intimately associated with T follicular helper (T_{FH}) differentiation. Prolonged viral persistence seemed to preferentially generate T_{FH} cells [24]. Consistent with this, signal through IL-6R on CD4 T cells was required to sustain T_{FH} response in a Bcl-6-dependent manner during the later phase of chronic infection [25]. Thus, CD4 T cells are likely to have an indirect role in controlling chronic infection. Despite phenotypic characterization of CD4 T cell response, the knowledge on the transcriptional control of high-quality CD4 help is still lacking.

A.2 RESULTS

AP4-deficient mice show significantly delayed viral clearance during chronic infection

Given that AP4 regulates the magnitude and duration of CD8 T cell expansion during acute infection, and that functional CD8 T cell response is also required for the timely resolution of chronic LCMV infection [26], we hypothesized that kinetics of viral clearance would be significantly delayed in mice lacking AP4 in CD8 T cells. To address this, we infected *Tfap4*$^{F/F}$;Cd8-Cre and WT mice with LCMV clone 13 and monitored serum viral titer over 60 days. We also included *Tfap4*$^{-/-}$ and *Tfap4*$^{F/F}$;Cd4-Cre mice in our pilot experiments to determine whether successful response to LCMV clone 13 requires the presence of AP4 in non-CD8 T cells, in particular, CD4 T cells. On day 7 post infection, all groups developed similarly severe viremia (**Figure 1**). By day 30 post infection, while WT mice began to control viral replication [24], all three groups of AP4-deficient mice retained significantly higher serum viral titer (2 to 3 logs compared to WT) (**Figure 1**). Delayed viral clearance in AP4-deficient animals was also apparent on day 45 post infection, although by day 60, viral transcripts in the blood fell below detection limit for all groups of mice (data not shown). Interestingly, both *Tfap4*$^{-/-}$ and *Tfap4*$^{F/F}$;Cd4-Cre mice retained substantially higher viral load than *Tfap4*$^{F/F}$;Cd8-Cre animals, suggesting immune response against chronic viral infection may require AP4 in CD4 T cells and/or other cell types.

Antigen specific CD8 T cells exhibit profound "exhaustion" phenotype in the absence of AP4

Because viral titer was significantly higher in AP4-deficient mice compared to WT controls regardless of where AP4 is deleted, we expected a more profound "exhaustion" phenotype exhibited by CD8 T cells from *Tfap4*$^{-/-}$, *Tfap4*$^{F/F}$;Cd4-Cre, and *Tfap4*$^{F/F}$;Cd8-Cre mice. Indeed, LCMV GP_{33-41}-specific splenic CD8 T cells from AP4-deficient mice expressed 10- to 20-fold higher level of surface PD-1 compared to WT controls at day 60 post LCMV clone 13 infection (**Figure 2a and b**). Next, we assessed production of effector cytokines, IFNγ and TNFα, by splenic CD8 T cells when re-stimulated with cognate LCMV antigens. Whereas the frequency of GP33-tetramer positive splenic CD8 T cells was only slightly reduced in AP4-deficient mice compared to WT controls at this point, IFNγ and TNFα production was severely compromised (**Figure 2c**). Based on these data, we concluded that CD8 T cells from AP4-deficient mice were more "exhausted" than WT controls. While we considered this defect secondary to prolonged viral persistence in the absence of AP4, we have not ruled out the possibility that AP4-deficient CD8 T cells are intrinsically prone to "exhaustion" and therefore fail to eliminate pathogens efficiently in the first place.

The requirement for AP4 during robust CD4 T cell responses is CD4 T cell-intrinsic.

To determine whether AP4 is required for robust CD4 T cell responses during chronic infection, we infected WT, *Tfap4*$^{-/-}$, *Tfap4*$^{F/F}$;Cd4-Cre and *Tfap4*$^{F/F}$;Cd8-Cre mice with LCMV clone 13 and analyzed immune responses on day 7 post infection. We

included *Tfap4*$^{F/F}$;Cd8-Cre mice as control because Cd4-Cre is active at the DP stage in thymic development, resulting in the deletion of AP4 in both CD4 and CD8 lineages. The choice of an early time point for analysis was made based on the finding that on day 7, viral titer was not different between WT and AP4-deficient mice. Consistent with our data from experiments using LCMV-Arm, in the absence of AP4, antigen-specific CD8 T cells showed highly impaired clonal expansion 7 days after infection with LCMV clone 13 (**Figure 3a and c**). Interestingly, the number of effector CD4 T cells was also moderately reduced specifically in *Tfap4*$^{-/-}$ and *Tfap4*$^{F/F}$;Cd4-Cre mice, but not in *Tfap4*$^{F/F}$;Cd8-Cre animals, compared to WT controls (**Figure 3b and d**), suggesting that AP4 is required for the expansion of CD4 T cells in a cell-intrinsic manner. We have not yet tested whether the functions of CD4 T cell were also affected in the absence of AP4.

N-terminal Flag-tag and S139A mutation enhance the stability of AP4 protein

Many attempts have been made to reverse CD8 T cell "exhaustion" induced by viral persistence [7, 10, 11], with most focusing on targeting the inhibitor receptor PD-1. Recently, whole genome microarray analysis on exhausted CD8 T cells revealed that several pathways involved in glucose metabolism and ribosome biogenesis were down-regulated compared to effector T cells [12, 13], a signature partly reminiscent of *Tfap4*$^{-/-}$ T cells during acute infection. These studies, together with the finding that AP4 protein was hardly detectable in exhausted P14 cells (data not shown), led us to hypothesize that forced expression of AP4 in antigen-specific CD8 T cells may restore expansion capacity and effector function lost during exhaustion. A major obstacle that hindered us from carrying out the experiment was the instability AP4 protein, with an estimated half-life of

2 hours in *in vitro* activated CD8 T cells and readily subject to proteosomal degradation (**Chapter 2 Figure 1e and f**). Compounding this was the observation that overexpression of AP4 resulted in proteolytic cleavage of the full-length form into a 5-kDa shorter product. This cleavage product, existing at approximately 3:1 ratio with the full-length AP4, lost the nuclear localization sequence and was constantly found in the cytoplasm (**Figure 4**). Thus, its intrinsic nature of instability and unexpected cleavage event prevented us from overexpressing AP4 at the maximal level. To overcome this problem, we sought to construct an AP4 mutant with prolonged half-life and reduced proteolytic cleavage when overexpressed.

Since serine/threonine phosphorylation commonly signals for proteasome-dependent degradation [27], we hypothesized that AP4 protein may undergo certain post-translational modifications that impact its stability. To test this, we utilized a publicly available proteomics software (PhosphoSitePlus) to search for phosphorylation sites in AP4. PhosphoSitePlus is not a prediction program. Rather, it sieves published phospho-mass spectrometry data into a list of peptides with confirmed phosphorylated residues. We found three highest hits in AP4 protein: T37, S124, and S139 (**Table 1**).

We mutated each of the three phosphorylated residues to alanine: T37A, S124A, and S139A, and tested the stability of each construct in primary CD8 T cells. Remarkably, S139A, but not T37A or S124A, significantly prolonged the half-life of AP4 (**Figure 5a** and **b**). Despite its enhanced stability, AP4-S139A still underwent proteolytic cleavage (**Figure 5a and b**). To determine at which termini the cleavage occurred, we Flag-tagged AP4 at either the N- or C-terminus, and analyzed the cleavage pattern by Western blot. Both the full-length and 5-kDa shorter products of C-terminal flag-tagged AP4 could be

detected with an anti-Flag antibody, suggesting that the cleavage occurs at the N-terminus (**Figure 5c**). Consistently, the very same antibody did not detect any cleavage product of N-terminal Flag-tagged AP4 (**Figure 5c**). Strikingly, anti-AP4 antibody also failed to detect the cleaved form, suggesting that N-terminal Flag-tag significantly reduced proteolytic cleavage (**Figure 5c**). From these structural studies, we concluded that N-terminal Flag-tag and S139A mutation enhance the stability of AP4 protein.

We also confirmed that the addition of Flag tag and point mutation did not impair the transcriptional activity of AP4, as both mutants were able to restore CD25 expression when overexpressed in *Tfap4*$^{-/-}$ CD8 T cells, compared to a mutant lacking the DNA binding domain (**Figure 6**).

Stabilized AP4 sustains CD8 T cell activation after IL-2 withdrawal

We found that S139A on AP4 is critically important for its stability. Another group has also confirmed this finding[28]. We next generated a mouse where an inducible enhanced AP4 is knocked into the *Rosa26* locus (**Figure 7**). mCherry expression allows tracking of CD8 T cells that have undergone Cre-mediated deletion of the STOP cassette following in vitro activation and transduction of a Cre-expressing retrovirus (**Figure 8a**). Consistent with their significantly elevated AP4 expression levels, mCherry^{+} CD8 T cells sustain high levels of CD25 and a blasting phenotype compared to control cells after IL-2 withdrawal (**Figure 8b, c**).

Interestingly, both the frequency and number of TCRβ^{+} cells in the spleen were reduced in *Rosa26*$^{sAP4/+}$ Cd4-Cre mice compared to controls at the steady-state (**Figure**

9a-c). Thymocyte development was normal, however (data not shown), suggesting that overexpression of AP4 has negative effects on peripheral T cell homeostasis. An increased proportion of both $CD4^+$ and $CD8^+$ T cells displayed an activated phenotype in *Rosa26*$^{sAP4/+}$ Cd4-Cre spleens compare to WT controls (**Figure 9d**), a phenomenon also seen in mice with constitutive PI3K activity (unpublished observation).

A.3 CONCLUSIONS AND FUTURE DIRECTIONS

In this preliminary study, we identified key phosphorylated residues on AP4 that are required for proteasome-mediated degradation of the protein. In addition, we also uncovered the proteolytic cleavage of AP4 when the protein is expressed at supraphysiological levels. The truncated form of AP4 is excluded from the nucleus, suggesting another layer of regulation of AP4 activity in addition to its short half-life and low transcript levels. This cleavage event was prevented by tagging the N-terminus of AP4. Thus, by mutating S139 to alanine and adding a N-terminal Flag-tag, we significantly enhanced the stability and function of AP4 in CD8 T cells *in vitro*. Whether this mutant form of AP4 is able to prevent CD8 T cell exhaustion during LCMV clone 13 infection remains to be tested. Expression of a constitutive form of PI3K and genetic deletion of *Vhl* in T cells enhanced effector functions, but also resulted in lethal immunopathology during LCMV clone 13 infection [29]. It will be interesting to test whether mutant AP4 is sufficient to promote T cell effector functions without inducing immunopathology.

Rejection of antigenic tumors requires T cell responses [30]. However, tumors establish an immunosuppressive environment that induces dysfunction or hyporesponsiveness of infiltrating T cells, thereby evading T cell-mediated destruction [31, 32]. Chronic TCR stimulation, lack of co-stimulation signals, suppression by other cells, and deprivation of mitogenic cytokines all contribute to T cell dysfunction [33]. Indeed, depleting regulatory T cells and blocking the PD-1 inhibitory receptor with checkpoint blockade therapies sufficiently reinvigorate T cell functions to mediate tumor rejection [34, 35]. Despite the efficacy seen in a wide variety of cancer patients, many tumors show little

susceptibility to checkpoint blockade therapies [36], suggesting that other inhibitory pathways are engaged in T cells. Defining, characterizing, and targeting these cell extrinsic pathways may prove fruitful, but is time-consuming and costly.

The use of autologous tumor-specific T cells as anti-cancer therapy provides an opportunity to engineer cell-intrinsic pathways for sustained effector functions, thus circumventing the need to target multiple surface receptors. By targeting common signaling pathways dampened by inhibitory receptor engagement, engineered T cells may be resistant to signals through multiple inhibitory receptors. This strategy is best exemplified by the successful use of CD137 and intracellular domain of CD28 to improve CAR T cell functions [37]. Because these signaling pathway ultimately activate transcription factors that promote the expression of genes related to survival, proliferation and cytokine production, directly targeting key transcription factors, either by modulating their transcriptional activities using small molecules or overexpression/silencing with a retrovirus/lentivirus may prove to be a successful ambition.

For this reason, enhanced AP4 mutant offers therapeutic potential. By overexpressing mutant AP4 in autologous or CAR T cells, one may prolong the effector functions of the transferred cells. Although such a strategy, like many others involving the use of a retrovirus, raises the critical concern of whether AP4 has oncogenic potential and whether transferred T cells can cause immunopathology, the risk can be significantly minimized by inserting a suicide cassette into the retroviral construct [38, 39, 40].

A.4: REFERNECES

1. Zajac, A.J. *et al.* Viral immune evasion due to persistence of activated T cells without effector function. *Journal of Experimental Medicine* **188**, 2205-2213 (1998).
2. Virgin, H.W., Wherry, E.J. & Ahmed, R. Redefining Chronic Viral Infection. *Cell* **138**, 30-50 (2009).
3. Wherry, E.J., Blattman, J.N., Murali-Krishna, K., van der Most, R. & Ahmed, R. Viral persistence alters CD8 T-cell immunodominance and tissue distribution and results in distinct stages of functional impairment. *J Virol* **77**, 4911-4927 (2003).
4. Moskophidis, D., Lechner, F., Pircher, H. & Zinkernagel, R.M. Virus Persistence in Acutely Infected Immunocompetent Mice by Exhaustion of Antiviral Cytotoxic Effector T-Cells. *Nature* **362**, 758-761 (1993).
5. Riley, J.L. PD-1 signaling in primary T cells. *Immunol Rev* **229**, 114-125 (2009).
6. Workman, C.J. *et al.* Lymphocyte activation gene-3 (CD223) regulates the size of the expanding T cell population following antigen activation in vivo. *J Immunol* **172**, 5450-5455 (2004).
7. Blackburn, S.D., Shin, H., Freeman, G.J. & Wherry, E.J. Selective expansion of a subset of exhausted CD8 T cells by alphaPD-L1 blockade. *Proceedings of the National Academy of Sciences of the United States of America* **105**, 15016-15021 (2008).
8. Velu, V. *et al.* Enhancing SIV-specific immunity in vivo by PD-1 blockade. *Nature* **458**, 206-U205 (2009).

9. Grosso, J.F. *et al.* Functionally Distinct LAG-3 and PD-1 Subsets on Activated and Chronically Stimulated CD8 T Cells. *J Immunol* **182**, 6659-6669 (2009).

10. Pellegrini, M. *et al.* IL-7 engages multiple mechanisms to overcome chronic viral infection and limit organ pathology. *Cell* **144**, 601-613 (2011).

11. Kao, C. *et al.* Transcription factor T-bet represses expression of the inhibitory receptor PD-1 and sustains virus-specific CD8+ T cell responses during chronic infection. *Nat Immunol* **12**, 663-671 (2011).

12. Wherry, E.J. *et al.* Molecular signature of CD8+ T cell exhaustion during chronic viral infection. *Immunity* **27**, 670-684 (2007).

13. MacIver, N.J., Michalek, R.D. & Rathmell, J.C. Metabolic regulation of T lymphocytes. *Annual review of immunology* **31**, 259-283 (2013).

14. Sun, J.C. & Bevan, M.J. Defective CD8 T cell memory following acute infection without CD4 T cell help. *Science* **300**, 339-342 (2003).

15. Wiesel, M. & Oxenius, A. From crucial to negligible: functional CD8(+) T-cell responses and their dependence on CD4(+) T-cell help. *European journal of immunology* **42**, 1080-1088 (2012).

16. Matloubian, M., Concepcion, R.J. & Ahmed, R. CD4+ T cells are required to sustain CD8+ cytotoxic T-cell responses during chronic viral infection. *J Virol* **68**, 8056-8063 (1994).

17. Walton, S., Mandaric, S. & Oxenius, A. CD4 T cell responses in latent and chronic viral infections. *Frontiers in immunology* **4**, 105 (2013).

18. Elsaesser, H., Sauer, K. & Brooks, D.G. IL-21 Is Required to Control Chronic Viral Infection. *Science* **324**, 1569-1572 (2009).

19. Frohlich, A. *et al.* IL-21R on T Cells Is Critical for Sustained Functionality and Control of Chronic Viral Infection. *Science* **324**, 1576-1580 (2009).

20. Yi, J.S., Du, M. & Zajac, A.J. A vital role for interleukin-21 in the control of a chronic viral infection. *Science* **324**, 1572-1576 (2009).

21. Chevalier, M.F. *et al.* HIV-1-Specific Interleukin-21(+) CD4(+) T Cell Responses Contribute to Durable Viral Control through the Modulation of HIV-Specific CD8(+) T Cell Function. *Journal of Virology* **85**, 733-741 (2011).

22. Williams, L.D. *et al.* Interleukin-21-Producing HIV-1-Specific CD8 T Cells Are Preferentially Seen in Elite Controllers. *Journal of Virology* **85**, 2316-2324 (2011).

23. Bergthaler, A. *et al.* Impaired antibody response causes persistence of prototypic T cell-contained virus. *PLoS Biol* **7**, e1000080 (2009).

24. Fahey, L.M. *et al.* Viral persistence redirects CD4 T cell differentiation toward T follicular helper cells. *The Journal of experimental medicine* **208**, 987-999 (2011).

25. Harker, J.A., Lewis, G.M., Mack, L. & Zuniga, E.I. Late interleukin-6 escalates T follicular helper cell responses and controls a chronic viral infection. *Science* **334**, 825-829 (2011).

26. Storm, P., Bartholdy, C., Sorensen, M.R., Christensen, J.P. & Thomsen, A.R. Perforin-deficient CD8+ T cells mediate fatal lymphocytic choriomeningitis despite impaired cytokine production. *J Virol* **80**, 1222-1230 (2006).

27. Westermarck, J. Regulation of transcription factor function by targeted protein degradation: an overview focusing on p53, c-Myc, and c-Jun. *Methods in molecular biology* **647**, 31-36 (2010).

28. D'Annibale, S. *et al.* Proteasome-dependent degradation of transcription factor activating enhancer-binding protein 4 (TFAP4) controls mitotic division. *J Biol Chem* **289**, 7730-7737 (2014).

29. Doedens, A.L. *et al.* Hypoxia-inducible factors enhance the effector responses of CD8(+) T cells to persistent antigen. *Nat Immunol* **14**, 1173-1182 (2013).

30. Vesely, M.D. & Schreiber, R.D. Cancer immunoediting: antigens, mechanisms, and implications to cancer immunotherapy. *Ann N Y Acad Sci* **1284**, 1-5 (2013).

31. Crespo, J., Sun, H., Welling, T.H., Tian, Z. & Zou, W. T cell anergy, exhaustion, senescence, and stemness in the tumor microenvironment. *Curr Opin Immunol* **25**, 214-221 (2013).

32. Wherry, E.J. T cell exhaustion. *Nat Immunol* **12**, 492-499 (2011).

33. Gajewski, T.F., Schreiber, H. & Fu, Y.X. Innate and adaptive immune cells in the tumor microenvironment. *Nat Immunol* **14**, 1014-1022 (2013).

34. Pardoll, D.M. The blockade of immune checkpoints in cancer immunotherapy. *Nat Rev Cancer* **12**, 252-264 (2012).

35. Chen, L. & Han, X. Anti-PD-1/PD-L1 therapy of human cancer: past, present, and future. *J Clin Invest* **125**, 3384-3391 (2015).

36. Kyi, C. & Postow, M.A. Checkpoint blocking antibodies in cancer immunotherapy. *FEBS Lett* **588**, 368-376 (2014).

37. Kershaw, M.H., Westwood, J.A. & Darcy, P.K. Gene-engineered T cells for cancer therapy. *Nat Rev Cancer* **13**, 525-541 (2013).

38. Bonini, C. *et al.* HSV-TK gene transfer into donor lymphocytes for control of allogeneic graft-versus-leukemia. *Science* **276**, 1719-1724 (1997).

39. Straathof, K.C. *et al.* An inducible caspase 9 safety switch for T-cell therapy. *Blood* **105**, 4247-4254 (2005).

40. Wang, X. *et al.* A transgene-encoded cell surface polypeptide for selection, in vivo tracking, and ablation of engineered cells. *Blood* **118**, 1255-1263 (2011).

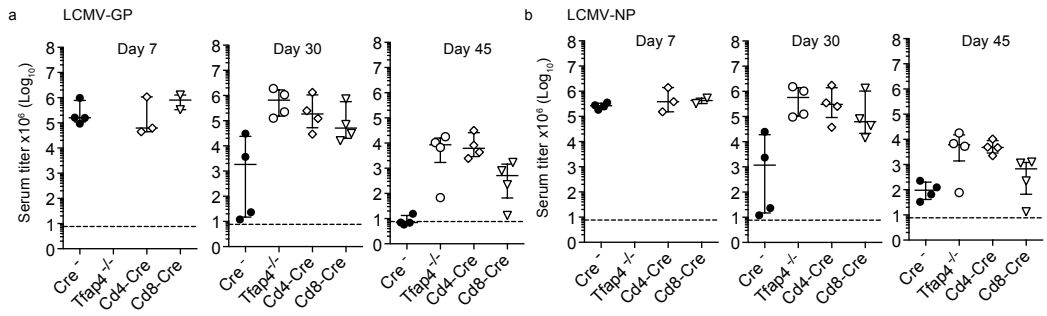

Figure A.1. AP4-deficient mice exhibit delayed kinetics of viral clearance. (a,b) Analysis of plasma LCMV loads in *Tfap4*$^{-/-}$, *Tfap4*$^{F/F}$ Cd4-Cre, *Tfap4*$^{F/F}$ Cd8-Cre and control *Tfap4*$^{F/F}$ Cre(–) mice at various time points after infection with LCMV clone 13. Data are shown by means ± SD.

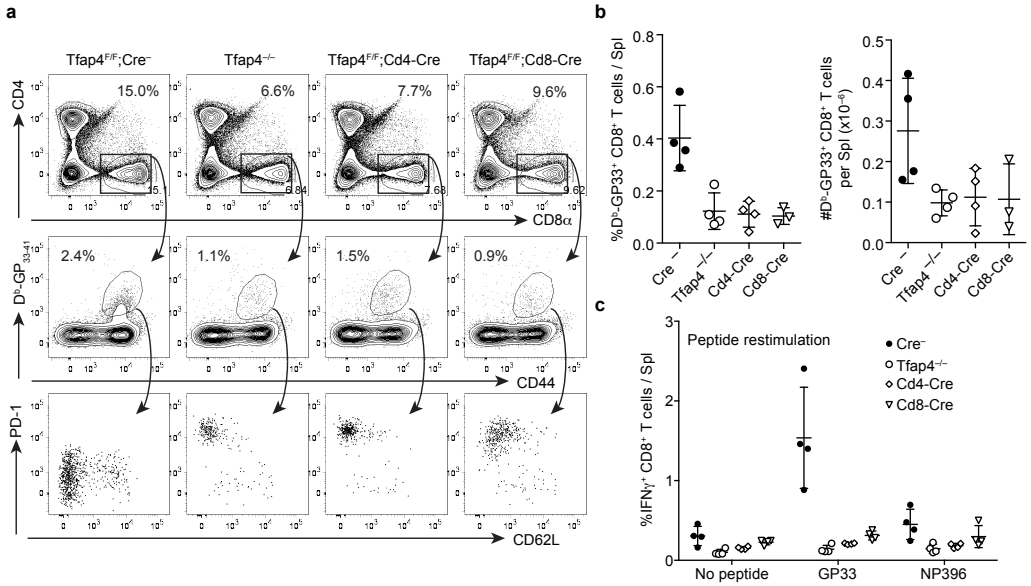

Figure A.2. CD8 T cells from AP4-deficient mice appear more "exhausted" than WT controls. (a) Expression of CD4, CD8α, CD44, PD-1, and CD62L on splenocytes as well as H-2D^b-GP(33-41) binding by CD8α$^+$ cells 30 days after infection with LCMV clone 13. **(b)** Statistical analysis showing the frequency and absolute number of H-2D^b-GP(33-41)-specific CD8α$^+$ cells per spleen in (a). **(c)** Frequency of IFNγ$^+$ CD8α$^+$ splenocytes in (a) after re-stimulation with indicated peptides, as determined by intracellular flow cytometry. Data are shown by means ± SD.

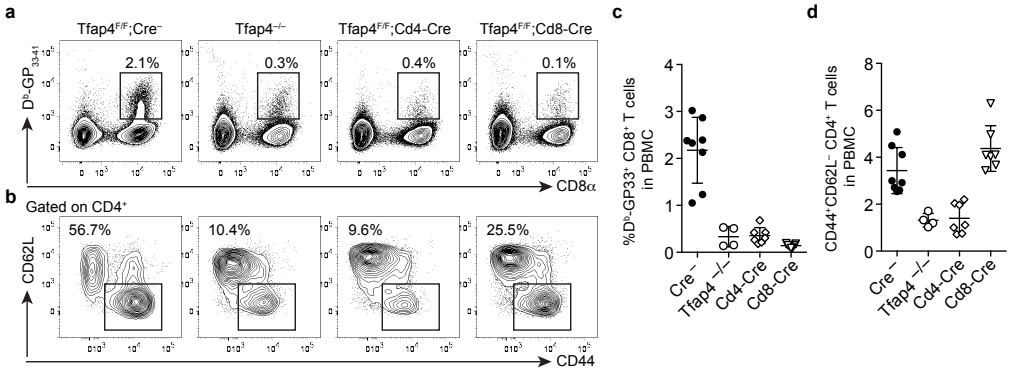

Figure A.3. AP4 is required for optimal expansion of both CD4 and CD8 T cells during chronic infection. (a) Frequency of CD8α$^+$ H-2D^b-GP(33-41)-binding cells in PBMC 30 days after infection with LCMV clone 13. **(b)** Expression of CD62L and CD44 in CD4$^+$ PBMC in (a). **(c)** Statistical analysis showing the frequency of H-2D^b-GP(33-41)-specific CD8α$^+$ cells in PBMC in (a). **(d)** Statistical analysis showing the frequency of CD44$^+$CD62L$^-$CD4$^+$ cells in PBMC in (a). Data are shown by means ± SD.

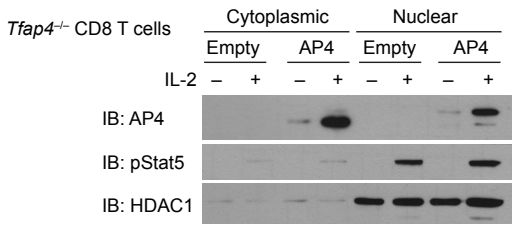

Figure A.4. AP4 protein is unstable and subject to rapid proteosomal degradation. Western blot analysis showing expression of AP4 and phospho-STAT5 in the cytoplasm or nucleus of *Tfap4*$^{-/-}$ CD8^{+} T cells transduced with a control retrovirus or one expressing AP4, and subsequently cultured in the presence of absence of IL-2. Note the difference in size between cytoplasmic and nuclear AP4 protein.

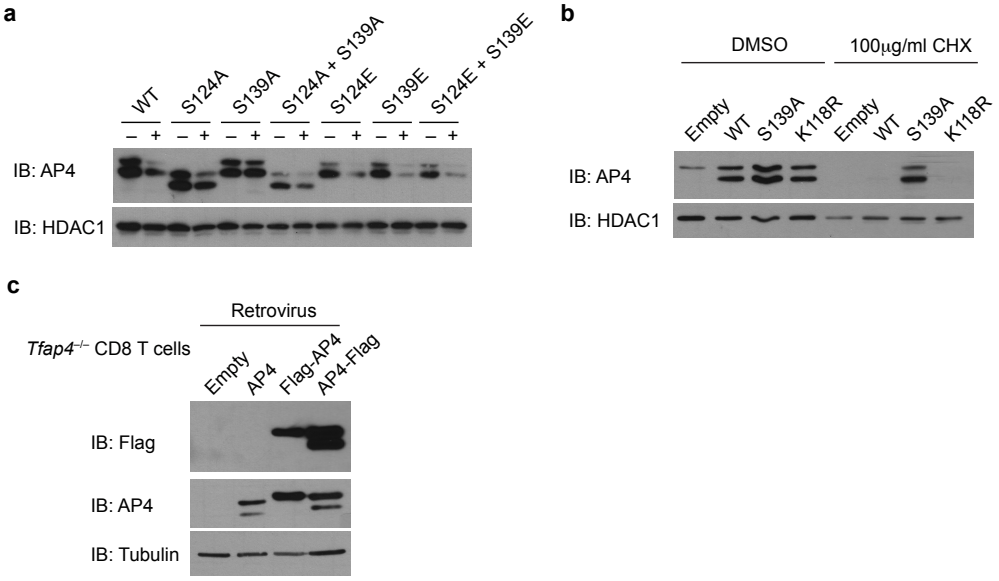

Figure A.5. Point mutation at S139 and N-terminal Flag tag confer AP4 with enhanced stability. (a,b) Western blot analysis showing expression of AP4 in CD8T cells transduced with retrovirus expressing WT AP4 or AP4 with point mutations, and subsequently cultured in the presence or absence of IL-2 (a) or CHX (b). **(c)** Expression of Flag-tagged AP4.

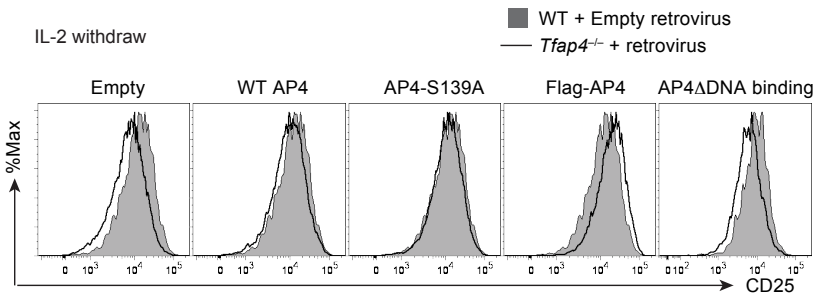

Figure A.6. S139A and N-terminal Flag-tagged AP4 still retain their transcriptional activity. Flow cytometric analysis showing expression of CD25 on *Tfap4*$^{-/-}$ CD8^{+} T cells transduced with WT or mutant forms of AP4.

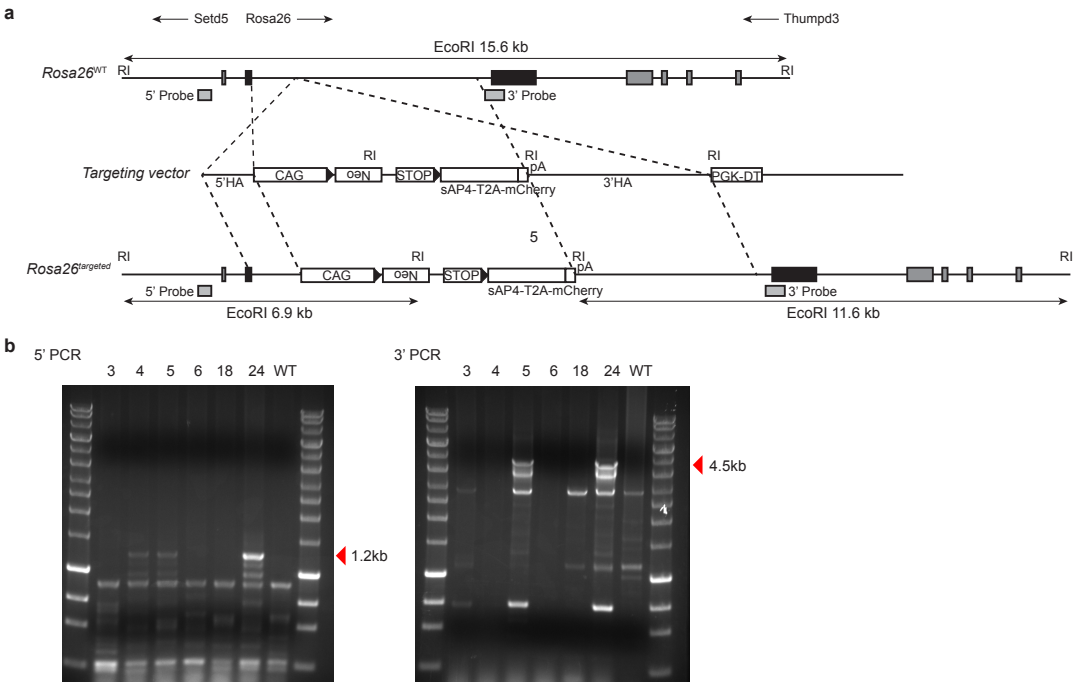

Figure A.7. Generation of the inducible super-AP4 knock-in allele. (a) A targeting strategy to knock-in an inducible stabilized mutant AP4 (sAP4) into the *Rosa26* locus. **(b)** PCR analysis of targeted ES clones. The expected band size for corrected targeted ES cell clones is indicated with a red arrow. Clones 5 and 24 were used for microinjection.

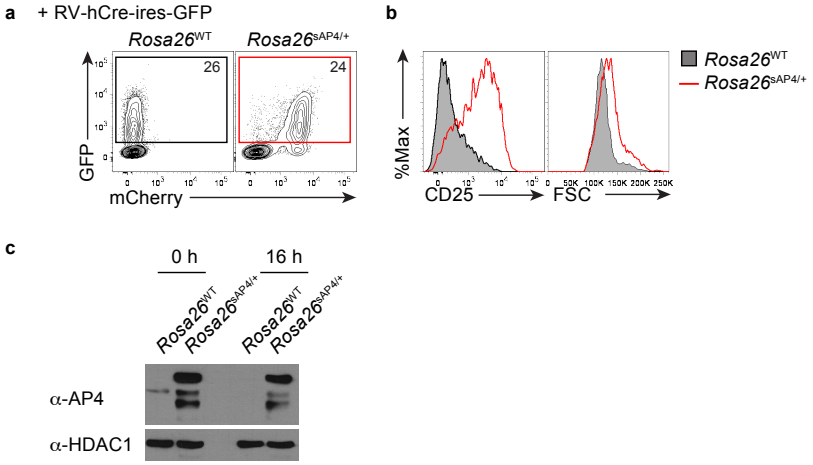

Figure A.8. Stabilized AP4 sustains CD25 expression and cell size after IL-2 withdrawal. (a) Expression of GFP and mCherry in *Rosa26*^{WT} or *Rosa26*$^{sAP4/+}$ CD8 T cells transduced with a retrovirus expressing the Cre-recombinase. (**b**) Expression of CD25 and forward scatter of CD8 T cells in **a**. (**c**) Western blot analysis showing AP4 protein expression in CD8 T cells in **a**.

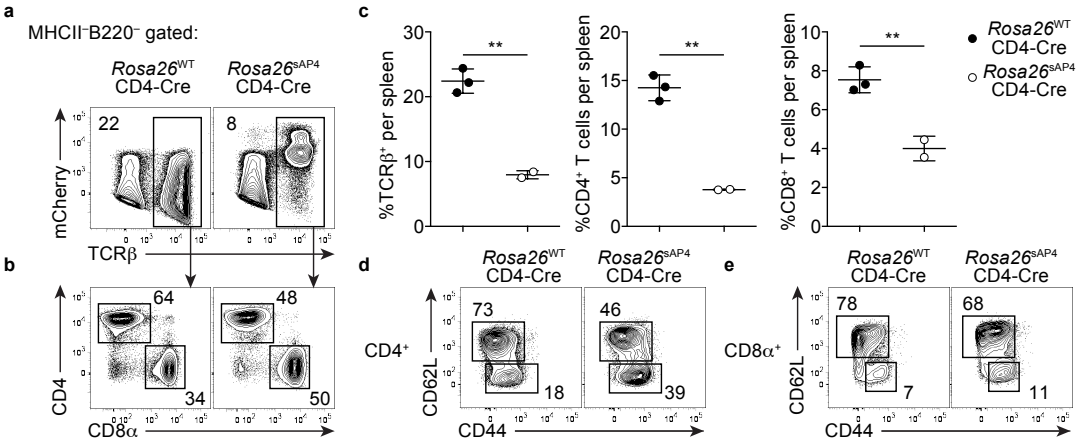

Figure A.9. CD4 and CD8 T cells expressing ectopic sAP4 display effector phenotypes under the steady state. (a,b) Flow cytometric analysis showing the expression of mCherry, TCRβ, CD4 and CD8α in MHCII$^-$B220$^-$ splenocytes from *Rosa26*^{WT} CD4-Cre and *Rosa26*$^{sAP4/+}$ CD4-Cre mice. (c) Frequencies of TCRβ$^+$, CD4$^+$ and CD8$^+$ cells per spleen. (d,e) Expression of CD62L and CD44 on CD4$^+$ (d) and CD8α$^+$ (e) splenocytes.

MS		MOUSE		HUMAN
1	Y3	_____MEYFMVPTQK	Y3-p	_____MEyFMVPTQK
1	S13	VPTQKVPSLQHFRKT	S13-p	VPTQKVPsLQHFRKT
18	T37	SLANIPLTPETQRDQ	T37-p	SLANIPLtPETQRDQ
2	K114	LQQNTQLKRFIQELs	K114-u	LQQNTQLkRFIQELs
2	S121-p	KRFIQELsGSsPKRR	S121-p	kRFIQELsGssPKRR
3	S123	FIQELsGSsPKRRRA	S123-p	FIQELsGssPKRRRA
24	S124-p	IQELsGSsPKRRRAE	S124-p	IQELsGssPKRRRAE
7	S139-p	DKDEGIGsPDIWEDE	S139-p	DKDEGIGsPDIWEDE
1	K189	HMYPEKLKVIAQQVQ	K189-u	HMYPEKLkVIAQQVQ
2	T282	AIQHIEGTQDKQELE	T282-p	AIQHIEGtQEKQELE

Table A.1. A list of phosphorylated peptides from AP4 protein. Data generated by PhosphoSitePlus (http://www.phosphosite.org/homeAction.action)